MASTER'S THESIS

ON THE INFLUENCE OF STORM CHARACTERISTICS ON SURGE RESPONSE IN THE NEW ORLEANS COASTAL BASIN

L. Straatsma BSc
July 2015, Enschede

UNIVERSITY OF TWENTE.

UNIVERSITY OF TWENTE.

On the influence of storm characteristics on surge response in the New Orleans coastal basin

Master's thesis

in Water engineering & Management
Faculty of Engineering Technology
University of Twente

Author	Leonie Straatsma BSc
Contact	L.straatsma@live.nl
Location and date	Enschede, July 4, 2015
Thesis defence date	July 10, 2015
Graduation committee	
Graduation supervisor	Prof. dr. S.J.M.H. Hulscher — University of Twente
Daily supervisors	Dr. ir. P.C. Roos — University of Twente
	W.L. Chen BSc — University of Twente
External supervisors	Dr. H.M. Schuttelaars — Delft University of Technology
	Dr. ir. M. van Ledden — Royal HaskoningDHV
	Dr. J.P.M Mulder — MULKUST

Abstract

Storm surges are of great interest to the city of New Orleans. Storm surges are flood like phenomena caused by storms. Different methods for surge prediction are used until now. Nevertheless, these methods are not always capable to provide insight in observed surge patterns in the New Orleans basin. This study focuses on assessing and explaining spatial and temporal patterns of surge response depending on different storm characteristics. This is done with the newly developed idealized storm surge model. For the first time this model is applied to a realistic case study. First model performance is assessed and then a sensitivity study to storm parameters is done.

Hurricanes create low pressure and high wind stresses at the ocean's surface. These forces induce both local and large scale water movements. Six storm parameters based on the Holland model are used as model input for the meteorological part. The hydrodynamical part is forced by the meteorological model and solves the linear shallow water equations using the finite element method and a temporal Fourier transformation. The domain is a schematic representation of the north east corner of the Gulf of Mexico (Figure 1). This large scale domain is chosen to capture both the local and large scale processes of a storm surge. Dirichlet boundaries with an inverse barometer effect represent the open connection with the Gulf.

The realistic case study shows that reproduced water level are in fair agreement with observed water levels. The maximum surge levels are comparable but the water level trend is underestimated prior and after landfall. The timing of these peaks levels on the other hand, is comparable at all locations. The qualitative trend of observed water levels is reproduced by the model. A sensitivity study for storm parameters is done with six synthetic storm scenarios. These scenarios are based on three different storm directions (NE, N, NW) and two combinations of central pressure and storm size (900 mbar & 32 km; 930 mbar & 47 km).

The simulations demonstrate that in this study, storm direction is the dominant storm parameter. Water level time series (Figure 2) show a clear distinction per direction. Directions affect maximum surge, timing of the surge and the trend of the water level. The water level deviations caused by storm direction in the range from 40 cm to 2 m. The combinations of central pressure and storm size on the other hand, show only small differences in maximum surge (3-35 cm).

Local processes mainly determine the surge pattern through the basin. These are induced by geometry and bathymetry and wind direction. This pattern is different for each storm direction. In addition, direction affects the relative importance of large scale processes. Only a north west storm direction shows this contribution, as it generates a forerunner propagating along the coast of Florida towards New Orleans. This can be seen in both water levels and the

amplitude spectra.

We conclude that the storm direction is an important parameter for the surge response in New Orleans affecting local and large scale surge response. This is notable because literature focusses on central pressure and storm size as main contributors. The effect of geometry should be noted . Therefore, it is important to extend this sensitivity study and focus more studies on a coastal geometry rather than commonly used, a straight coastline.

Preface

This report represents the final project of my study Water Engineering and Management at the University of Twente. The study focusses on the influence of storm characteristics on surge response in the New Orleans coastal basin. The newly developed storm surge model is used for the first time to simulate a realistic case. Making it a interesting study for both the model's applicability for real cases as the outcome of the storm sensitivity study.

The last few months I have had the opportunity to focus on the most fascinating forces of nature; the combination of wind and water. I worked with great pleasure on the subject of hurricanes and storm surges and learned a lot about these huge weather systems and massive amounts of water that are involved. I had a great time!

This project has proven the value of good advice and support. I would like to thank all the members of the large group of supervisors! Your different backgrounds gave me a broad view on the topic and brought up many different issues and good suggestions. Pieter, I would like to thank you for your enthusiasm and support, the thorough feedback and the fact that the door that was always open. Wenlong, thank you for letting me into the world of you storm surge model and especially for your endless efforts and patience to help me manage with the model. Suzanne your questions and focus on the scientific quality of this thesis is really appreciated. Henk, thank your for being a solid mathematical corner stone of my project. Mathijs, thank you for your engagement to my project. Your help in finding sources and telling me about your experiences in New Orleans really helped me. Jan, thank you for relating my project to practice and the use for coastal managers. Finally, Pieter again, thank you for informing me about this project and luring me away from another graduation project I was already accepted for. I have never ever regretted the choice for this project.

Furthermore, I would like to express my sincere gratitude towards Jorin and Sander, who were willing to read all the pages of my thesis and help me with writing a readable thesis.

Last but not least, I would like to thank family and friends for their support and great time at the university.

Leonie Straatsma
Enschede, July 4, 2015

Contents

Chapter 1

Introduction

Hurricane induced storm surges are a major threat to the low-lying city of New Orleans. Half of the city lies below sea level and high water levels cause a real threat. This was illustrated in 2005, when hurricane Katrina made landfall in New Orleans. Half of the city flooded causing a lot of damage and casualties. However, tropical storms making landfall in New Orleans are rather a norm than an exception. Each year several tropical storms cause high waters levels along the coasts of the Gulf of Mexico. Better understanding of the processes causing these high water levels can help to protect the city for future flooding by storms surges.

This chapter introduces the phenomenon of storm surges and explains how storm surges were predicted currently and in the past (Sections 1.1 and 1.2). Some surge predictions show a lack of understanding of the processes of a storm surge. This results in the objective of this study (Section 1.3). Research questions and a research plan are presented next (Sections 1.4 and 1.5). Finally an outline of this report is given (Section 1.6).

1.1 Storm surges

Storm surges are flood-like phenomena which are caused by a storm. In the case of New Orleans these storms are tropical cyclones which are formed at the Atlantic Ocean or the Gulf of Mexico. Under certain conditions the cyclone develops such high wind speeds (over 33 m/s) that it is called a hurricane and given a name. Hurricanes cause several hazards for people and environment, both directly and indirectly. Directly, as the storm causes high wind speeds, wind gusts and a lot of rainfall. Indirectly, due to the creation of a storm surge causing flooding in unprotected coastal areas.

Low pressure at the sea surface and high velocity winds are the main drivers of the storm surge. A storm surge is basically a volume of water pushed towards the shore by the wind swirling around the moving depression. Together with other processes along the coast, such as the tides and waves, it generates the water levels at the coast which can be up to 8 m higher than normal.

1.2 Prediction of storm surges

In the past, storm surges have caused a lot of damage over the world. Well known cases are the North Sea surge of February 1953 and the surge at Galveston, Texas

*Table 1.1: Saffir-Simpson hurricane scale (1974) and how hurricane Katrina (at landfall)
fits within this scale (orange)*

Saffir-Simpson category	Central pressure [mbar]	Max wind speed [m/s]	Storm surge [m]
1	980	33.0 - 42.5	1.2 - 1.5
2	965 - 979	42.9 - 49.2	1.8 - 2.4
3	945 - 964	49.6 - 58.1	2.7 - 3.7
4	920 - 944	58.6 - 69 3	4.0 - 5.5
5	< 920	> 69.3	> 5.5

(400 km west of New Orleans) in September 1900 (Pugh, 1987) and recently the surge of hurricane Katrina. The storm surge caused by hurricane Katrina in 2005 resulted in higher water levels than expected prior to landfall; this is one of the motivations behind this research.

Historically, the Saffir-Simpson scale (Simpson, 1974) has often been applied as an indicator of the storm impact (see Table 1.1). The Saffir-Simpson scale is based on hurricane intensity, where the central pressure of the hurricane and the wind speeds give an indication for the expected storm surge. Based on the Saffir-Simpson scale, various studies on storm surges have been conducted. These studies include parameters as bottom slope (Harris, 1959), landfall location, forward speed and direction (Weisberg and Zheng, 2006). All these studies emphasize storm intensity as the main factor for the predicted storm surge. However, there are still too many exceptions to fit the scale. Irish et al. (2008) pointed out that, while the Saffir-Simpson scale has historically proved an adequate categorization of hurricane damages, it could not predict the storm surge of hurricane Katrina. Irish et al. (2008) stress that it is a misconception not considering storm size (measured as radius between storm centre and location of maximum wind speed) as an important factor regarding to storm surge generation. Indeed, the size of hurricane Katrina was large compared with other severe hurricanes that were higher on the scale of Saffir-Simpson. So, besides pressure, storm size is an important parameter as well. Including the storm size would have predicted more realistic storm surges.

Surge levels of hurricane Katrina were the most extreme in years. New water defence measures were designed based on extensive probability studies (Cobell et al., 2013). However, a few years after hurricane Katrina a smaller storm in sense of hurricane category (Isaac in 2012, category 1) caused even higher water levels at some locations along the coast of New Orleans (Figure 1.1). So, despite the lower intensity and the smaller storm size, the water levels still exceeded the forecasts of the storm surge. This emphasizes the strong variations in surge response and that other parameters could be important as well.

Furthermore, it is observed by Van Ledden (personal communication) that the storm surge of hurricane Katrina has some remarkable properties. In AD-CIRC simulations of the storm surge (Westerink et al., 2005) it seems that the storm surge 'bounces' from the Mississippi river dikes to the opposite shore (yellow dashed lines in Figure 1.1), crossing the path of the hurricane. This bouncing could indicate that some processes of a storm surge can lead to even more variation in observed water levels.
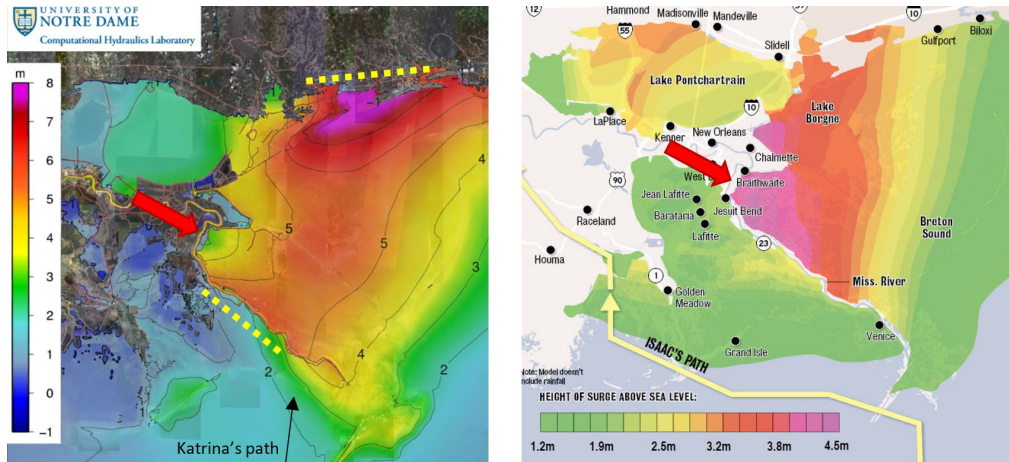
Figure 1.1: Maximum storm surge of hurricane Katrina (left)(Westerink et al., 2005) and tropical storm Isaac (right)(The Times-Picayune, 2014). The location of the red arrow shows the point where the surge of hurricane Isaac is higher than the surge of Katrina. Yellow dashed lines represent the coastal zones where the surge of Katrina is observed to have a 'bouncing effect'. Please note the different scales on the colour bars!

In this research I will endeavour to assess and explain the processes leading to the differences observed at different places along the coast of New Orleans of the succeeding events.

1.3 Research objective

The current storm surge prediction methods are able to explain some of the observed water levels in the New Orleanscoastal basin. Nevertheless, these models do not provide sufficient insight in the processes. Each storm creates a different storm surge and different processes seem to interact causing temporal and spatial differences in surge response. Many previous studies are focussed on straight coastlines and storms with straight storm paths. This may imply that processes in the semi enclosed basin of New Orleanscould affect the storm surge in a different way than found in literature. The research objective of this study is:

> "To assess and explain the spatial and temporal patterns of surge response variations inside the semi-enclosed basin of New Orleans depending on storm characteristics, by idealized process-based modelling."

This study will be conducted using an idealized storm surge model (Chen, 2014) which computes the hydrodynamic behaviour of the storm surge. The model is forced by characteristic storm scenarios. These scenarios are parametrized by central pressure, storm size, Holland-B parameter, forward speed, landfall location and storm direction.

1.4 Research questions

The following research questions are formulated to achieve the research goal:

1. How can the domain, parameters, forcing and boundary conditions of the idealized storm surge model be formulated to calculate the storm surges at the coasts of New Orleans?

2. How does the idealized storm surge model behave and perform when applied to a realistic case study?

3. What is the sensitivity of the storm surge response to storm parameters?

4. How can the (characteristic) storm surge response be explained?

1.5   Methodology

To answer the research question and achieve the goal, the following methodology is used:

- First an analyses of the study area will be made. The New Orleans coastal basin is a big and dynamic basin. Sufficient background knowledge is necessary for studying storm surges.

- An overview of the development of a storm surge is made, starting with the meteorological processes originating at the Atlantic Ocean and the formation of a hurricane. Secondly, the hydrodynamical processes are described which are involved when the storm surge comes to shore. A selection of processes will be incorporated in the model.

- Then, water level data and meteorological data of hurricanes for the New Orleans coastal basin and bathymetric data of the Gulf of Mexico are collected. Based on availability of meteorological and water level data, representative hurricanes are selected for assessing model performance and sensitivity. Data processing and preparation will be done before data are used as basis for the idealized model.

- The idealized process-based storm surge model of Chen (2014) will be used to calculate the storm surges. It uses the Holland model (1980) to describe the pressure and wind fields of a tropical cyclone. Six storm parameters will be the input; central pressure (P_c), radius to maximum wind speed (R_{max}), Holland-B parameter (B), forward velocity (C_f), location of the origin $(x,y)_{origin}$ and track (ϕ) of the storm.

- Next, an appropriate domain size will be selected. The size of the domain will be based on the selected processes from step 2. Domain boundaries conditions will be specified to allow or prevent water to flow in and out of the domain. Bathymetry will be an idealized representation of the continental shelf and the deep part of the Gulf of Mexico.

- Assessing model performance and behaviour of the idealized model will be done using historical data, both meteorological and hydrodynamical. Model performance will be judged with hindcast of historical storms (base cases) using the maximum water level, timing of the maximum water level and the hydrographs of the total surge. Model behaviour will be investigated by systematically varying input parameters and comparing the outcome with the base cases. Some adaptation to the model set-up can be necessary as well.

- With the tested model a sensitivity study to storm surge response will be conducted by systematically varying the storm parameters. These combinations of storm parameters will be described in different storm scenarios relevant for the New Orleans area. The impact on the surge response will be analysed by for the different parameters using the same indicators as for the model sensitivity, complemented with the amplitude spectra of the Fourier modes. To study the water levels and amplitudes, six locations are chosen which are previously selected as interesting points.

- Based on the found surge responses, these results of the water levels and elevation amplitude spectra will be interpreted and explained by linking them to physical processes present in the New Orleanscoastal basin.

1.6 Report outline

The report is structured as described below. A summary is given at the end of each chapter listing the main points of that chapter.

Chapter 2: Storm processes around New Orleans This chapter provides some basic knowledge about the New Orleansarea. Secondly, it gives an overview of the development of a storm in the New Orleansarea. It also explains the processes leading to the observed storm surge of a hurricane at the coasts of New Orleans.

Chapter 3: Model set-up This chapter covers the building and testing of the model. Assumptions and model choices are explained. The first research question is answered in this chapter.

Chapter 4: Model performance and behaviour Assessing the model performance for a realistic case study and investigating model behaviour is reported in this chapter, addressing the second research question.

Chapter 5: Sensitivity analysis and physical interpretation This chapter covers the sensitivity study of surge response, beginning with a selection of the storm scenarios. The sensitivity to storm parameters is presented in several figures and tables giving an objective overview. The physics behind the found characteristic surge responses is explained as well. This chapter answers research questions three and four.

Chapter 6: Discussion This chapter forms the discussion about the limitations of the chosen approach. Also the model input and the implications of excluding certain processes are discussed.

Chapter 7: Conclusion and Recommendations This final chapter covers a summarized conclusion for the different research questions. Finally, recommendations for further research are presented.

Chapter 2

Storm processes around New Orleans

The New Orleans coastal area is a large area which is prone to hurricanes. As this research is focussed on New Orleans and the surrounding waters, this chapter provides some background information about historic storms which have made landfall in the vicinity of New Orleans (Section 2.1).

These hurricanes generate storm surges when making landfall. Therefore the final parts of this chapter explain the development of storm surges. In Section 2.2 the development of a storm in the New Orleans area is described. Followed by Section 2.3, where the effect of this meteorological system on the water movements in the Gulf of Mexicois described.

2.1 New Orleans area

The New Orleans area is a complex system of many water bodies and swamps and it is a major economical centre for the state of Louisiana as well. This section provides more information about this area and gives an impression of orders of magnitude (km and m surge etc.) for the remainder of this report.

2.1.1 New Orleans

New Orleans is a major city situated at the north coast of the Gulf of Mexico, located at 29°N latitude in the Northern Hemisphere. The port of New Orleans is one of the major ports of the United states. It forms the largest city of the state Louisiana and is an important economic centre.

In 2012 the population was about 340.000, but the whole metropolitan area of New Orleans populated roughly 1.2 million inhabitants. This number is significantly smaller than before hurricane Katrina in 2005. Many houses and public places were destroyed which resulted in many people moving from the city (Population Division, 2012) .

The city is forced to take good care of their water management because only 51% of the city is at or above the sea level. The lowest points of the city even reach 6 m below the sea level (Williams, 2007). Therefore, flooding due to storms forms a major threat for the city. This threat is even more alarming because of the long evacuation times of New Orleans that are caused by the lack of major highways and the dense population (Roth, 2010).
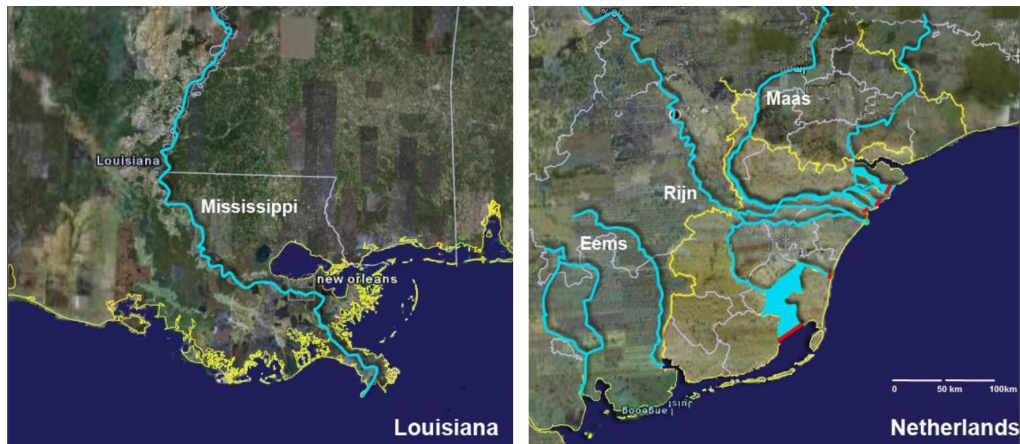
*Figure 2.1: Size of the Mississippi delta (left) compared with The Netherlands (right).
Note that both images have the same scale (Dijkman, 2007).*

2.1.2   Mississippi river delta

The city of New Orleans is located in the south east of Louisiana, straddling the
Mississippi river. It is built on both sides of the banks of the Mississippi, 169 km
away from the mouth at the Gulf of Mexico. Even though this is upriver, the
city still belongs to the Mississippi river delta. This 7th largest delta on earth
has been formed over the last 7000 years. As can be inferred from the shape
of the coastline, this delta is a river-dominated system. The delta is formed by
the deposited sand, clay and silt from the largest river of North America. In the
past extensive coastal wetlands covering more than 11.000 km^2 were formed in
the delta. To give an indication of the large scale of this river delta, Figure 2.1
shows the Mississippi delta compared with The Netherlands (both images have
the same scale!).

The Mississippi River nowadays flows along a ridge formed by its own nat-
ural deposits creating a natural levee system. Throughout the history the delta
experienced natural growth and shrinkage as a result of variations in sediment
deposition. Therefore the water depth in the delta is very limited and in large
sections not even reaching below 2 m. A detailed map of the water depth can
be seen in Figure 2.2. Unfortunately, the levee system, navigation channels and
other structures upstream in the Mississippi river prevent the natural deposition
of sediments resulting in the erosion of the delta and wetlands. It is estimated
that Louisiana has lost about 5000 km^2 of land since the beginning of the 20th
century (Barras, 2005). This increases the risk of flooding. The coastal erosion
increases salt water intrusion from the Gulf of Mexico into the coastal wetlands.
This intrusion weakens the ecosystem and makes it vulnerable to destruction
by hurricanes and unable to withstand heavy storm surges. For example after
hurricanes Katrina and Rita in 2005, 520 km^2 of wetlands was lost and became
open water (Barras, 2005).

2.1.3   Storms around New Orleans

The location of New Orleans in the Gulf of Mexico makes it prone to hurricanes.
On average, ten tropical storms are formed in the North Atlantic annually. Some
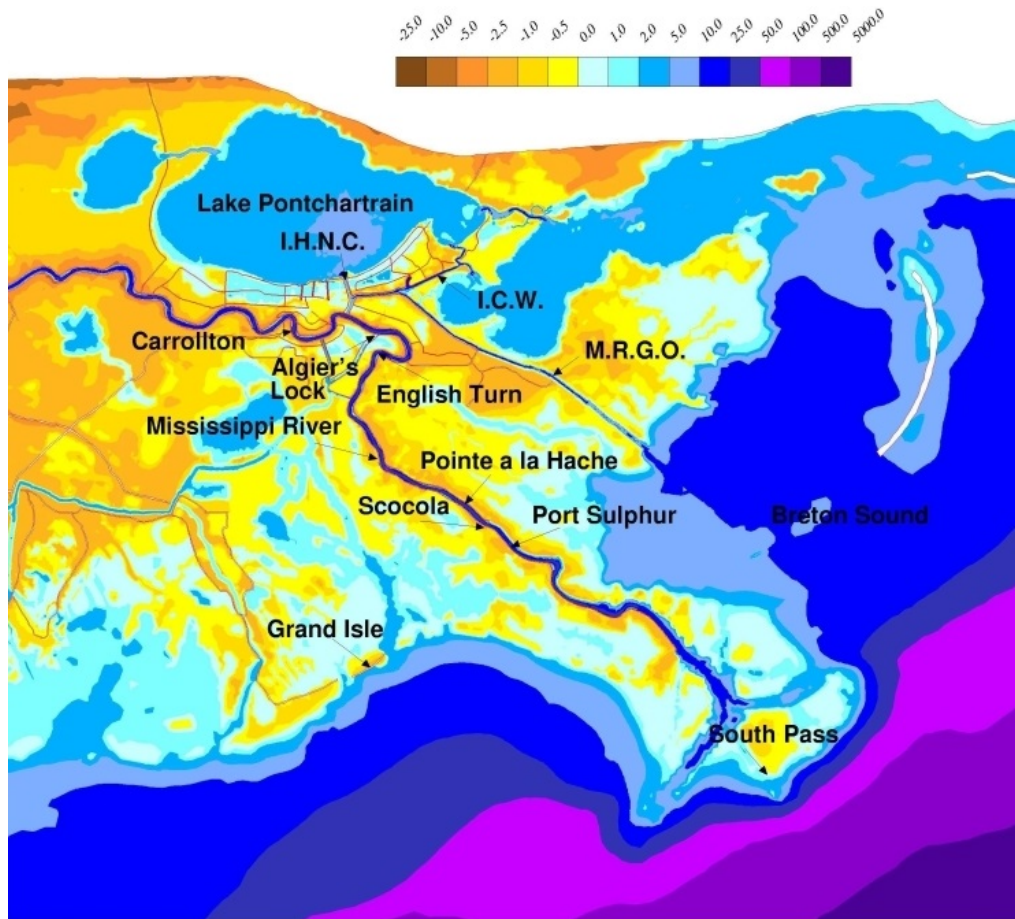of these storms make landfall causing enormous damages.

Figure 2.2: Bathymetry of New Orleans (Westerink et al., 2005)

Historical storms

Since the city of New Orleans was established in the 18th century nearly 52 hurricanes made landfall in or near the city. Several historical hurricanes are listed in Section 2.1.3. Twenty other not-named hurricanes have made landfall in New Orleans before 1964, but those are left out of the table. The three largest storms in terms of their storm surge levels are Betsy (1965), Camille (1969) and recently Katrina in 2005. As can be seen, the three largest storms in essence differ strongly, especially regarding the size and the Saffir-Simpson category, but their surges were comparable. Those storms are briefly described below.

Hurricane Betsy (1965) came to land at Grand Isle with wind gusts of 160 mph (258 km/h). The island was completely flooded by the surge of 4 m and many oil rigs and public utilities were severely damaged (Fitzpatrick, 1999). When the storm hit the city of New Orleans still wind gusts of 135 mph were measured and a surge of 3 m was recorded. The hurricane caused 81 casualties and the damage was up to 1.4 billion US$.

Hurricane Camille (1969) was one of the three hurricanes of category 5 that made landfall during the 20th century. The hurricane had a relatively small size. However, the wind gusts were severe and a wind speed of 201 mph was measured. The storm caused massive flooding and landslides in Louisiana. Damage was suffered in a much bigger area as the hurricane

Table 2.1: Historical hurricanes making landfall in New Orleans (characteristics are at moment of landfall). Missing values could not be obtained from used sources (National Weather Service, 2014; U.S. Army Corps of Engineers, 2006).

Storm name (year)	Central pressure [mb]	Storm size* [km]	Saffir-Simpson category [-]	Observed storm surge [m]
Hilda (1964)	960	39	3	2.3 - 3.0
Betsy (1965)	945	74	3	4.1 - 4.8
Camille (1969)	910	22	5	6.4 - 6.9
Babe (1977)	995	-	1	1.5
Bob (1979)	986	-	1	1.5
Elena (1985)	959	-	3	3
Juan (1985)	975	-	1	1.5 - 2.4
Danny (1997)	990	-	1	1.2 - 1.8
Cindy (2005)	991	-	1	1.2 - 1.8
Katrina (2005)	919	47	3	7.5 - 8.5
Gustav (2008)	954	-	2	4.5
Isaac (2012)	965	-	1	2.5 - 3.4

*radius from hurricanes centre to location of highest wind speed.

travelled further inland. In total 355 people died, which is remarkably low given this extremely violent storm. An early warning system and the success of evacuation worked and there were no casualties among the thousands of offshore oil workers. The total damage is estimated at 11 billion US$.

Hurricane Katrina (2005) was one of the worst natural disasters of the US history. Despite being classified as only a category 3 storm, surge levels were much higher than could be deduced from the Saffir-Simpson scale. Computer models made forecasts predicting a surge of 15 to 20 feet (4.5-6 m). However, when the hurricane made landfall Katrina produced a surge as high as 27 feet (8.2 m). The storm and the surge levels caused many breaches in the 350 mile levee system surrounding the city. In a total of 18 hours 80% of the city flooded 6-20 feet (2-6m) (Homeland security Council, 2006). The storm caused 1836 casualties and a total damage of 120 billion US$ in the whole US.

Hurricane season

Each year several cyclonic storms are formed on the Atlantic Ocean during the hurricane season. According to the National Oceanic and Atmospheric Administration (NOAA) the official hurricane season is between the first of June and the 30th of November, with a peak in hurricane activity in the period between mid-August until mid-October. During the season an average of 10 tropical storms is formed above the Gulf of Mexico, the Caribbean Sea or the Atlantic Ocean. In 2-3 year time 5 hurricanes make landfall in the US, two of which are severe hurricanes (category 3-5). Since 1851 a total of 75 hurricanes of Katrina's landfall strength (category 3) hit the mainland of the US.
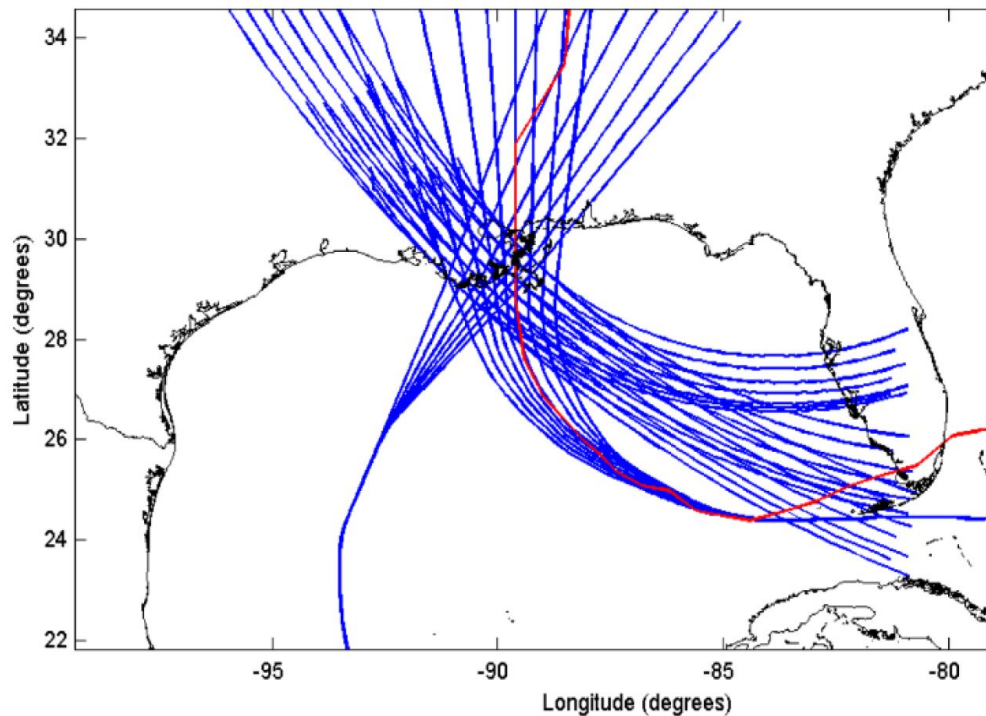
Figure 2.3: 34 Hypothetical storm tracks (blue) making landfall in the vicinity of New Orleans, including the track of hurricane Katrina (red) (U.S. Army Corps of Engineers, 2008a).

Hurricane tracks

Despite hurricane Katrina being the most memorable in face of the destruction, the track of Katrina is far from unique. All hurricanes making landfall near New Orleans are formed near the Gulf of Mexico and the Atlantic Ocean. Because of the Coriolis force and general wind patterns on the earth, the paths of hurricanes have 3 general directions. U.S. Army Corps of Engineers (2008a) used these three, complemented with a fourth path, in their study to create 34 hypothetical hurricane paths Figure 2.3. The fourth path, however, was only different far away from the landfall location and lined up with the other directions close to the shore. These tracks are a good representation of the hurricane activity near New Orleans.

2.2 Hurricane development

Storm surges are driven by meteorological processes. Low pressure weather systems can bring the water of the oceans into motion. These meteorological processes can cause a variety of storms. Because this study is focussed on the Gulf of Mexico, a storm is defined as a severe cyclonic wind storm ranging from tropical storm to a hurricane. Additionally, this section will only describe the formation of tropical storms rather than extratropical and subtropical storms and depressions. This difference is important because tropical storms have the potential to quickly develop into hurricanes while the latter two do not (Weather Underground, 2014). Because of their nature, extratropical and subtropical storms will not occur in the Gulf of Mexico.

The development of a hurricane starts with a low pressure area above a tropical sea or ocean. First it forms a tropical depression, then a tropical storm which may develop into a hurricane. In the development of a cyclonic storm many processes are happening at the same time. These processes, schematized in Figures 2.4 and 2.5, are explained below.

2.2.1 Meteorological processes

All cyclonic storms start with a low pressure area above a water surface. Disturbances over the Atlantic Ocean form the origin for the storms in the New Orleans area. The prevailing wind blowing over this ocean is directed from Central Africa to the west. When the water in the ocean is warm enough (over 26°C) and a constant wind is present, a tropical storm can develop. Wind blowing over the surface of the warm ocean induces evaporation at the ocean's surface (Figure 2.4, process 1). The warm humid air rises (2) and condensates in the atmosphere forming clouds (3) and releasing latent heat warming the air around (4). Hot air will rise further up and as the wind keeps evaporating sea water it generates more warm air pulling up the clouds and forming a column of clouds in the centre of the depression (5) (National Weather Service, 2014).

As the column increases to go higher and higher, a high pressure area forms on top of the cloud column and wind starts blowing from this high pressure to the surrounding area with lower pressure (see the red arrows in Figure 2.5). In the Northern Hemisphere those winds will bend to the right because of the geostrophic winds around a high pressure area combined with the Coriolis force. The cooled air flows to the outer boundaries of the storm and can fall down to the sea surface again. At the same time the rising warm air causes a pressure drop at the sea surface underneath the cloud column in the eye of the storm. This generates winds at the sea surface towards the centre of this low pressure area. Due to the Coriolis force these winds circulate in a counterclockwise direction around the low pressure area (see green arrows Figure 2.5), so in the opposite direction compared with the overcast. The rising air inside the centre of the storm creates the eye of the storm rotating in the counterclockwise direction as well.

The continuous supply of air at the sea surface moving towards the centre creates more and more clouds. Around the storm's eye rain bands form with the same circulating properties. These are bands of thunderstorms often accompanied with heavy rainfall and gusty winds. When a tropical depression is above an ocean with warm water for a longer time, the continuous evaporation at the sea surface makes the hurricane's eye start spinning faster and faster. When wind
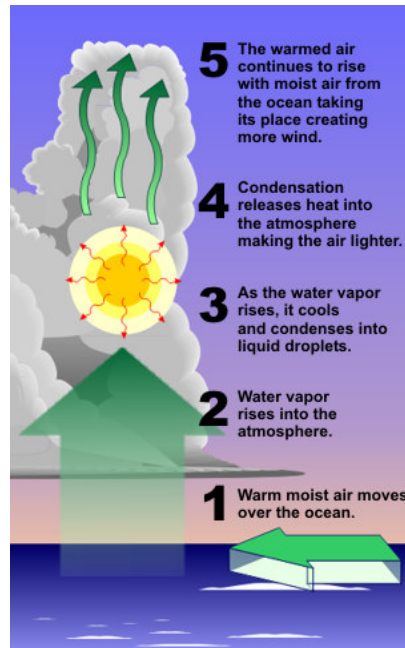
Figure 2.4: Initial development of a column of clouds, the starting point for a tropical storm (National Weather Service, 2014).
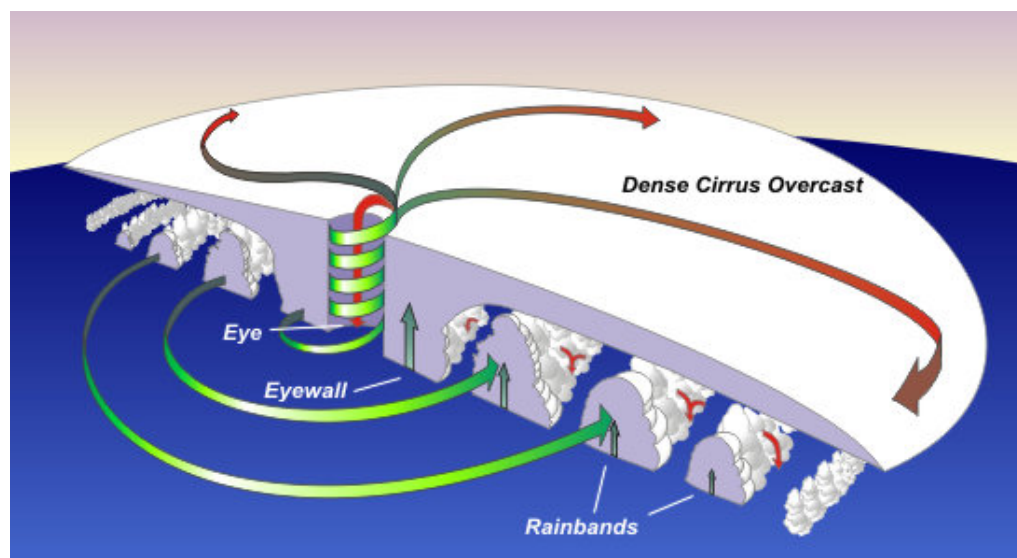

Figure 2.5: Wind structure and cloud of a tropical cyclone (National Weather Service, 2014).

speeds reach 39 mph (17 m/s) the depression is termed a tropical storm and it is given a name. If a tropical storm remains over warm water for a long enough period, the core temperature will become warmer and wind speed increases even more. The thunderstorm activities will then come closer to the centre and when wind speeds exceed 74 mph (33 m/s) the tropical storm is grown into a hurricane.

2.2.2   Hurricane varieties

Each tropical storm or hurricane is different. The wind speeds, pressure inside the eye, the eye's size and the amount of rain it spills over the land can all be different. Even a single storm itself is not the same over the whole lifespan. When a storm develops the size and wind speed increase, but when it makes landfall the wind speeds generally reduces due to friction by trees, houses or other objects and the absence of the hot water energy source. When the storm moves further on shore it gradually ceases to exist. Another difference are the observed wind speeds in a single hurricane; the wind speeds at the right side (in the Northern Hemisphere and viewed in the direction of forward motion) of the hurricane are higher than those on the left side. This is caused by the forward speed of the storm combined with the anti-clockwise circulation. Imagine the hurricane in Figure 2.5 moving to the top right corner of the figure. The winds at the right side of the hurricane are in the same direction as the storms movement contributing the observed velocities, while the wind at the left side of the hurricane point in the opposite of the hurricane's direction causing the observed wind speeds to be lower.

2.3   Storm surge development

When large amounts of water travel to the shore other factors such as bottom slope and angle of approach become important.

Hurricanes cause several hazards such as the high wind speeds, wind gusts and a lot of rain. Still, in coastal areas the storm surge caused by the hurricane is one of the biggest concerns. A storm surge can cause enormous floods. The low pressure at the sea surface and the high velocity winds are the main drivers of the storm surge. A storm surge is basically water sucked up by the low pressure and pushed towards the shore by the force of the wind swirling around the storm.

A storm surge is influenced by for instance, the geography and a variety of different physical processes. Furthermore, it is found that large scale effects due to the geometry of the Gulf of Mexico contribute to the surge as well. Along with four other processes these create the final observed storm surge along the coasts. These processes create the total water level observed at the coast are schematized in Figure 2.6 and explained below the figure. The first two processes are described in more detail in the following sections.

Total water level

The storm surge during a hurricane is, despite being the biggest, not the only contributor to the final observed water levels along the coast during a hurricane. The total water level is built up by the following factors influencing the sea level at that specific moment. The last four are outside the scope of this research and will therefore only be shortly touched upon.
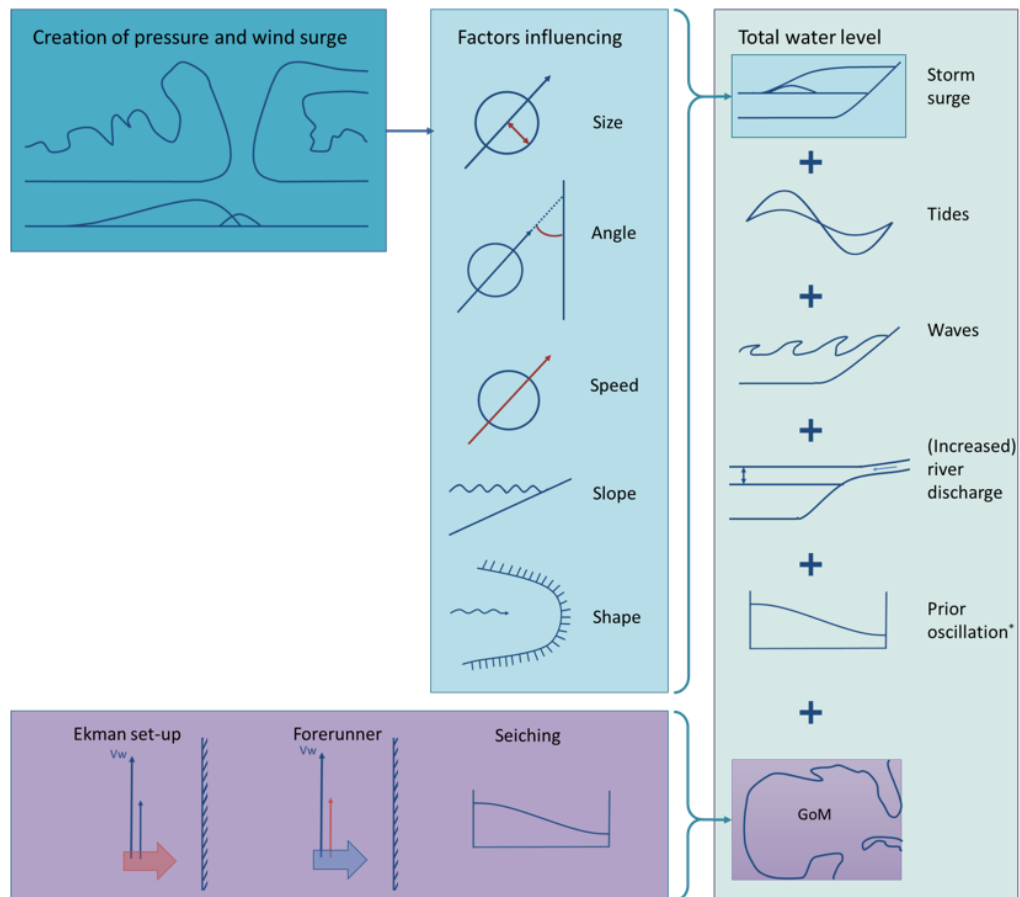
Figure 2.6: Schematic overview of storm contribution to the total water level at the coast (green, right). The storm surge is created by the pressure and wind effect (blue, left), influenced by different local factors (blue, middle). Large scale processes (purple, bottom) generate an increase in water level farther away from the storm. However these can propagate towards the location of landfall increasing the total water level as well. *Only oscillations are meant which were driven by an earlier event. So, not the oscillations caused by the storm event causing the present storm surge.

Storm surge: The direct surge of the storm (dark blue) driven by the pressure and wind field of the hurricane. The surge is influenced by many different factors (light blue), ranging from site specific properties to the storms forward speed, creating a local surge (Section 2.3.1).

Large scale processes: These processes (purple) can force the water along the coast to increase with 1 m even if the storm is several 100 km away. These processes could propagate and reach the landfall location before or during moment of landfall enhancing the effect of the storm surge (Section 2.3.2).

Tides: Every day the water levels along the coast rise and fall due to the gravitational pull of the Moon and the Sun. New Orleans experiences one high and one low tide a day (diurnal tide) with a relatively small tidal range of 0.5 m. However, tide-surge interactions make it difficult to simply add up the tidal water level and the surge water level (Bode and Hardy, 1997).

Wind waves: Near the coast wind waves increase the water level in two different ways: by wave run-up and wave set-up. Wave run-up is caused by breaking waves which spill the water onshore letting the water reach further inland. Wave set-up is caused when waves propagate towards the shoreline and increases the mean water level with a typical order of less than 0.5 m.

River discharge: Storms are generally accompanied by heavy thunderstorms in the outskirts of the storm. In a short time this excessive rainfall increases the river discharge in the region. Especially near deltas (such as the Mississippi delta) the local water levels will rise.

Prior sea level oscillations: Oscillations can occur in a water body, for example when a storm travels over a basin pushing the water against one shore (wind effect). The oscillation can remain in the basin after the storm passed. The surge of a second storm can be enlarged by these prior oscillations. When the time between the two successive storms matches the natural period of a basin resonance can occur and amplify the water level of a storm surge as observed in the North Sea by Weenink (1956). A single storm itself can also cause resonance of the water in a basin, though these oscillations do not fall in the context of the above mentioned oscillations.

2.3.1   Local processes

Local processes are processes in the direct vicinity of the hurricane. Physically the atmosphere of a storm acts on the sea in two distinct ways; i) changing vertical acting forces on the sea surface due to the atmospheric pressure changes and ii) forces generated by wind stress at and parallel to the sea surface. Although both forces can be described separately, the effect of the forces can usually not be separately identified (Pugh, 1987). While for extratropical storms the pressure effect and the wind effect are equally important, for tropical storms the wind effect is dominant resulting in much higher surge levels (see Figure 2.7).

Reduced atmospheric pressure influences the water level, which is called the inverted barometer effect (Proudman, 1953). A local low pressure area causes the water level to rise compare to the surrounding regions. The atmospheric pressure inside the eye of a hurricane can be as low as 910 mbar
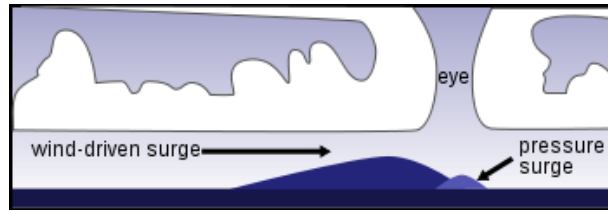
Figure 2.7: Wind-driven and pressure-driven surge of a hurricane (National Weather Service, 2014).

(Hurricane Camille, 1969) (U.S. Army Corps of Engineers, 2006). Compared to the normal ambient pressure around new Orleans (1030 mbar), the inverted barometer effect in this hurricane forces the water level to rise 1.15 m.

Wind exerts horizontal stresses at the sea surface. Energy and momentum are transferred from the more rapidly moving wind to the water layer. The wind stress brings the water into motion. Velocities of the water are highest in the top layer of the water and could reach up to 3% of the winds speed (Pugh, 1987). This results in piling up of the water at the coast (wind set-up). When a storm is travelling to shallow water the Ekman transport can also add to this wind set-up. This Ekman transport is induced by the Coriolis force and is a function of wind stress and latitude. Wind stresses induce a net transport of water with an angle due to the wind direction. In the Northern Hemisphere this transport is directed 90° to the right of the wind direction if the water depth is sufficient. However, in shallow areas the Ekman spiral cannot develop completely resulting in a smaller angle of the net transport due to the wind direction. Furthermore, due to the increased bottom friction in shallow water, turbulence increases reducing the angle even more (Pugh, 1987).

Thus, when a hurricane enters a shallower part of the oceans (continental slope) the wind-driven surge will increase while the pressure driven surge will not change.

Factors influencing the storm surge

After creation of the storm surge, several factors contribute to the height of a storm surge at each specific location. Several studies have pointed out the most important factors:

Central pressure A lower central pressure in the eye of the hurricane produces a higher surge. This can be derived from the inverted barometer effect. The central pressure is a minimal contributor compared to the other factors.

Wind speed Stronger winds circulating around the eye of a hurricane produce a higher wind set-up, resulting in an higher surge.

Storm size The storm size is measured as the radius from the hurricane's centre to the location of highest wind speed. A larger storm produces a higher storm surge (Irish et al., 2008). This is caused by two things: the winds of the storm affect a larger area of the ocean, bringing more water into

motion. Secondly, the storm affects a specific location for a longer period (because of the size it costs more time for the whole storm to pass over a certain point).

Angle of approach The angle at which the storm approaches the coastline has effect on the height of the storm surge. Storms making landfall with a big angle or perpendicular to the coast are likely to produce higher surge levels than storms with a smaller angle.

Forward speed Faster moving storms generate in general a higher storm surge. All the water of the wind-driven surge is driven to the shore in a much shorter time than when the storm is moving slower. However, when a storm is moving over a bay or another enclosed water body, slower storms create a higher surge. The fast moving storms have already moved over the bay before a wind-driven surge can be built up. So depending on geometry forward speed can both enhance and decrease a surge.

Bottom slope Higher storm surges occur where the bottom is gently sloping in contrast to steeply sloping shelves. This is particularly important for the New Orleans area because the continental shelf is very shallow and deepens gradually offshore.

Shape of coastline A storm will produce higher surges when it makes landfall on a concave coastline than on a convex coastline. In very narrow basins funnelling can cause a large amplification of the storm surge. Depending on the shape a surge could even be coastal trapped and propagate like edge waves causing enormous devastation (As-Salek, 1998).

Local features The final height of the storm surge is highly dependent on local features as for example: man-made barriers, barrier islands, wetlands or inlets. These features will affect the flow of the water and can either reduce or amplify the storm surge (Resio and Westerink, 2008).

2.3.2   Large scale processes

The large scale meteorological nature of a hurricane does not only generate a local surge at the location of landfall. In the Gulf of Mexico large shelf scale processes are observed during the hours before, during and after landfall. The Gulf of Mexico constitutes one big basin with a deep middle section and a broad continental shelf along the coasts. Together with the concave geometry around New Orleans this has led to hurricane induced surges that impacted over 1000 km of coastline. Recently more detailed studies (Hope et al., 2013; Kennedy et al., 2011) are done to hurricanes and the affected water levels within the Gulf of Mexico. These studies show processes as geostrophic set-up, forced early rise of water in coastal bays and propagation of a free wave along the shelf. These processes are most important for hurricanes with a large wind fields (over few hundreds of kms).

Geostrophic set-up A large hurricane can induce strong shore parallel currents in the Gulf of Mexico. Due to the shape of the Gulf and the counterclockwise ration of the hurricane's wind field, hurricanes from the south

east create a steady wind field along the Florida to New Orleans coast. Ekman transport induced by the steady winds causes water to pile up along the coast, creating a geostrophic set-up.

Forerunner The cross-shore barotropic pressure gradient and Coriolis acceleration in its turn force an alongshore current in the same direction as the wind. The geostrophic balance between along shelf current velocities and surface elevation can create a forerunner in the Gulf of Mexico. This propagating wave along the shelf is most significant on wide, shallow shelves and has a typical amplitude under 1 m (Kennedy et al., 2011). Forerunners are observed to propagate with an average speed of 5-6 m/s. Kennedy et al. (2011) specified the forerunner of hurricane Ike as a non-dispersive free continental shelf wave which has a sub-inertial nature. This alongshore forerunner induces an early rise of connected inland lakes and bays well before landfall which facilitates the inland surge penetration. A forerunner is also found for hurricane Katrina (Figure 2.8). The forerunners is observed along the coast from Florida to New Orleans.

Seiching Blain et al. (1994) showed that even larger scale processes are important in the Gulf of Mexico. When a hurricane suddenly enters the Gulf of Mexico resonant modes of the whole Gulf can be excited. These resonant modes may even depend on interaction between the Gulf and contiguous basins. The large scale seiching modes could have amplitudes of several tens of cm (Kennedy et al., 2011).

2.4 Summary

The city of New Orleans is very vulnerable to storm surges; half of the city lies below sea level making it prone to flood caused by the storm surges. The dense population and lack of major highways increase evacuation times, resulting in an even bigger risk for the population. Erosion of the Mississippi delta increases the risks of flooding even more. Roughly five hurricanes make landfall in the US every 2-3 years. For these hurricanes roughly three different paths can be differentiated.

Hurricanes develop from a low pressure weather system at the Atlantic Ocean. The pressure in the centre of the hurricane is low and increases toward the outer boundaries of the hurricane. On the contrary, wind velocities are highest at the edge of the hurricane's eye and decrease further from its centre.

Local processes underneath the hurricane induce a pressure-driven and wind-driven surge that are influenced by the local bathymetry and geometry of the shoreline. Large scale processes on the other hand, create a rise of water levels at locations far away from the hurricanes centre. This can generate a forerunner propagating towards the location of landfall. Combined with the wind- and pressure-driven surge this results in an additional rise of water level.
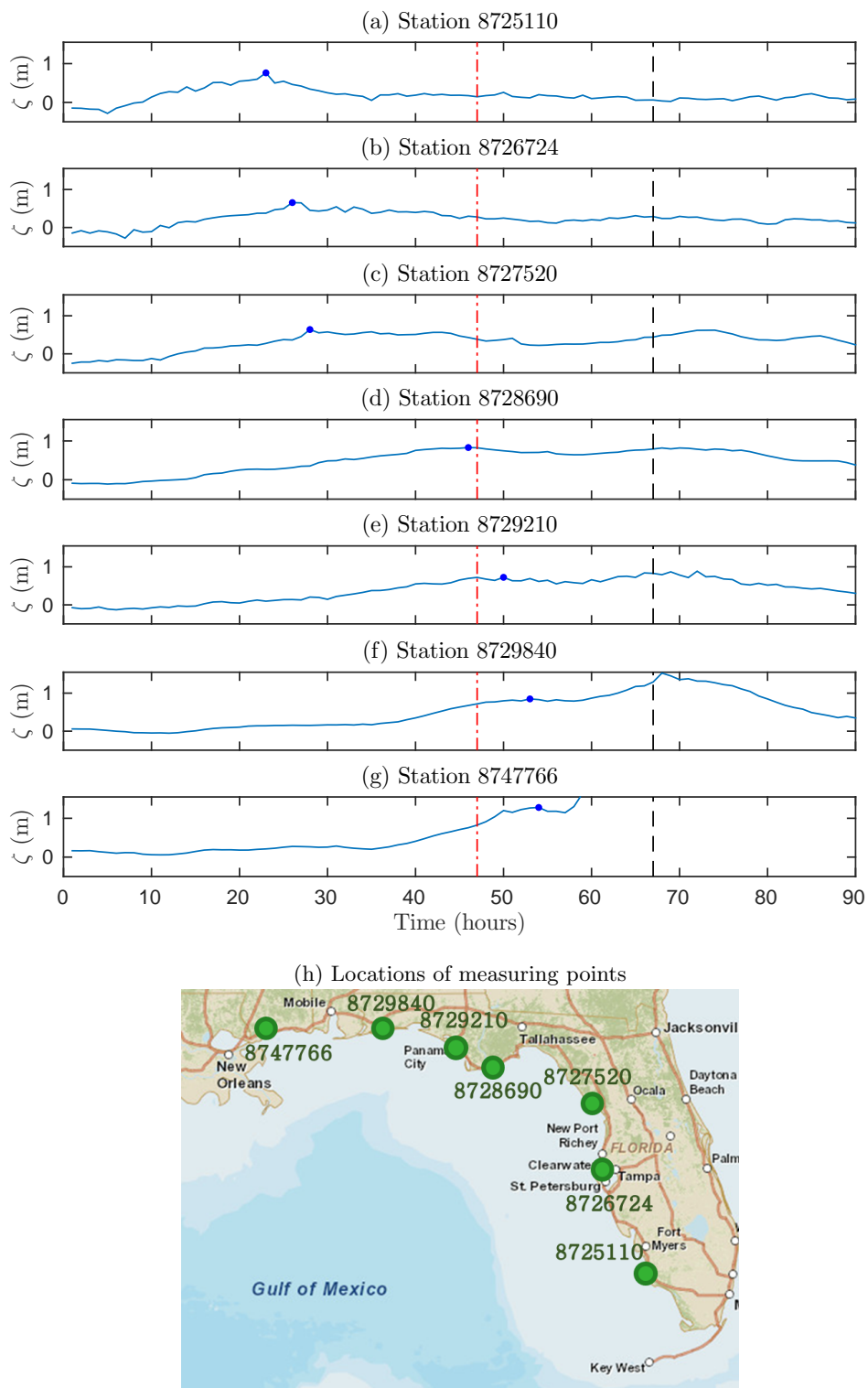
Figure 2.8: *The forerunner of hurricane Katrina. (a-g) Water surface anomaly over time as observed along the coast (observed water levels excluding tides (National Oceanic and Atmospheric Administration (NOAA), 2015)). A forerunner can be observed when comparing all highest water levels (blue points) from the top to the bottom. The maximum surge travels from southern point of Florida to New Orleans. Vertical lines indicate time of landfall (black) and 20 hours prior to landfall (red). (h) The locations of water level measurements a-g.*

Chapter 3

Model set-up

The model used in this study is the newly developed storm surge model by Chen (2014). The model is developed for his PhD project at the University of Twente.

This semi-analytical storm surge model is developed to cope with large computer demands which arise when one would like to make a systematic analysis of storm surge response. The model calculates three-dimensional flow, including Coriolis effects and bottom friction, forced by a time-periodic wind stresses and pressure gradients.

The idealized model combines a temporal Fourier transformation and the Finite Element Method (FEM). This can be used to gain insight in the dominant processes of a storm surge because the Fourier transformation makes it possible to assess the surge reaction to each of the corresponding modes (Chen, 2014).

The model consists of two parts: a meteorological model and a hydrodynamical model. The meteorological model generates input for the hydrodynamical model through wind stress and atmospheric pressure gradients. The model is schematically visualized in Figure 3.1.

This chapter presents successively the meteorological and hydrodynamical parts of the model. Then the implementation of the model for this specific study is presented (Section 3.3). This chapter answers research question one.

3.1 Meteorological part

The meteorological part of the model generates the forcing for the hydrodynamical part. The atmospheric pressure field of a storm and the movement of the storm is described by the Holland-B model (Holland, 1980). This parametric pressure model is a simplification and thus an approximation of the pressure field of a real storm. Wind is a result of pressure gradients and can therefore be determined using the approximated pressure field of the storm.

3.1.1 Pressure field

Despite the complexity of a hurricane's pressure field, it is found that this field can be well represented by a relatively small set of parameters, primarily the storm intensity, storm size, peakedness and forward speed (Resio and Westerink, 2008). Using the Holland storm model ((Holland, 1980)), these four parameters, along with the angle and landfall location of the hurricane prescribe a specific pressure field for a moving hurricane at each moment in time. The following six
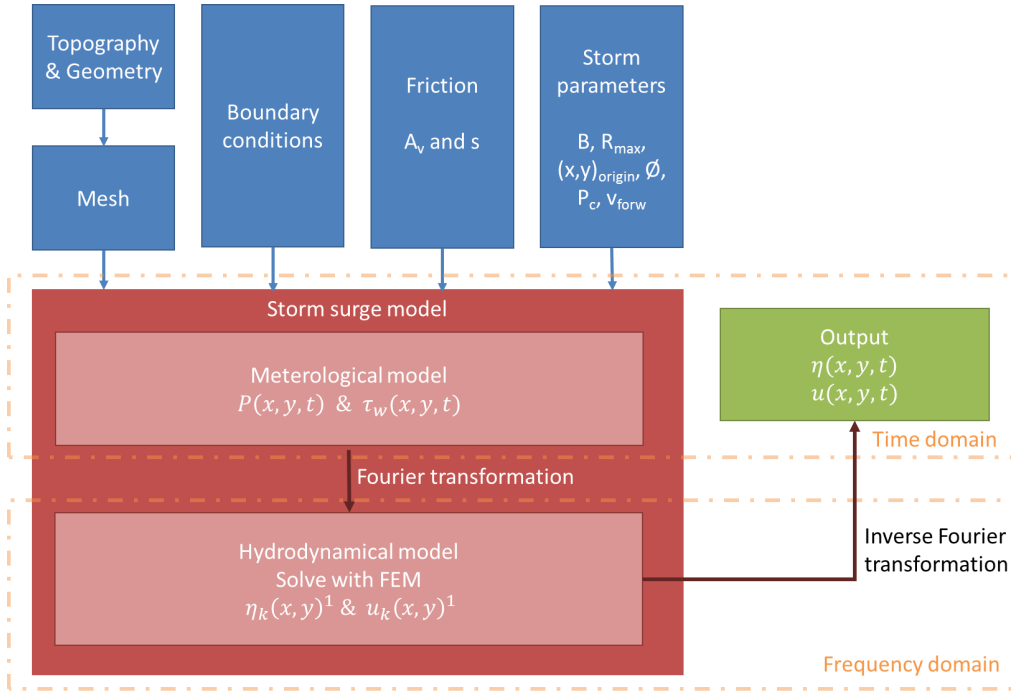
Figure 3.1: Schematic representation of the idealized storm surge model by Chen et al. (2014). η_k and u_k are the complex amplitudes of respectively surface elevation and velocity at frequency ω_k.

input parameters (storm parameters) are specified for the model to generate the pressure field:

- Central pressure, P_c [Pa];

- Radius to maximum winds, R_{max} [m];

- Holland-B parameter, B [-];

- Forward velocity of storms centre, C_f [m/s];

- Point of origin, $(x, y)_{origin}$;

- Storm direction, ϕ [°].

Holland model

The parametric pressure model by Holland (1980) uses the six parameters to generate a wind- and pressure-field of a hurricane. It is specifically useful for tropical storms. These storms have no front and their pressure field has a circular shape. The pressure field can therefore be described by the radial distance from the hurricane's centre with the following relation:

$$P = P_c + (P_n - P_c) \exp\left(-\left(\frac{R_{max}}{r}\right)^B\right) \qquad (3.1)$$

Here, r is the radial distance from the hurricane's centre, P is the atmospheric pressure as function of r and P_n is the ambient atmospheric pressure and other

parameters are as described above. Input for the model is reduced by assuming constant ambient pressure of 1030 mbar (consistent with the New Orleansarea).

The Holland-B parameter (B) and the radius to maximum wind speed (R_{max}) determine the shape of the radial pressure profile in the hurricane. Hence, using the gradient wind equations the wind profile can be derived from the pressure profile (Holland, 1980). The influence of the Holland-B parameter on both pressure and wind profiles with a given R_{max} can be seen in Figure 3.2. As can be seen, the bigger the value of the Holland-B parameter, the steeper the pressure profile at the R_{max} of 20 km and the higher the wind speeds at that location.
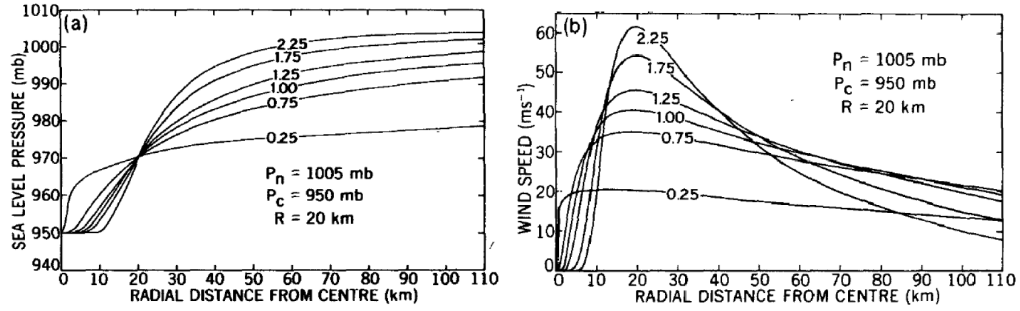

Figure 3.2: The effect of varying the Holland-B parameter on (a) pressure profile and (b) the gradient wind profile (Holland, 1980).

3.1.2   Wind field

The wind field is derived using the pressure field. It is modelled as a so-called gradient wind. The forward movement of the storm and friction influence both wind direction and speed. How the wind field is calculated is explained below.

Forward speed of the storm

Although the wind profile can be derived from the pressure profiles, for a moving cyclonic storm this derivation is more complicated than for a non-moving storm. As described in Section 2.2, observed wind velocities at the east side of a moving storm are higher than at the left side. The forward speed of the hurricane and the wind velocities are enhancing each other while at the west side of the hurricane the opposite happens. Therefore the wind velocities are calculated using Chen (2014):

$$V_w = \frac{2}{3}\left(-W + \sqrt{W^2 + \frac{(P_n - P_c)B}{\rho_a}\left(\frac{R_{max}}{r}\right)^B \exp\left(-\left(\frac{R_{max}}{r}\right)^B\right)}\right) \quad (3.2)$$

with $W = \dfrac{C_f \sin \kappa - rf}{2}$ in which V_w denotes the wind speed (m/s), ρ_a air density (kg/m^3), $f = 2\Omega \sin \varphi$ the Coriolis parameter and ξ the angle (°) between the storm track and the vector from the storm centre towards the point of interest.

Surface friction

Gradient wind blows parallel to the pressure isobars. However, the actual wind at the sea surface is influenced by friction. The wind speed decreases and direction

slightly changes. To correct the wind speeds, Brunt (1934) derived the following equation:

$$V_s = V_g(\sin\beta - \cos\beta) \approx \frac{2}{3}V_g \tag{3.3}$$

Where V_s is the surface wind (m/s) at 10m above the surface and β the deflection of the surface wind towards the storm's centre. With a value of $\beta = 17°$ (as used by Jong (2012)) this results in a ratio of 2/3 as seen in Equation (3.2).

Wind stresses

Finally the wind stresses acting on the water surface are computed using:

$$\vec{T_w} = C_d\rho_a \left|\vec{V_w}\right|\vec{V_w} \tag{3.4}$$

where $\vec{T_w} = (T_{w,x}, T_{w,y}), \vec{V_w} = (V_{w,x}, V_{w,y},)$ and C_d the dimensionless drag coefficient ($= 2.54\mathrm{e}^{-3}$)[1].

Altogether, the meteorological part generates the pressure and wind stresses as function of time and space. The wind stress is used as the surface boundary condition at z=0 and the pressure as input variable for the calculations. Both the pressure field and wind field of a hurricane can be seen in Figure 3.2.
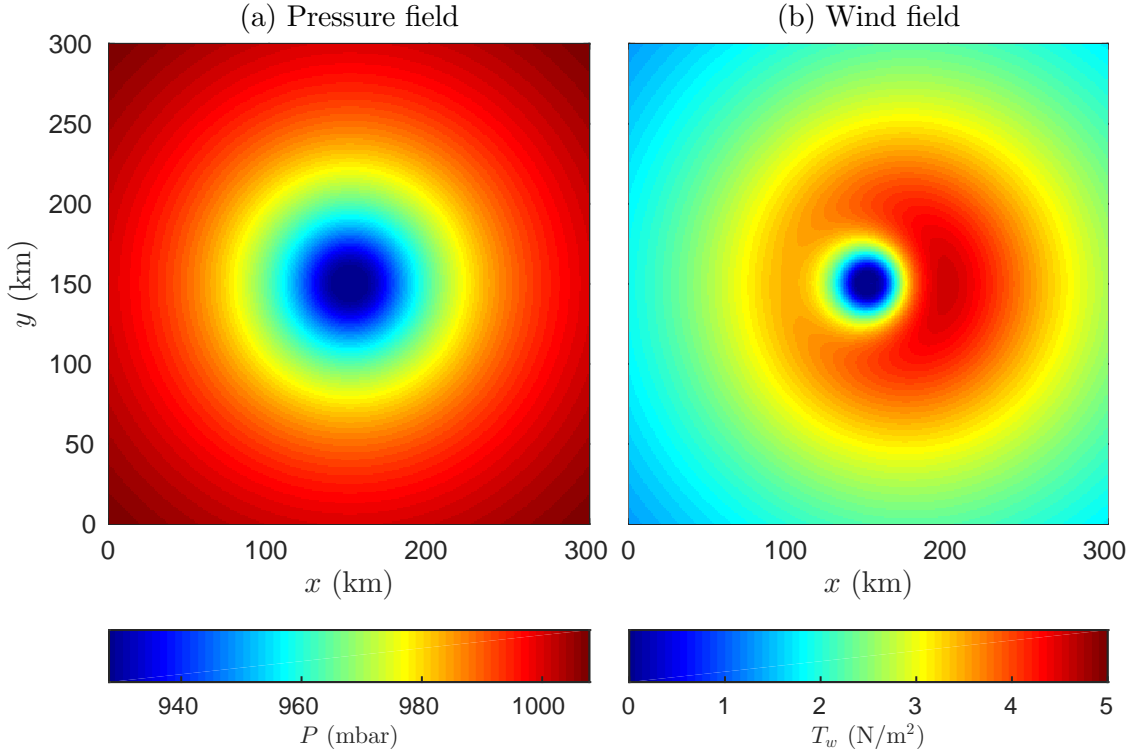

Figure 3.3: The pressure (left) and wind field (right) of a hurricane with parameters $P_c = 92800$ (Pa), $R_{max} = 52$ (km), $B = 1$ (-) and $C_f = 7.8$ (m/s).

---

[1]Based on the analysis in Chapter 4, this value replaces the default value of $1.4\mathrm{e}^{-3}$.

3.2 Hydrodynamical part

The hydrodynamical part of the model calculates the solution for the surface elevation and velocity field at each point in the domain as a function of time. The time and space-dependent pressure and wind force the system. Fourier transformation combined with the Finite Element Method is used to solve the problem.

3.2.1 Shallow water equations

Assuming vertical displacement to be small compared to the water depth, the three dimensional linearised shallow water equations are used to express conservation of momentum and mass:

$$\frac{\partial u}{\partial t} - fv = -g\frac{\partial \eta}{\partial x} - \rho^{-1}\frac{\partial P}{\partial x} + \frac{\partial}{\partial z}(A_v\frac{\partial u}{\partial z}), \tag{3.5}$$

$$\frac{\partial v}{\partial t} - fu = -g\frac{\partial \eta}{\partial y} - \rho^{-1}\frac{\partial P}{\partial y} + \frac{\partial}{\partial z}(A_v\frac{\partial v}{\partial z}), \tag{3.6}$$

$$\frac{\partial \eta}{\partial t} + \int_{-h}^{0} \left[\frac{\partial u}{\partial x} + \frac{\partial v}{\partial y}\right]\partial z. \tag{3.7}$$

Here, P is the atmospheric pressure from the meteorological model, η is the sea surface elevation, g is the gravitational acceleration u and v are flow velocities in $x-$ and $y-$direction, respectively. Furthermore, η represents the free surface elevation relative to the undisturbed water level $z = 0$ and the bed level $z = -h$

Turbulence is represented using a uniform eddy viscosity A_v along with a partial slip condition at the bed with resistance parameter s. This means with a large s, there is no slip as the bottom boundary condition and a $s = 0$ means a free-slip for which the problem is independent of vertical coordinate. This is captured in the following boundary conditions for an imposed wind stress at the free surface and the partial slip-condition at the bottom. The linearisation procedure causes the free surface condition to be imposed at $z = 0$ instead of at $z = \eta$.

$$A_v \left.\frac{\partial u}{\partial z}\right|_{z=0} = \frac{T_{w,x}}{\rho}, \qquad A_v \left.\frac{\partial v}{\partial z}\right|_{z=0} = \frac{T_{w,y}}{\rho} \tag{3.8}$$

$$\rho A_v \left.\frac{\partial u}{\partial z}\right|_{z=-h} = su, \qquad \rho A_v \left.\frac{\partial v}{\partial z}\right|_{z=-h} = sv \tag{3.9}$$

3.2.2 Solution method

To be able to calculate the solution the hydrodynamical model is divided in two parts (as can be seen in Figure 3.1). The first part contains a Fourier transformation of the pressure field and wind stresses to write them in a time-periodic fashion. This means the continuous signal is decomposed in a number of signals (modes indicated with index (k)) with different frequencies (ω_k) and amplitudes (P_k or $T_{w,k}$). Which means:

$$P(x,y,t) = \sum_{k=-K}^{K} P_k(x,y)e^{-i\omega_k t} \tag{3.10}$$

$$\vec{T_w}(x,y,t) = \sum_{k=-K}^{K} \vec{T_k}(x,y)e^{-i\omega_k t} \tag{3.11}$$

The second part of the hydrodynamical model calculates the solution for each of these modes. The shallow water equations are transformed and expressions are created for both horizontal velocities, in terms of the surface slopes and wind stresses. Substituting these expressions into the continuity equation and integrating this from bottom to surface gives an elliptical equation for the surface elevation. A complete derivation of this solution method can be found in Chen et al. (2015).

This equation is finally solved numerically using the Finite Element Method finding the surface elevation for each mode in the domain. With the surface elevation the horizontal velocities for each mode can be derived. Linearity of the model ensures that the basins response to forcing can be obtained by the superposition of the responses to the Fourier forcing.

3.3   Model implementation

To simulate the storm surge response with the model of Chen (2014) the complex New Orleans coastal basin is schematized. This section gives an overview of the model choices to represent the schematized coastal basin of New Orleans. As the model is constructed using successive loops of improvements only the final model set-up is presented here.

3.3.1   Domain

The New Orleans coastal basin is a complex basin with many features such as barrier islands and the large swampy areas along the coastline. In order to make a sensitivity study on the most basic elements of the coastal basin most of these features are simplified or left out of the geometry to study only the most important processes.

For simulation purposes a small domain concerning only the local scale of the New Orleans coastal area is preferred because of calculation time. However, this local scale domain showed to be inadequate to compute the storm surge response as also pointed out by Blain et al. (1994). Since cross-shelf boundaries are in regions of significance for surge generation in a small domain. Surge and boundary conditions could not be known a priori. Therefore a domain must be chosen sufficient for simulating large scale processes as well. If the domain is chosen to small entire flow phenomena may be merely model artefacts and which appear and disappear.

To include the large scale processes the domain covers the whole north east corner of the Gulf of Mexico as shown in Figure 3.4. For simplicity the coasts of the basin are represented by straight lines. Inside the New Orleans coastal basin the lines follow the coasts during high water, so swampy areas which flood during high water are not present in this domain.

3.3.2   Bathymetry

As already seen in Figure 2.2, New Orleans is situated at a continental shelf. The bathymetry is shallow near the coast with a steep drop to the deep open water of the Gulf of Mexico. Because the New Orleans coastal basin is the region
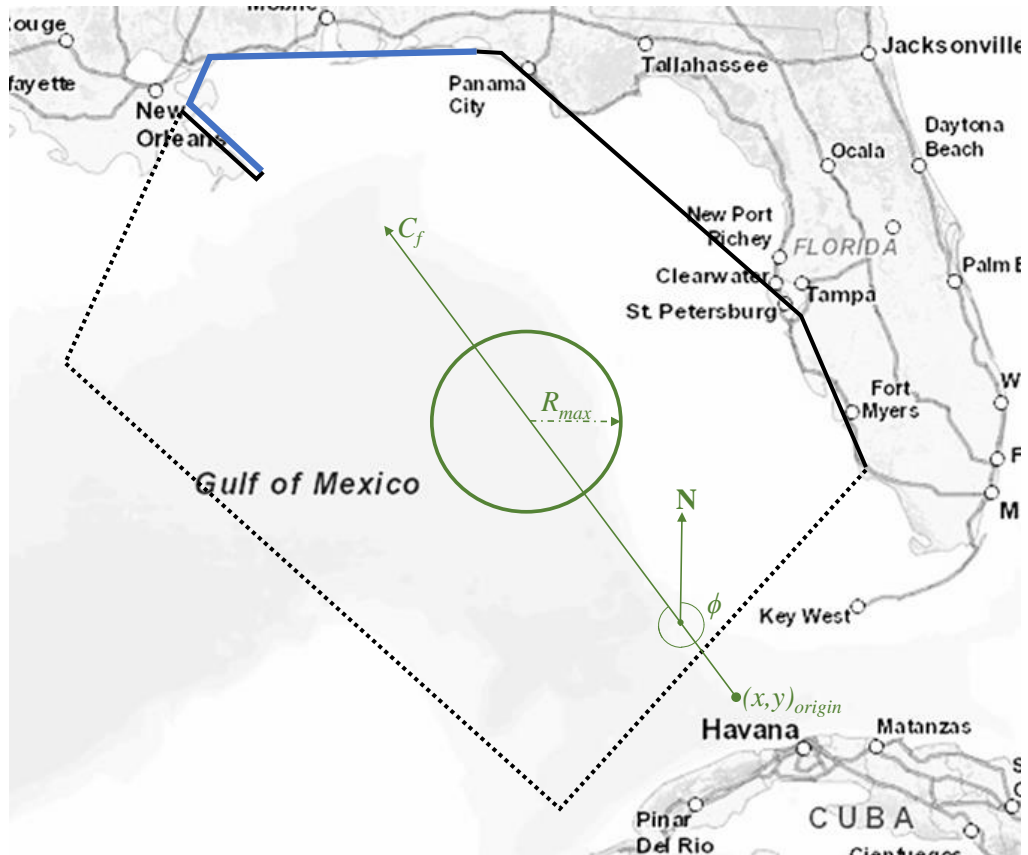
Figure 3.4: Schematized model domain of the north east corner of the Gulf of Mexico. **Blue:** *New Orleans coastal area.* **Black:** *domain boundaries, where dashed lines resemble inverted barometer boundaries.* **Green:** *schematic representation of a storm and storm track, parametrized by hurricane size (R_{max}), forward speed (C_f), point of origin (x,y) and storm direction (ϕ). Central pressure (P_c) is not shown.*

of interest, the bathymetry of this basin is schematized in more detail than the rest of the domain. The bathymetry for the whole basin is a simplified version of the real bathymetric data (see Figure 3.5). The shallow water depths represent the swamps. During high tide the swamps are flooded but during low tide the swamps are almost dry. This is difficult to implement in the model since it is a linear model and cannot work with water depth of zero. The water depth for the swamps is therefore exaggerated to 3 m. Between the swamps and the barrier island the water level decreases slowly to 20 m with a big topographical step to the continental shelf at 100 m.

In the rest of the domain, the continental shelf is represented with a water depth of 20 m along the coast and 100 m further from the shore. The deepest part of the Gulf of Mexico is 1000 m.

3.3.3 Boundary conditions

The model domain is surrounded by 2 different boundaries; closed boundaries representing the physical coastline and inverted barometer boundaries connecting open water with the Gulf of Mexico. The closed boundaries are represented by a reflecting boundary where no normal flux is allowed. This means the vertical integration of the normal velocities at these boundaries is zero (Dirichlet boundary condition for velocities).

An open boundary is used to represent the open side of the basin. Both a non-reflective boundary and a Dirichlet boundary with an inverse barometer effect are considered for this case. Eventually the inverse barometer boundary showed to be best option for this study.

The non-reflective boundary allows water to flow into the basin and makes it possible for waves to propagate out of the domain. Even though this could be a better presentation of reality than a Dirichlet boundary, this non-reflective boundary gives difficulties if large differences in water depth are present near the boundary. Furthermore, this boundary uses an assumption that the open water outside of the domain has the shape of a 'channel' with the width of the open boundary and an infinite length. Because the open boundaries are cross-shelf boundaries, a large change in water depth is present along this boundaries. Choosing for this non-reflecting boundary condition means that it is not specifically known how the boundary behaves with the large topographical step and it incorrectly assumes the width of the Gulf of Mexico. This can have big influences for the amount of water transported by the hurricane towards and into the basin. Both of these aspects are important for this study so therefore the Dirichlet boundary condition is considered an option as well.

The Dirichlet boundary prescribes a certain water level at the seaward boundary. This water level can either be a fixed water level, a periodic function (e.g. tidal signal) or a calculated value from the inverted barometer effect. This implies that the water level has a given value but still water can flow in and out of the domain since the velocity flux over the boundary is not zero.

Despite non-linear interactions with storm surge, tides are not considered in the model because the tidal range around New Orleans is relatively small (around 0.5 m). Furthermore, surface elevation due to the wind at open boundaries is assumed to be small compared to the inverse barometric effect. Pascal's law can then be used to determine the surface elevation (ζ):
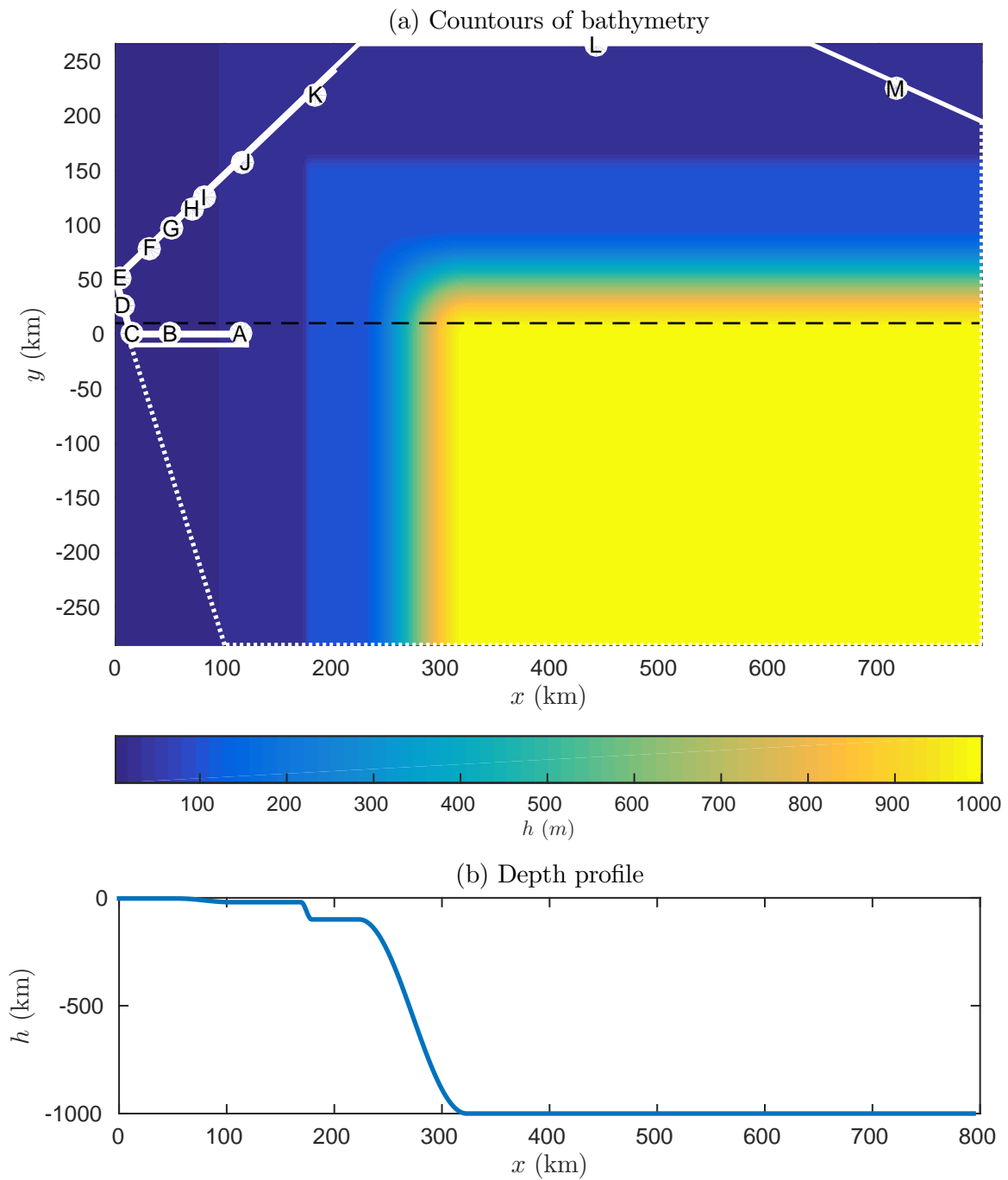
Figure 3.5: (a) Schematized bathymetry including domain boundaries and locations. For dashed black line the depth profile is shown in (b). Both show the different water depths, 3 m, 20 m, 100 m and 1000 m successively from west to east at the dashed line.

$$\zeta = \frac{\Delta p}{g\rho_w} \tag{3.12}$$

However, using this boundary implies that a wave generated inside the domain cannot propagate out of the domain.

Furthermore this boundary condition will lead to a discrepancy when, on the one hand, there will be a wave reflected from the closed (coastal) boundary, giving the points (nodes) at (or near) the boundary a value, and on the other hand, the boundary condition prescribes other values at these nodes. This discrepancy arises when the boundary is not sufficiently far away from the dynamic area in the domain and could possibly make the open boundary a 'partially-reflecting' boundary. However, as shown by Chen et al. (2014), a large topographical step in a basin causes a circulation within the shallower part of the basin and mimics in this way the effect of a Dirichlet boundary at the topographical step.

Therefore, taking this into account and compared with the non-reflecting boundary condition, the Dirichlet boundary is considered the best option for this domain. Prescribing the water level with the inverse barometric effect showed to be the best representation for this study. Due to the low pressure inside the eye of the hurricane the water level rises underneath it. This water level rise is used as boundary condition for the model both inside and outside the eye of the hurricane.

3.3.4   Storm parameters

The six storm parameters of the Holland-B model specify the different storms. For calibration these parameters are based on historic hurricanes which deviate in strength along there track. Therefore these parameters are time dependent. For the sensitivity study however, the parameters are kept constant for the whole timespan of the simulation. For historic storms parameters are only known (or specified) for the first 66-72 hours. The recurrence time is much longer and therefore the parameter set of the last known time step is assumed for the remainder of the simulated time.

3.3.5   Friction parameters

Friction due to turbulence is represented by the vertical eddy viscosity (Av) and a partial slip condition with resistance parameter (s) at the bottom. The values of both of these parameters could be linearly proportional to the local water depth or uniform over the entire basin. It is chosen to work with constant values as used by Chen et al. (2014): $A_v = 0.025$ and $s = 0.01$.

3.3.6   Numerical choices

Several numerical choices must be made for simulation of the same problem. Each of the choices influences the accuracy of the results or the correctness of the model. Below the numerical choices are explained.

Grid size for calculation

The storm surge model uses the finite element method which divides the whole domain in smaller simpler parts (finite elements). The equations are solved for each of the elements. Analogous to creating a circle with straight lines, the
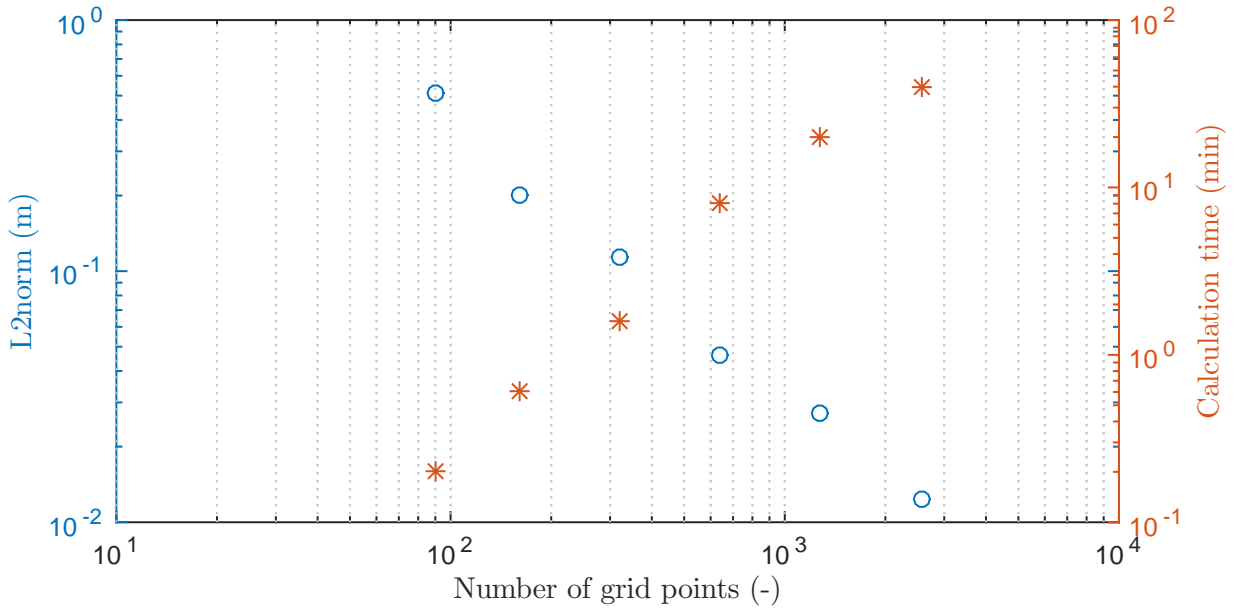
Figure 3.6: L2 norm (o) for different grid sizes within the local basin of New Orleans, together with associated calculation time (*).

error decreases when the lines are smaller. This means that small elements are preferred. However, with decreasing element size, the calculation time of the computer increases rapidly.

Since this study requires many simulations, calculation time cannot be too long. Selection of the appropriate grid size is therefore based on the calculation error and the calculation time of the computer. A sensitivity study for the local coastal basin of New Orleans is conducted to determine the optimal grid size for the calculations. Several simulation runs are made with different grid sizes. The L_2-norm[2]

is used to determine the error between a certain grid size and the smallest grid size which is assumed to be the best fit (Figure 3.6). A grid with 320 grid points is considered appropriate. For the large scale basin this corresponds with a grid size of 6 km. This grid size is used at the boundaries of the model and in the New Orleans coastal area. For the wider part of the domain a bigger grid size is used (20 km). This results in 10130 grid points (Figure A.2).

The storm surge model uses triangular elements, which can be either structured or unstructured. Because of the geometry of the New Orleanscoastal basin a structured mesh is not appropriate for this study. The unstructured triangle mesh is used.

---

[2]The L_2-norm is defined as follows (Kumar et al., 2015) :

$$L^2(\Omega) = \{\phi \ such \ that \ \|\phi\|_2 = \left(\iint_\Omega |\phi|^2\right)^{1/2} < \infty\}, \qquad (3.13)$$

where ϕ is the difference between the numerical solution with the finest grid and the coarser grid.

Recurrence time

The Fourier transformation in the hydrodynamical model decompose the continuous signal of the forcing into a number of different signals with different frequencies. The smallest frequency of the Fourier modes is determined by the recurrence time of the model:

$$\omega_1 = \frac{2\pi}{T_r} \qquad (3.14)$$

where ω_1 is the smallest frequency and T_r is the recurrence time.

   Because the solution is based on a discrete Fourier analyses, the simulation has no initial starting point and the storm is simulated again and again inside the basin. The period between two successive storms must thus be chosen and is called the recurrence period. If the recurrence period is too small, the water level oscillation of the previous storm could still be present in the basin and enhance the surge of the following storm. A large recurrence period means that smaller frequencies (longer wave periods) can be captured in the Fourier analysis. However, in that case more modes are needed to get the same accuracy. Simulations showed the first used recurrence period of 20 days to be insufficient to exclude sloshing from previous storms. The recurrence period was increased to 30 days to reduce the effect of sloshing. However, sloshing did not disappear. Combined with the found results for the number of modes, the recurrence period had to be reduced to 7 days to give a proper representation of the forcing.

Number of modes

The Fourier transformation in the hydrodynamical model decomposes the continuous signal of the forcing into a number of different signals with different frequencies.

$$\omega_n = \omega_1 * n \qquad (3.15)$$

where ω_n is the frequency of the nth-mode and $n = 1, 2, ..., N_{max}$, with N_{max} the chosen maximum number of modes.

   Analogous to the number of elements, increasing the number of modes gives a more accurate signal because the highest frequency gets smaller and smaller. However, more modes increase the calculation time. The number of modes is also related to the recurrence period of the storm (Equation (3.14)), the longer the period the more modes are needed for the same accuracy.

   The default value of 30 modes is too small to represent the sudden change in wind stresses and pressure caused by the hurricane. As illustrated in Figure 3.7, 128 modes and a recurrence time of 7 days give a relative good representation for the forcing of hurricane Katrina. Even more modes should be used to reduce the still present deviation in Figure 3.7 b and d. In combination with the calculation time a maximum of 128 modes chosen for the simulations. Resulting in a resolution to capture waves with a period of at least 1.31 hour.

Time series time step

Even though a Fourier transformation is used, water levels can be calculated both for the Fourier modes and as a time series. For these time series a inverse Fourier transformation is used. Results can be calculated with each desired time step.
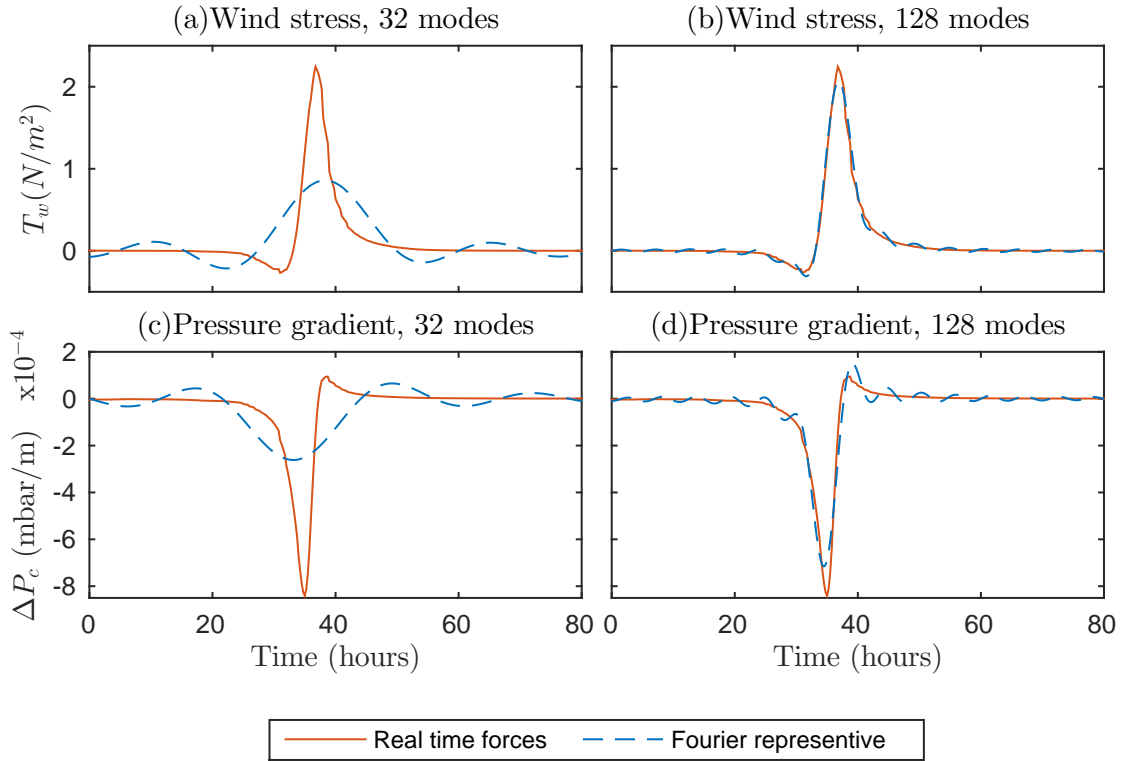
Figure 3.7: *Real and Fourier representative of forces. (a) and (c): Fourier representative with 32 modes. (b) and (d): Fourier representative with 128 modes. Both with a recurrence time (T_r) of 7 days.*

The observed data has a time step of 1 hour. Furthermore, with chosen number of modes (128) and recurrence time (7 days) the period of the highest frequency is 1.31 hour. Choosing a time step bigger than this period ensure that results are do not show small variations created by merely the highest frequency. Therefore it is chosen to use a time steps of 2 hours for the time series of the water levels, which decreases the calculation time as well when compared to a 1 hour time step.

3.4 Summary

The meteorological model generates the radial profiles of the pressure field and wind stresses of a hurricane for each point in the domain as a function of time. These forces are used as input for the hydrodynamical model, which is based on the linearised three dimensional shallow water equations. A Fourier transformation and the Finite Element Method make it possible to calculate a solution for the surface elevation at each point.

Domain and bathymetry are chosen to give an adequate representation of the north west part of the Gulf of Mexico. An inverse barometer effect is used to simulate the open boundaries with the Gulf, while closed reflecting boundaries simulate the shoreline of Louisiana, Mississippi and Florida. Numerical choices are based on the trade-off between accuracy and calculation time. This has resulted in a grid size along boundaries and in the New Orleans area of 6 km, a recurrence time of 7 days and 128 modes.

Chapter 4

Model performance and behaviour

The newly developed idealized storm surge model has never been used before for a realistic case study. Therefore, during this first comparison to reality, the model performance is assessed and the model behaviour using different physical parameters is systematically explored. This is done to gain trust in the model's ability to simulate storm surges and judge its applicability for a realistic case study.

First the selection of historical data is presented (Section 4.1) and uncertainties of the historical data are quantified. These data are used for a hindcast and to assess model behaviour (Section 4.2). Simulated water levels are shown with maximum surge level and timing of these peaks. When necessary also results of Fourier modes are presented. This chapter answers the second research question.

4.1 Historical data

Each year, many tropical storms make landfall in the US. Not all these storms can be included in the dataset. Most common storms to calibrate and validate models for the New Orleans area are the BRICKA storms (Betsy, Rita, Ivan, Camille, Katrina and Andrew). These hurricanes are considered to form a good representation of the range of realistic hurricanes for this study area. However, many more storms have passed new Orleans. Suitable storms for the performance assessment are selected using the following criteria.

- Data about storm parameters should be available during the course of the hurricane towards the coast and at moment of landfall.

- Water level data should be available at coastal stations in and around the coastal basin of New Orleans.

- For a storm to be selected data about both storm parameters and water levels should be available for the same time span.

- A storm should make landfall in the proximity of the city of new Orleans or the coastal basin.

- Water level data should have been recorded for a period of 10 days before and after the storm to be able to see extra sloshing in the basin.

Table 4.1: Selected hurricanes for assessing model performance and behaviour. Data from National Climatic Data Center (2014). Water levels are relative to NAVD88 (2004.65).

Storm name	Date	Max storm surge [m]	Max wind speed [km/h]	Min central pressure [mbar]
Rita	24-9-2005	1.94*	281	897
Katrina	29-8-2005	4.04*	233	918
Ivan	16-9-2004	2.23*	–	–
Andrew	26-8-1992	1.76*	–	–

*Sensor ceased transmission at this point and did not record maximum elevation.

- Water level data about one storm should be available at more than 3 different stations spread along the coast of the coastal basin.

- Storms should be tropical storms with a hurricane category (SS-scale) of 1 or higher.

Based on these criteria, data from hurricane Katrina, Ivan and Rita and Andrew were found to be sufficient enough for the performance assessment. For other hurricanes often no data were available for either storm or water level data or the data were too old. For example, before 2004 the National Oceanic and Atmospheric Administration (NOAA) (2015) did not record any data giving information about the size of a hurricane.

4.1.1　Hydrodynamic data

The search for hydrodynamic data was difficult. Even though many storms pass the New Orleans area consistent observations water level data were hard to find. The National Data Buoy Center (NDBC) employs 15 floating buoys in the Gulf of Mexico, however data have to be paid for and only wave levels were recorded. The NOAA deployed many water level gauges and stations along the coasts of the Gulf. In the New Orleans basin several hundred measuring points are available. Unfortunately not all of them are active any more and no record is present about when data was measured. So based on trial and error, stations have been individually assessed for suitability. A second set of hydrodynamic data during hurricane Katrina is obtained from a model study done by Dietrich et al. (2012). This ADvanced CIRCulation (ADCIRC) model has calculated the surface elevation including tides for the whole Gulf of Mexico. Water level data at 6 locations is extracted for the purpose of this study.

Data preparation

Despite the verification of the NOAA, the observed water level data still showed measuring gaps and inconsistencies. Some of the stations were destroyed during hurricane Katrina and unable to record the maximum surge as well as the surge of hurricane Rita two weeks later. Furthermore, the water levels were measured with respect to the MLLW (Mean Lowest Low Water level). This MLLW is different for each station so water levels could not be compared. The following steps are made to prepare the data for use:

Table 4.2: *Water level observations/simulations at different locations for one or multiple hurricanes. Observed maximum surge is shown (relative to NAVD88 (2004.65)). Locations A to K are shown in Figure A.1. (National Oceanic and Atmospheric Administration (NOAA), 2015)*

Location	Station name	Station ID	Rita surge [m]	Katrina surge [m]	Ivan surge [m]	Andrew surge [m]
A	SW Pass, LA	8760922	1.132	2.362	1.164	0.978*
	ADCIRC	1	-	3.322	-	-
B	ADCIRC	2	-	5.175	-	-
C	ADCIRC	3	-	4.476	-	-
D	ADCIRC	4	-	4.692	-	-
E	ADCIRC	5	-	6.220	-	-
F	Waveland, MS	8747766	-	2.737*	1.450	1.371
G	Gulfport, MS	8745557	0.9457	-	-	-
H	Ocean Springs, MS	8743281	-	4.043*	-	-
I	Pascagoula, MS	8741533	0.899	-	-	-
	Horn Island, MS	8742221	-	1.898*	-	-
	ADCIRC	6	-	4.071	-	-
J	Dauphin Isl., AL	8735180	1.233	1.942	2.177	0.826
K	Pensacola, FL	8729840	1.119	2.038	2.230*	0.808

*Sensor ceased transmission at this point and did not record maximum elevation.

Gaps in recordings were present in the observed data. Time stamps of this missing data were also missing so the data series just became shorter. Missing time steps are searched manually and inserted with NaN-values for the water levels.

Tides are included in the data. With tide predictions (NOAA) for the same time-period these were removed from the recordings. However, small deviations were still present because tide predictions did not include wind set up or other temporary factors. By excluding the tides the tide-surge interactions are neglected. It is assumed that these interactions can be neglected in the scope of this research.

The reference level for each station is different. A deviation from the NAVD88 (2004.65) (the NAP for the US) was not known for all stations. The same method is used as by U.S. Army Corps of Engineers (2008b). They resolved this by assuming the MSL (Mean Sea Level) to be constant for the whole Louisiana coast and on average to lie 0.5 ft above MLLW. The MSL was on average 0.44 ft above NAVD88 (2004.65) so the MLLW data is corrected with +0.06 ft.

ADCIRC data are only available including tides. To be comparable with other observations, the best fit tidal predictions at nearby stations during hurricane Katrina are subtracted from these simulated time series.

Conversion from feet to meters was needed to be able to compare the simulations with the observed data. At the end, all data are available in m +NAVD88 (2004.65).

The available stations of NOAA and the ADCIRC simulations have 3 locations which should show similar water levels. Figure 4.1 shows all measured
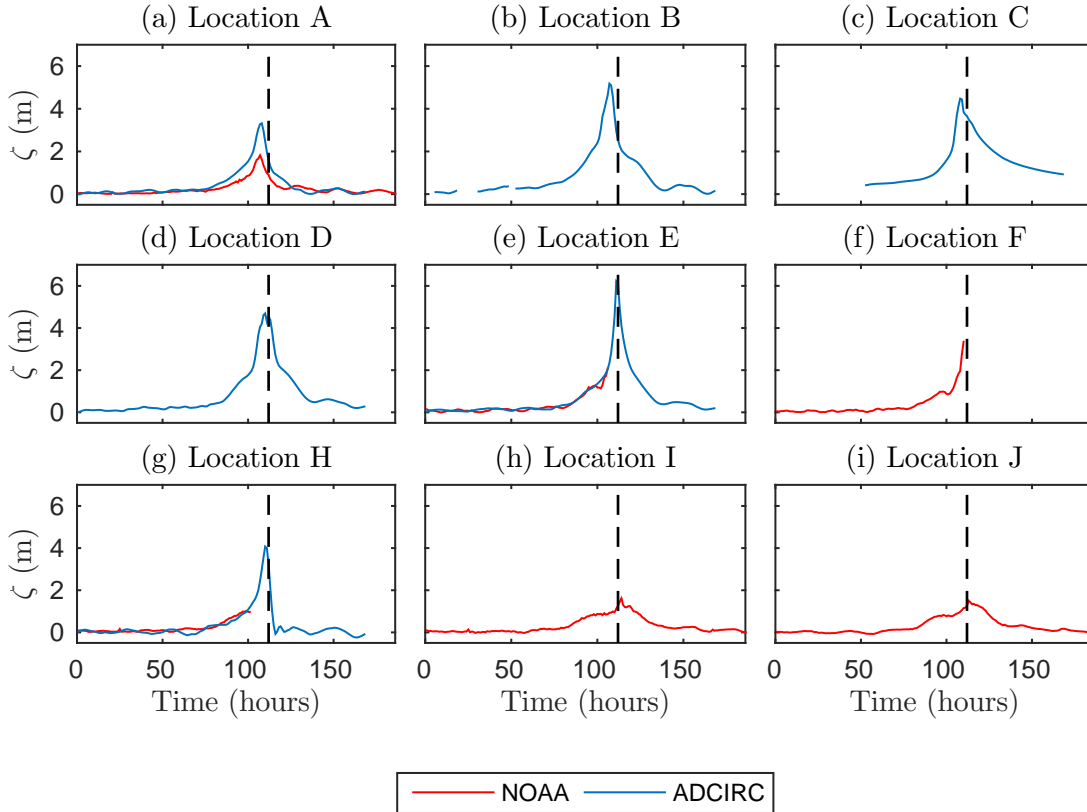
Figure 4.1: Observed (red) and ADCIRC simulated (blue) water level data during hurricane Katrina 24-8-2005 till 1-9-2005.

water levels for hurricane Katrina. It can be seen that at locations E/F and I the water levels are similar until the measuring stations are destroyed. For location A however, the maximum water levels deviate almost a meter. Therefore, the results of the model study will be either done with the NOAA observations or the ADCIRC simulations, both datasets will not be combined for the model assessment.

4.1.2   Meteorological data

The meteorological data should provide the six parameters to calculate the pressure and the wind field along the whole transect of the storm. Data for approximately 3 days before landfall is necessary because if landfall parameters would be used as constants for the whole track, the surge tends to be underestimated (Vickery and Wadhera, 2008). Tropical storms tend to decrease in size and intensity the 12 h prior to landfall.

Several studies use hurricane data, however all studies showed quite big deviations in used parameters. Again the NOAA provided raw data, which was finally used; the HURDAT2 (HURricane DATabase 2) (National Climatic Data Center, 2014). This database provided 6-hourly data about the central pressure and location of the storm's centre, which could be used to obtain the C_f, ϕ and $(x,y)_{origin}$. Vickery and Wadhera (2008) derived 3-hourly R_{max} and B from measured wind speeds and pressure profiles of the hurricanes. Unfortunately this data did not extend beyond the moment of landfall and was only available in graphs.
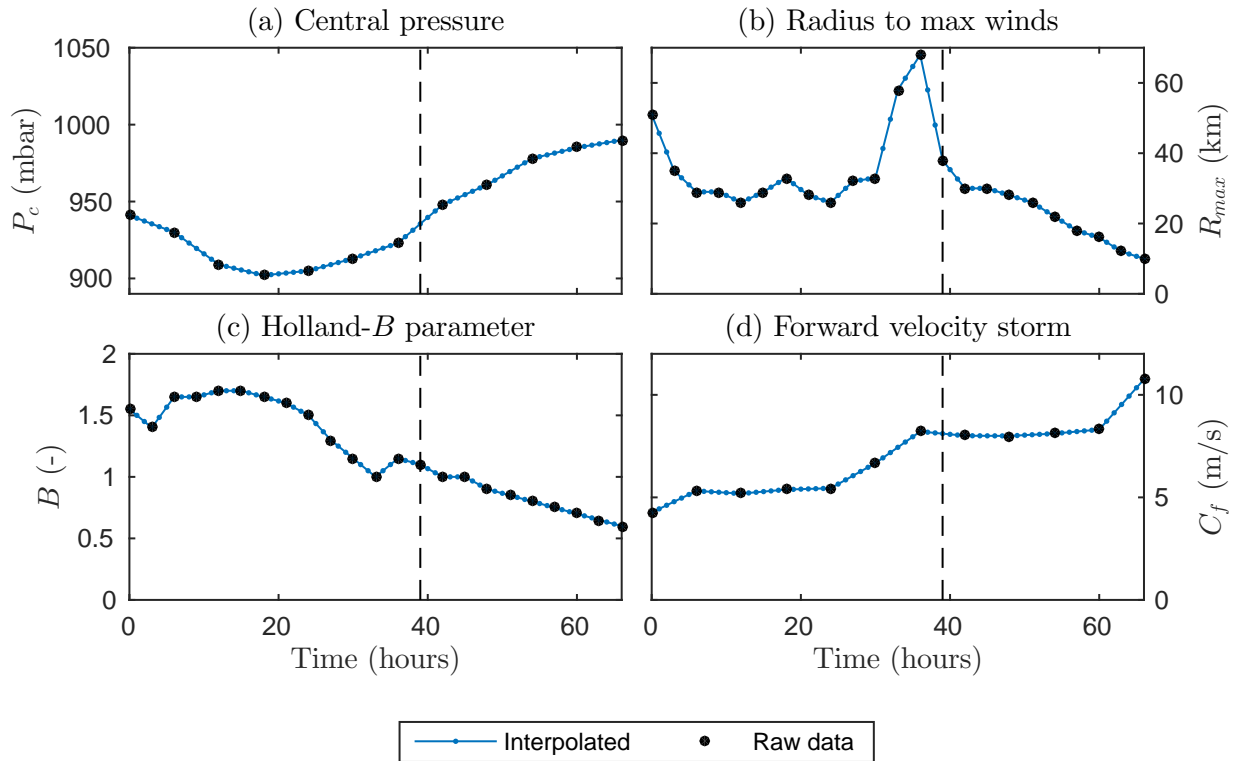
Figure 4.2: Hourly storm parameters P_c, B , R_{max} and C_f of hurricane Katrina from 28-8-2005 0.00h till 30-8-2005 18.00h.

Data preparation

With these two sources the six different parameters can be extracted from the database or derived from known values. A short description of this process is given below. Data about central pressure were usable without any preparation. The resulting parameters of hurricane Katrina can be seen in Figure 4.2, values for the storm direction (ϕ) and parameters of other storms can be found in the Appendix B.

C_f was calculated using the latitude and longitude of the hurricane's centre.

ϕ **and** $(x, y)_{origin}$ were derived from the latitude and longitude and translated to the coordinate system of the domain.

R_{max} **and** B have been read from the graphs and extended for the time after landfall. Vickery and Wadhera (2008) found hurricane size and Holland-B parameter to decrease after landfall. The data have therefore been extended with decreasing values after landfall (as suggested by U.S. Army Corps of Engineers (2008a)).

Linear interpolation has been finally done to determine the data for hourly intervals usable for the model calculations.

4.1.3   Qualification of uncertainty in historical data

Uncertainty of the model input and used observation data is described here. Because data were prepared and were used for an idealized model study it is dif-

Table 4.3: Quality assessment of used data

Hydrodynamic data	Data about	Uncertainty
NOAA (1hr)	$\zeta(t)$	low
ADCIRC (1hr)	$\zeta(t)$	medium
Meteorological data		
HURDAT2 (6hr)	P_c, $(lat, long)_{eye}$	low
FIS study (3hr)	B, R_{max}	high

ficult to make a quantitative analysis of the uncertainty. Therefore, uncertainty is qualified by using three categories: high, medium and low.

NOAA water level data are measured with gauges situated along the shore line. The uncertainty of the measuring devices is the order of mm and is therefore low compared with the uncertainty in the tide prediction (5 cm). The predicted tides are used to calculate the water level anomaly, the storm surge. Even though there are missing time steps in some of the observation time series the water levels are quite accurate. The uncertainty in the water level data is qualified as low.

While water level uncertainty is low, data compared to model simulations could still deviate a lot due to the very local effects near some stations. For example station SW Pass is in a swamp and in front of the station Waveland a barrier island is situated. Both of these features ar not simulated in the model.

ADCIRC water level data are obtained from another simulation model. Despite that model is calibrated and validated the uncertainty of these water levels is higher than real observed water levels. The typical error for the water levels of hurricane Katrina was 0.5 m for 72% of the measurement locations (Dietrich et al., 2012). This is higher than the uncertainty of the NOAA water levels. The uncertainty is therefore qualified as medium.

HURDAT2 data are measured during the whole course of a hurricane. With measuring stations, satellite images and aircrafts the pressure and the location of the storm are determined. Data are then analysed and if necessary revised. The uncertainty in this measurements is therefore qualified as low.

FIS study data (U.S. Army Corps of Engineers, 2008a) for both B and R_{max} are derived values. U.S. Army Corps of Engineers (2008a) derived these values from snapshots of wind field and data collected during hurricane reconnaissance flights. Because approximations and assumed relations are used, the uncertainty of this data is qualified as high.

4.2   Model properties

Water level data from historic storms are used to compare with the computed surge levels. The default physical parameters (as described in Section 3.3) are

used for these base cases. Assessing the model behaviour is done by systematically varying these physical parameters. This section describes the method and the results of the model performance and behaviour. The datasets of hurricane Katrina and Ivan are used for this, because these datasets were most complete.

4.2.1 Method

The model performance is judged by hindcasts of both hurricane Katrina and Ivan. In Chapter 3 the default values for the model input are determined. Together with storm data of both hurricanes (Appendix B) the hindcasts are made. These simulations are the base cases for the performance analysis. The results are discussed Section 4.2.2. The model behaviour is determined by investigating the effect of variations in model input on the model output. The default physical parameters will be systematically deviated within realistic ranges. The behaviour will be assessed using an individual parameter variation, thus only one parameter will be varied per simulation. The other parameters are kept constant. Simulated results are compared to the mentioned base case.

During this behaviour analysis storm parameters are not considered for variations. These are based on historic storm data and regarded to as fixed. This means that the forcing of the model is kept constant for each of the hurricanes. The following input varied instead:

Friction parameters The eddy viscosity (A_v) and the slip parameter (s). The default model values for the A_v and s were used for the base case, respectively 0.025 (-) and 0.01 m/s. Variations were made around these values resulting in the values 0.015 0.025 0.035 for A_v and 0.001 0.01 0.1 for s.

Secondly, the friction type was changed as well. In first instance the parameters were uniform over the water depth and constant over the whole domain. Runs were also made with both parameters still uniform over the water depth but linearly dependent on water depth over the basin. Which means that in shallow water the slip parameter and eddy viscosity are higher than in deep water.

Bathymetry The bathymetry of the Gulf is simplified for implementation in the model (Figure 3.5). To investigate the influence of depth, this bathymetry is varied by adapting the depths with +20% and -20%.

A third bathymetry is used which has a smoother transition between the continental shelf and the deep part of the Gulf (Figure D.1)

Drag coefficient The wind stresses are computed with Equation (3.4). The drag coefficient in the model has a default value of $1.4e^{-3}$ (-). However (Amorocho and DeVries, 1981) found an upper limit for this value. Surface winds above this velocity form a patches of foam. For wind velocities above 26.8 m/s the value should be $2.54e^{-3}$ (-), so a run is made with this value as well.

Number of modes The number of modes is chosen so that the forcing is represented best without a too large calculation time. A higher number of modes should increase accuracy. To see the effect, a run is made with an doubled number of modes (=256 modes).

Grid size The grid size is trade-off between accuracy and calculation time. A run is made with elements half the size of the used grid.

During the process of this performance and sensitivity analysis the results deviated so much from observations that multiple adoptions had to be made to the model set-up. This resulted in an iterative process for the model in combination with hurricane Katrina. This hurricane was used because of the amount of available data. At the end, only qualitative comparison of results is used to assess the influence of the parameters.

Selected indicators

Different indicators were used to judge the results of the model sensitivity analysis. For comparison with observed water level the model extracts simulated water levels at roughly the same locations as the observations. The model calculates with polynomial functions the value in a triangular element. If the point of interest is not on the grid node but inside the triangle, a quadratic function is used to calculate the value between the grid points. The following indicators are used as guide for the comparisons:

- Water level trend, $\zeta(t)$

- Maximum observed water level, ζ_{max}

- Timing of maximum water level, $t(\zeta_{max})$

4.2.2 Base cases

The results of the base cases are shown in Figure 4.3 and in Appendix C. The figures show the observations and simulations for 6 different locations. The reproduced water levels do so much deviate from observations that quantitative comparison using the selected indicators is not possible. Therefore the results are judged qualitatively and are eye-balled for comparison.

Compared with the NOAA observations of hurricane Katrina Figure 4.3 the following can be said about this base case simulation:

$\zeta(t)$ The simulated water levels trends are roughly in line with the observed water levels (NOAA). The water levels increase towards the moment of landfall and decrease afterwards. The simulated water levels show after the surge a periodic signal which is not registered by the measuring stations. This sloshing is probably model induced due to the chosen boundary conditions of the model and is therefore left out of further comparisons in this section.

At locations H-K the water levels running up to the start of the main surge (hours 10-30) are rather spiky compared to the observed levels. Recorded water levels show an early rise of water as well, but with a much smoother character. For location F however, the simulated water level before hour 38 does not show any sign of increase.

ζ_{max} Peak water levels are comparable with the observed. Unfortunately, it cannot be determined for locations F, H and I. High water marks at these locations reach up to 6-8 meter (Orders, 2006). Even though these high water marks include waves, the simulated peaks are probably underestimated.

$t(\zeta_{max})$ The timing of the maximum water level is fair. For locations with ob-
served maximum water levels the simulated highest water level was within
4 hours for the observed peaks.

If the simulations are compared with the ADCIRC simulations bigger devia-
tion with observed water levels are found. However, the course of simulated the
water level is still qualitatively comparable. In general the ADCIRC simulations
show a peak surge about 2 m higher than computed with the storm surge model.
The timing of the computed peaks on the other hand is rather consistent with
the ADCIRC simulations. Only location E shows a very different surge than is
computed with the model, which is neither comparable in qualitative water level
trend, nor in timing of the peak surge.

The base case simulation for hurricane Ivan shows a roughly comparable be-
haviour as well. This hurricane generated a lower surge than hurricane Katrina.
Less water is brought into the basin, therefore hurricane Katrina is used for the
behaviour assessment.

4.2.3   Results

The surge for hurricane Katrina with default parameter set is shown in Sec-
tion 4.2.2. Results of all other physical parameter sets are compared to this
default storm surge. It is important to keep in mind that the outcome of this
analysis, depends on the chosen storm parameters. For example, sensitivity for
certain parameters could be higher when more extreme storm parameters are
used. Nevertheless, this analysis shows the qualitative behaviour of the model.

For each of different input sets a brief judgement of the influence is given,
which is based on water level simulations and when relevant, amplitudes of the
Fourier modes. The effect is qualified in a qualitative way using three levels:
low, medium and high. Result of the drag coefficient are shown in Figure 4.4,
other figures of the results are shown in Appendix D.

Friction parameters' effect is shown in Figures 4.3 and C.1. This shows the
effect of the different combinations of A_v and s do not have a large influence.
These parameter combinations do not influence the water level trend and
only change the water level with a few centimetres. The effect of friction
parameters is qualified as low.

Bathymetry's effect is shown in Figure D.4. This shows a change in depth of
+ or - 20% does only influence the water levels in the order of centimetres.
The smoothed bathymetry on the other hand has more effect. At locations
H, I and J the peak surge is shifted with 2-4 hours. The surge levels
decrease slower to the original water level. Also the spiky signal before
land fall is not present as well. At location A, however, this spiky signal is
still visible.

The Fourier amplitudes show that for the smoothed bathymetry long pro-
cesses (low frequencies) are more important. There is almost no noise at the
higher frequencies, which is the case in all three not smoothed bathyme-
tries. Noise is only still at location A (the only location with the spiky
water level signal). The large peak in amplitude at mode 7[1] and around
mode 11 are also not present for the smoothed basin.

---

[1]Note: All 128 modes and associated frequencies only apply to this study where $T_{rec} = 7$
days.

(a) Location A

(b) Location F

(c) Location H

(d) Location I

(e) Location J

(f) Location K

Simulated   Observed

(g) Measure locations and track hurricane Katrina

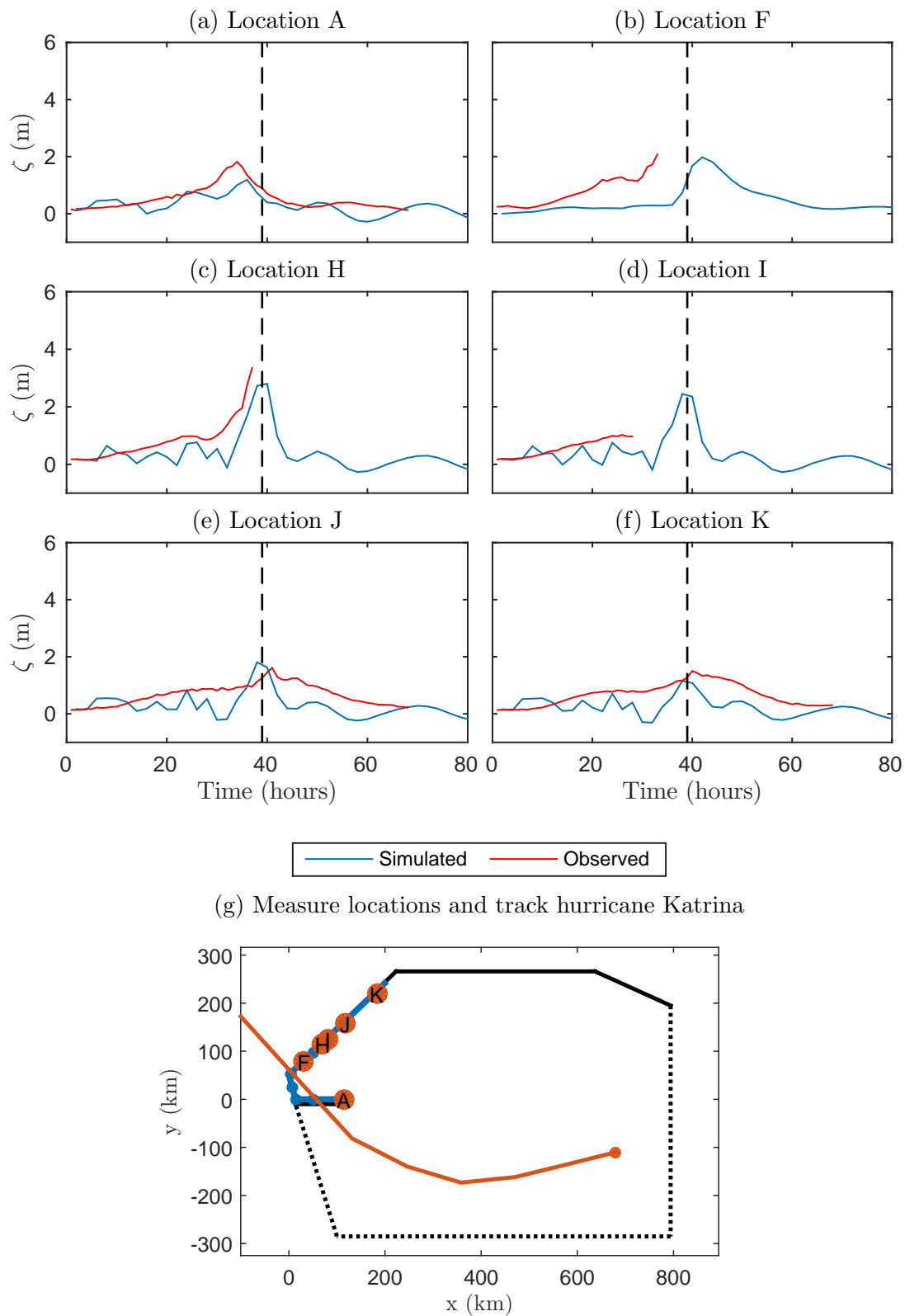*Figure 4.3: Simulation results for hurricane Katrina (a-f). Vertical dashed line represents the time of landfall (t=39). (h) shows measuring locations and the track of hurricane Katrina.*

This means that the effect of the bathymetry is low when only depth is changed. If the shape of the topographical step is changed the effect is bigger and qualified as medium.

Drag coefficient's effect is shown in Figure 4.4 . This shows that the drag has large quantitative effects on the peak water levels. These are increased with 1-1.5 meter at the most extreme locations. These peak water levels are in better agreement than simulated with the original drag coefficient. Also when comparing to the ADCIRC simulations (Figure D.6). The trend of the water levels is not qualitatively influenced. The drag coefficient in linearly implemented in the model, so almost doubling the drag coefficient doubles wind-driven surge. The pressure-driven surge, though is not influenced. Due to the large increase of peak levels the effect is qualified as high.

Number of modes hardly effect the water levels. This is shown in Figure D.7. Water level deviations are only centimetres and the peaks levels are not influenced at all. The effect of increasing the number of modes is therefore qualified as low.

Grid size's effect is shown in Figure D.8. This shows that the grid size mainly affects the water level trend prior to land fall. With the finer grid, the amplitude of the spiky signal is decreased, creating a better match with observed water levels[2] Peak water levels and the timing are only slightly influenced, changing respectively, maximum 15 cm and 2 hours. The Fourier amplitudes a change as well. The peak amplitudes of mode 12 are smaller as well as the noise of higher frequencies. This shows that due to grid size changes other modes are more important. This is important because the grid size is a numerical choice and physically there should be no differences between the two simulations. The effect of grid size is therefore qualified as high.

4.3   Summary

Historical data were gathered and prepared. These data were used as input for the storm parameters and as reference water levels to assess the model performance. The model performance is assessed using hindcasts of hurricane Katrina and Ivan. Simulated water levels are qualitatively comparable with observed water levels. On average the model underestimates the surge levels over the whole durations. The simulated water levels show also a spiky and a period signal which is not observed in data. Even though the height of the surge is not well represented, the timing of the simulated maximum water levels is reasonable. This implies that the surge moves in the same manner through the basin as in reality. Based on this, it is concluded that the most important processes are correctly simulated by the model. Therefore the performance of the model is considered to be sufficient to use it for a sensitivity study to storm parameters.

The behaviour study indicates that the friction parameters and number of modes hardly influence the results. The effect of bathymetry is different, changing only water depth has small effects compared to changing the slope of the

---

[2]This effect was discovered after sensitivity study mentioned in Chapter 5. Those scenarios are therefore simulated with the default parameter values.

topographical step. Changing the slope changes the processes of the storm surge. On the contrary, the drag coefficient and grid size have a larger effect on the results. The higher drag coefficient only influences the height of the surge creating much higher water levels which are in better agreement with observations. The default C_d-value is therefore replaced. The grid size mainly affect the 'spiky' signal prior to landfall, indicating the grid size still affects the processes of the storm surge. Unfortunately these findings could not be taken into account for the simulations of storm scenarios in Chapter 5. Since these were discovered after these simulations.

The quality of the used data could also explain some of the observed differences between observations and simulations. Main contributions are local features near observation stations and the high uncertainty for the Holland-B parameter and the storm size. Differences between simulated and observed data is therefore not merely caused by model performance. Though that is still considered as main contributor.
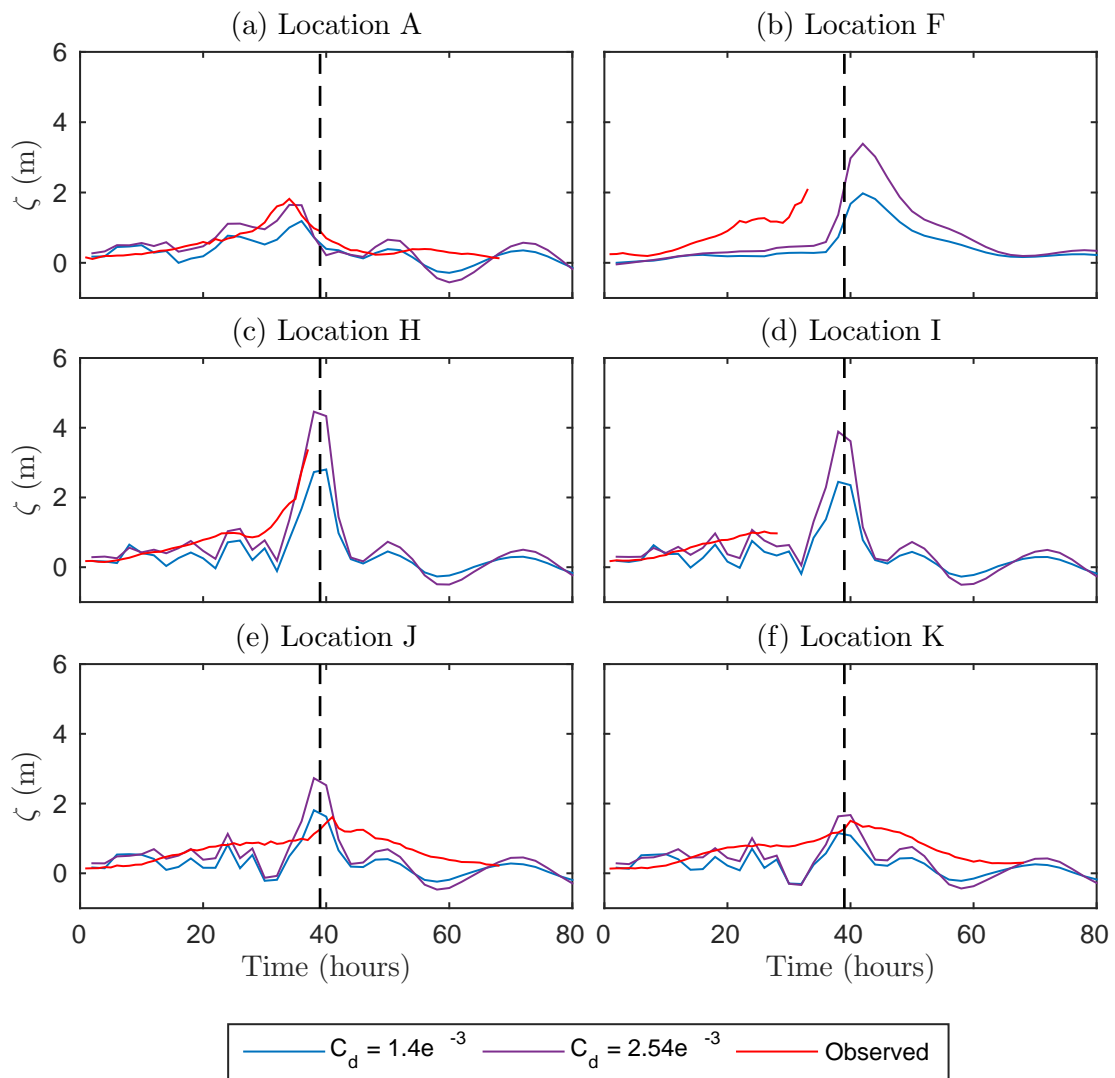
Figure 4.4: Simulated water levels for hurricane Katrina with different C_d-values. Vertical dashed line represents the time of landfall (t=39).

Chapter 5

Sensitivity analysis and physical interpretation

This chapter presents the sensitivity study of surge response to storm parameters. Several storm scenarios are designed and used for simulations (Section 5.1). The results of these simulations are presented (Section 5.2) and a qualitative interpretation of the sensitivities is made in Section 5.3. Finally, it is discussed how the surge response can be explained(Section 5.4). This chapter answers the third and fourth research questions.

5.1 Storm scenarios

For this part of the study a realistic but synthetic range of hurricanes is modelled. Based on historical and probable combinations of storm parameters, two different storms are developed which can approach the coast over three different paths, resulting in six storm scenarios. The parameter selection to form these scenarios is discussed below and more extensive in Appendix E.

As shown before, despite the complexity of a hurricane's wind and pressure field, it is found that the structure of the circulating wind can be well represented by a relatively small set of parameters. The first 4 parameters (P_c, R_{max}, B, C_f) determine the storm's pressure and wind field, while the latter two ($(x, y)_{origin}$, ϕ) describe the path of the hurricane.

Parameter constraints

Selection of parameters and combinations of parameters for a scenario is based on three different aspects: (i) Realistic ranges for storm parameters in the New Orleans area, (ii) interrelations between storm parameters, (iii) assumptions and constraints for parameters in combination with the FEM-model. Each of these three aspects is covered in Appendix E.

A fourth restriction was time, this formed the main restriction for the scenario selection. Many scenarios can be formulated with selected parameters but only a small set of scenarios can be run during this study.

Parameter choice

The parameter selection is aimed at selecting a synthetic set of probable hurricanes. An advantage of this, over methods that depend heavily on historical

storms, is that this also considers storms that might happen, whereas one otherwise only considers storms that did happen.

The parameters shown in Table E.1 are selected based on the different parameter constraints as described in Appendix E. Using these parameters 108 different scenarios can be formulated. This number is too large for this study so a selection of six scenario is made Table 5.1. The different storm directions are visually presented in Figure 5.1.

In the process of scenario selection it is chosen to study some parameters less intensively than others. So, the $P_c = 960$, $R_{max} = 21$, $C_f = 10$ and the second track of each direction $((x, y)_{origin} = A')$ are not studied in the first selection of scenarios.

Table 5.1: Selected storm scenarios based on the storm parameters. Holland-B parameter has a constant value of 1.1 and is therefore not shown in this table.

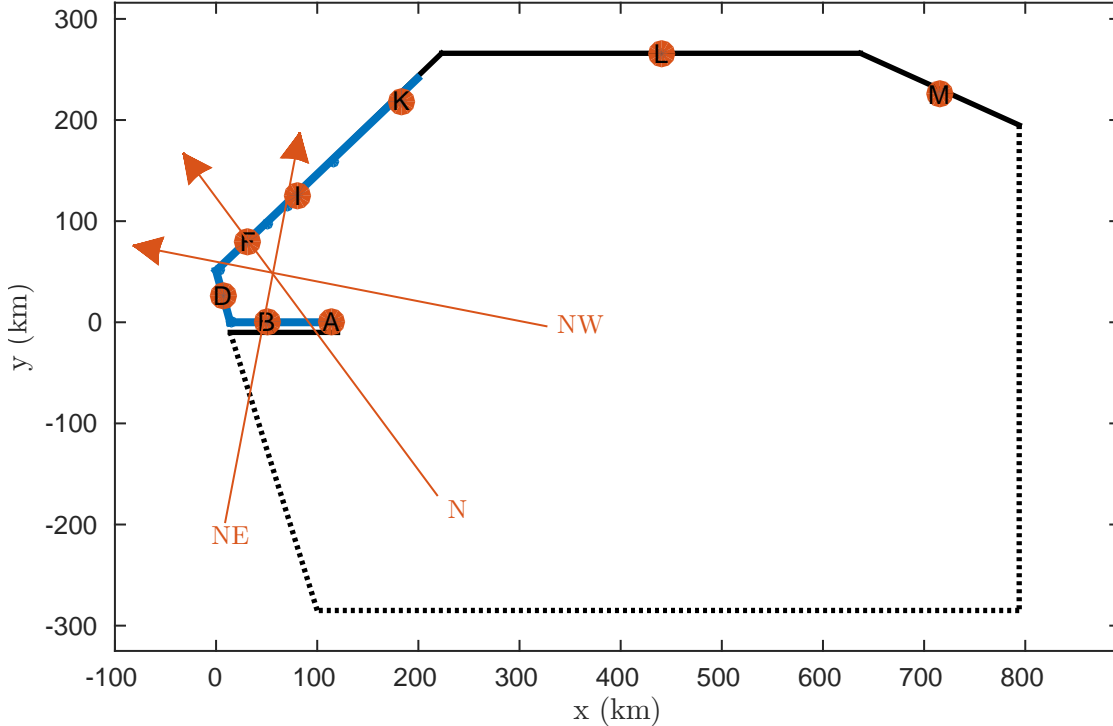| Scenario	P_c	R_{max}	C_f	ϕ^*	$(x, y)_{origin}$
1	900	32	6	7.5	A
2	930	47	6	7.5	A
3	900	32	6	322.5	B
4	930	47	6	322.5	B
5	900	32	6	277.5	C
6	930	47	6	277.5	C

*relative to the North.

Figure 5.1: The three main storm directions as specified in Table 5.1. Where NE, N and NW represent -7.5°, 322.5° and 277.5° respectively. Also the 8 measurement locations used for analysis are shown.

5.2   Simulation results

The results of the simulated scenarios are shown in this section. These results consist of graphs and tables based on water level time series and of frequency spectra and figures based on elevation amplitudes from the Fourier modes. These results will be discussed successively in Sections 5.2.1 and 5.2.2.

Features of the found water levels and elevation amplitudes are described per two scenarios with the same storm direction. This is done because Figure 5.2 shows that scenarios with the same angle have roughly the same results, which is also the case for the elevation amplitude of the Fourier modes.

This section gives a factual description of the results. An interpretation of these results is given in the following sections Sections 5.4 and 5.5. Just as assessing model performance and behaviour is done qualitatively.

5.2.1   Water level time series

Simulated water levels for the six scenarios are shown for six different locations (Figure 5.1 (Locations A, B, D, F, I & K)). The same three indicators are used for assessing the water levels as for the model performance (Chapter 4): water level trend $\zeta(t)$, peak value ζ_{max} and moment of peak value $t(\zeta_{max})$.

The six measuring locations are chosen in such way that at all boundaries of the coastal basin water level can be observed and important processes can be captured as well. Even so, these six locations have shown to be important for the city of New Orleans. Location D is located near the dikes defending the city and roughly at the location where hurricane Isaac had produced the highest surge (Figure 1.1), while hurricane Katrina generated the highest surge near locations A, B and I. Location K is used to assess if a forerunner can be observed propagating along the coastline from the east.

First the results for the water levels ($\zeta(t)$) for all storms are shown in Figure 5.2 and the ζ_{max} and $t(\zeta_{max})$ are shown in Table 5.2 together with Figure 5.3. More results for each scenario separately can be found in Appendix F.

Scenario 1&2

The results of storm scenarios 1 and 2 are shown in Table 5.2 and Figure F.1.

$\zeta(t)$ The water levels of both scenarios show a distinct surge at all locations around the moment of landfall. At locations A-F the maximum surge is measured before landfall while at locations I and K this is after landfall. After the water levels decrease even below 0. For scenario 2 only at location F the surge starts to decrease earlier.

ζ_{max} The maximum water level in both scenarios is the highest at location B. The second highest surge is at location I which is 6 hours later than at locations B. Both of these peaks are much higher than at the other locations which have maximum surges between 0.5 and 1.5 m. The difference in peak surge at location B between the two scenarios which is over 1 m.

$t(\zeta_{max})$ The timing of the maximum surge levels (Figure 5.3) shows that the surge propagates from location A to K passing all locations in between.
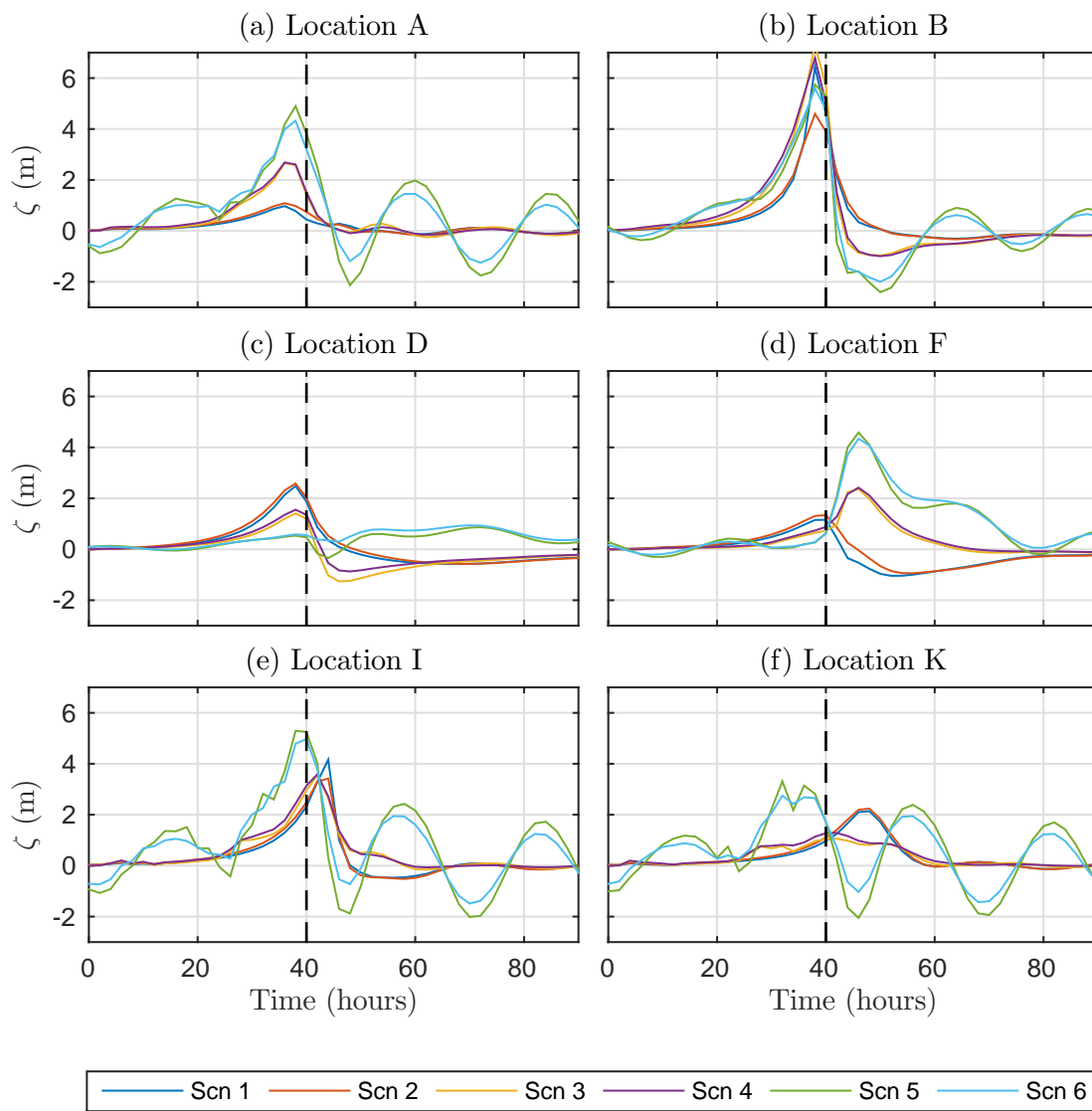
Figure 5.2: Simulated water levels for scenarios 1 to 6 at six locations. Locations are shown in Figure 5.1.

Table 5.2: Simulated maximum water levels and time of observation (hour). All storms make landfall at t = 40. Table organised per storm direction.

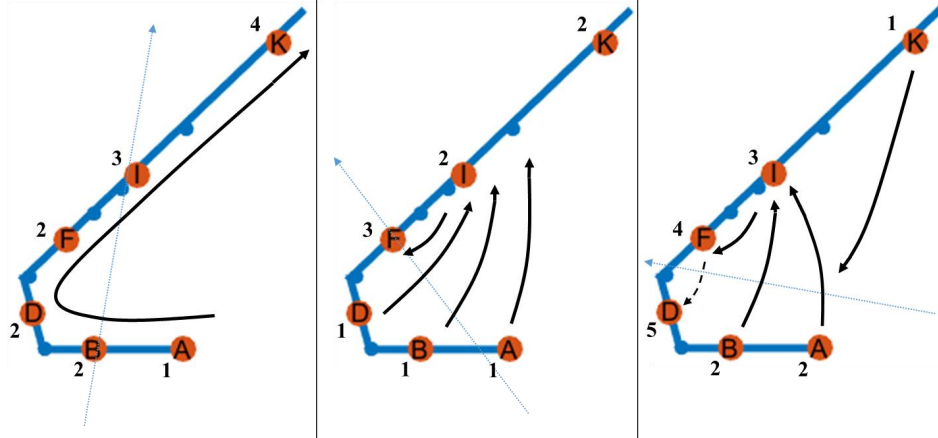|	Scenario 1	Scenario 2	Scenario 3	Scenario 4	Scenario 5	Scenario 6
	ζ_{max}	ζ_{max}	ζ_{max}	ζ_{max}	ζ_{max}	ζ_{max}
	$(t(\zeta_{max}))$	$(t(\zeta_{max}))$	$(t(\zeta_{max}))$	$(t(\zeta_{max}))$	$(t(\zeta_{max}))$	$(t(\zeta_{max}))$
A	0.97 (36)	1.09 (36)	2.66 (36)	2.69 (36)	4.90 (38)	4.32 (38)
B	6.43 (38)	4.59 (38)	7.31 (38)	6.78 (38)	5.74 (38)	5.60 (38)
D	2.48 (38)	2.58 (38)	1.41 (38)	1.55 (38)	0.87 (72)	0.94 (70)
F	1.16 (40)	1.34 (40)	2.36 (46)	2.42 (46)	4.58 (46)	4.34 (46)
I	4.17 (44)	3.42 (44)	3.56 (42)	3.59 (42)	5.29 (38)	4.97 (40)
K	2.14 (48)	2.24 (48)	1.06 (42)	1.29 (42)	3.31 (32)	2.75 (32)

Figure 5.3: Visual representation of Table 5.2. Surge pattern (black) through the New Orleans coastal basin based on (timing of) peak surges for three different storm directions (blue dashed line). Numbers at locations resembles timing of the peak compared to the first maximum surge. From left to right: scenario 1&2 (NE), scenario 3&4 (N), scenario 5&6 (NW).

Scenario 3&4

The results of storm scenarios 3 and 4 are shown in Table 5.2 and Figure F.2.

$\zeta(t)$ The water level trend of both scenarios show a distinct peak at locations A, B, D, F and I while at location K no distinct peak can be seen. The water levels show that the surge begins at the Mississippi dikes and then goes to the opposite shore without propagation into the shallow water (3 m) near D and F.

ζ_{max} The maximum surge is highest at location B, about twice as high as the second highest (location I) and multiple times higher than the other locations.

$t(\zeta_{max})$ The peak surges are measured at locations A, B and D before landfall, the other peaks after landfall.

Scenario 5&6

The results of storm scenarios 5 and 6 are shown in Table 5.2 and Figure F.3.

$\zeta(t)$ The water levels for scenario 5 and 6 are almost the same, only the water levels for scenario 6 are less extreme. The water levels show high peaks on each location except location D. At this location no significant surge is simulated. After the surge the water levels show a periodic signal. Before the highest peak surge a smaller surge can be observed at locations A, B, I, K between hours 14 to 24. This surge has a height of approximately 0.7-1 m, and seems to propagate from K to A along the coast. This is also visible in the simulations where can be seen that a wave propagates along the coast from east to west and keeps circulating after the storm is passed (resulting in the periodic signal).The surge does not propagate into the shallower part of the basin until storm is passed and only results in a surge at location F.

ζ_{max} Maximum surge of locations A, B and I are highest and comparable (3 m). At other locations (D, K) the maximum surge is lower, and at location D no distinct surge simulated at all.

$t(\zeta_{max})$ The timing of the peak surges are before landfall at locations A, B I and K while the surge at location F is after landfall.

5.2.2   Elevation amplitude of Fourier modes

The elevation amplitudes for the Fourier modes is shown for 8 different locations. The same six locations as used in the previous section, complemented with locations L and M. These extra locations are chosen to capture more information about the large scale processes. The spectral response is used to gain more insight in the processes of the surge responses.

Results of the Fourier modes are depicted in two manners: an amplitude spectrum for the eight locations (Figures 5.4 and 5.6 and appendix G) and a surface plot of modes with the highest amplitudes (Appendix G).

The spectra show mode 0 to mode 128. Where mode 0 is the time independent mode and mode 128 the highest frequency[1] (with a period of 1.3 hours).

Scenario 1&2

The results of scenarios 1 and 2 are shown in Figures 5.4, G.1, G.4 and G.5.

The amplitude spectrum shows that the lowest 8 modes create the highest amplitudes in the coastal basin. At locations B and I even higher modes still create an amplitude above the 0.02 m (horizontal line). For all locations applies: the higher the frequency, the lower the amplitude. In the shallow area mode 0 shows a rather small amplitude. The amplitudes of scenario 2 are at all locations slightly lower than scenario 1.

These observations can also be seen in the surface plots in which the lowest 8 modes are shown (Figure G.4). In these plots can be seen that the largest amplitude of the modes are all located at the shallow part of the basin which, in this case, is also underneath the storm track of the hurricane.

Scenario 3&4

The results of scenarios 3 and 4 are shown in Figures 5.5, G.2, G.6 and G.7.

---

[1]Note: All 128 modes and associated frequencies only apply to this study where $T_{rec} = 7$ days.
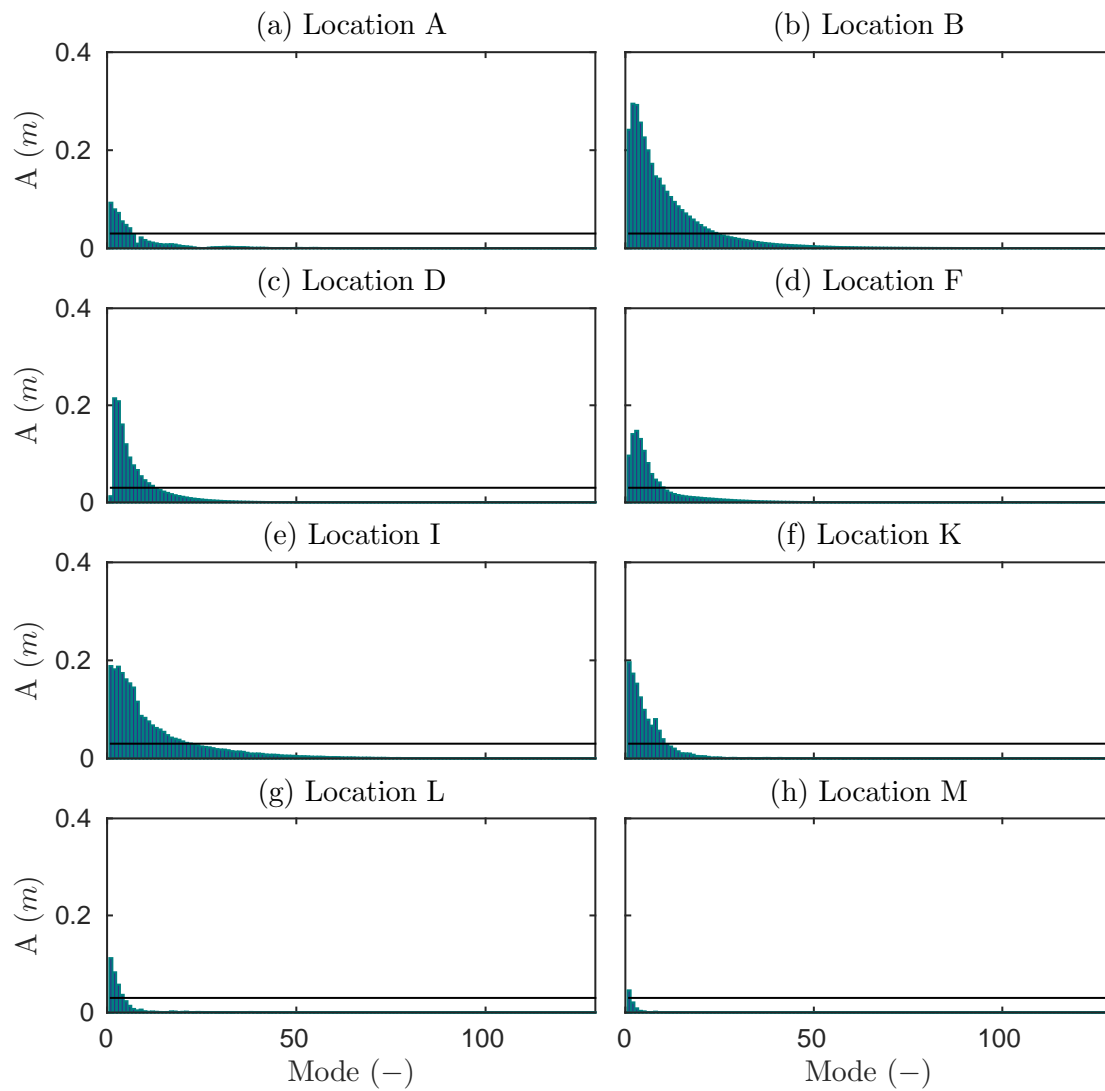
Figure 5.4: Fourier spectrum of elevation amplitude (m) for scenario 1.
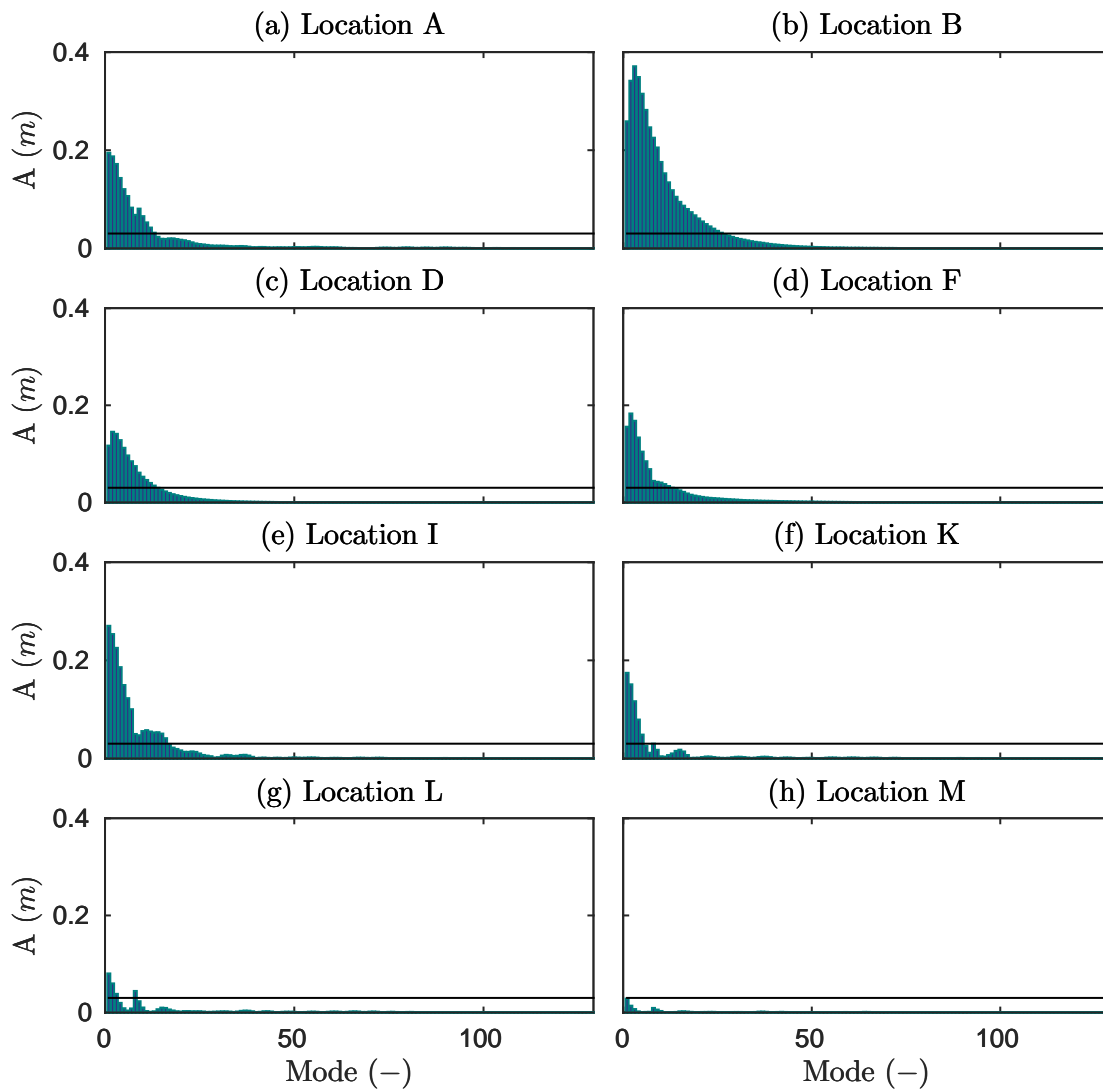
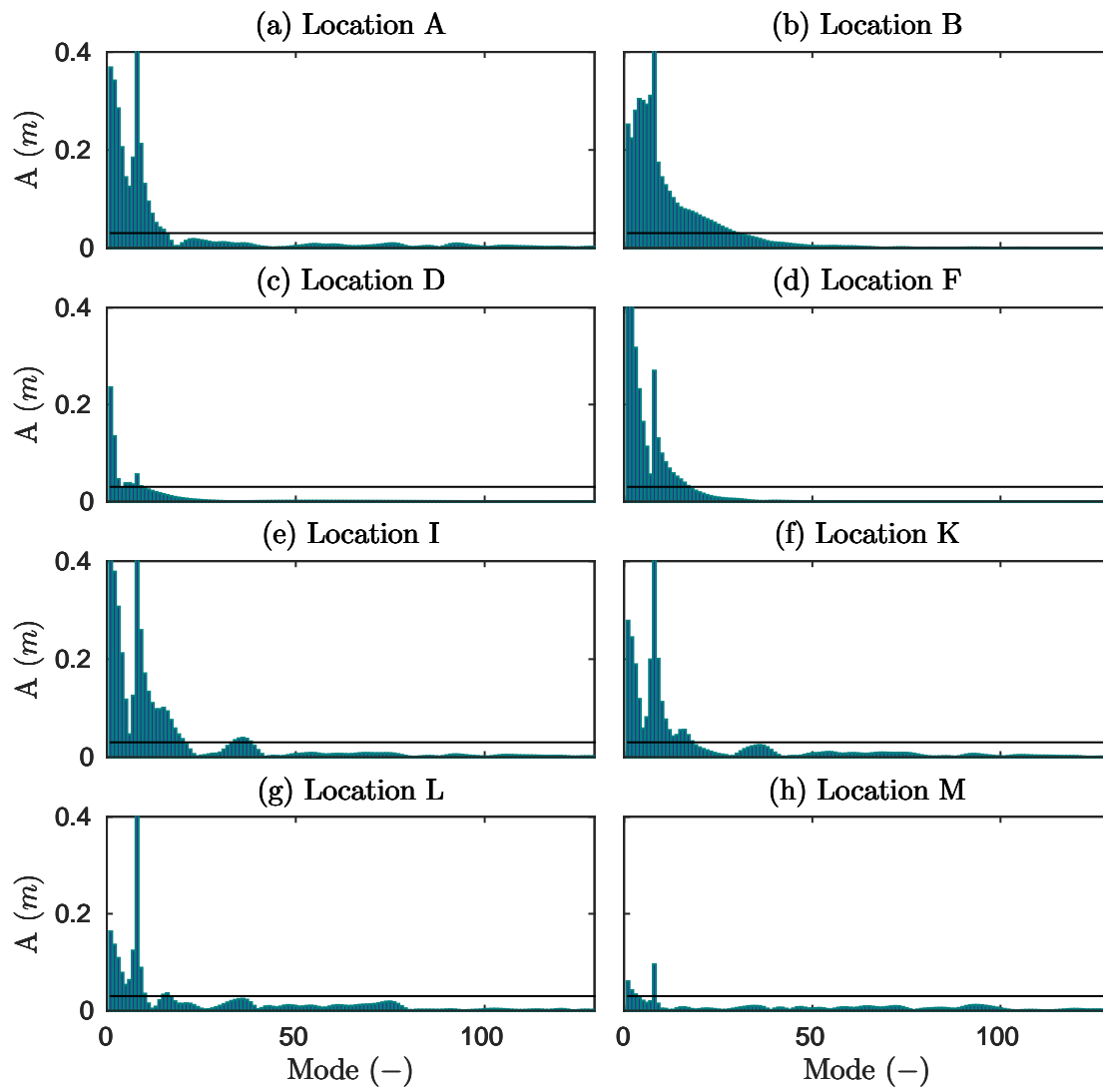*Figure 5.5: Fourier spectrum of elevation amplitude (m) for scenario 3.*

Figure 5.6: Fourier spectrum of elevation amplitude (m) for scenario 5.

The spectra of scenario 3 and 4 look like those of scenario 1 and 2. The lowest frequencies still have the highest amplitude. However, for location I the amplitudes of modes 9 to 15 are higher than mode 8. These modes have a period between 18 and 11 hours. A single amplitude peak for mode 7 can be seen at locations K and L, this mode has a period of 24 hours.

The higher influence of the 7th mode can also be seen in the surface plots. The light blue area extends to locations K and L. Secondly, these plots show again that the highest amplitudes for the first 8 modes are underneath the storm track.

Scenario 5&6

The results of scenarios 5 and 6 are shown in Figures 5.6, G.3, G.8 and G.9.

The spectra of scenario 5 and 6 are more divers than the ones of the other scenarios. Several separate peaks can be distinguished in the spectra; At all locations mode 7 shows a large amplitude compared to the modes which are slightly lower or higher. Second, Location I, K and L also show a peak at mode 15, which could be a higher harmonic, separately induced by the storm. Third, at these three locations an increase in amplitude can also be seen at modes 28 to 41, with a peak around mode 35. Fourth, location A, I, K, L and M show noise in the higher frequencies, which is absent at locations B, D and F.

The surface plots also indicate that the 7th mode has a large amplitude over almost the whole basin. Furthermore, these surfaces show that the maximum amplitude is spread over the whole basin. In contrast to the previous scenarios were this was more confined along the coastline and beneath the storm track.

5.3   Parameter sensitivity

Simulations of the different scenarios reveal sensitivity to used storm parameters. The varied storm parameters are two combinations of P_c and R_{max} and three different storm tracks $((x, y)_{origin}, \phi)$. These observed patterns and sensitivities are described in this section.

5.3.1   Track

The storm track shows to be a more important parameter than the difference in P_c and R_{max}. A clear distinction can be made between the water level trends of hurricanes with the three different directions (NE, N, NW) (Figure 5.2). This distinction can also be made based on the frequency spectra of the Fourier modes. Storms with the same direction show a similar qualitative pattern for the water levels Figure 5.3 and Fourier spectra Figures 5.4 to 5.6 and G.1 to G.3.

Direction NE and N are qualitatively more similar than direction NW. Water levels of direction NE and N show in general a steep increase to the maximum surge, with a relative constant water level before and after the storm. Storm direction NW on the other hand, is especially different because these storms cause a periodic signal after the storm surge and show a water level increase a day prior to landfall.

The maximum surge depends on the storm track as well. When comparing storm tracks, the difference in the surge at all locations is in the order of tens of cm to several m. A maximum difference of 2.36 m can be observed at location A (between scenario 1(NE) and 5(NW)).

Also the timing of the maximum surge is influenced by the storm track. Where the maximum surge at location F for scenario 1 and 2 is around moment of landfall, it is 6 hours later for scenarios with both tracks N and NW. The maximum surge levels also indicate that the storm surge for different directions moves in a qualitatively different path through the basin (Figure 5.3). The storm surge from NE track starts at the A to D and out of the basin at K. Whereas the surges of storm directions N and NW end up at the closed end of the basin.

The analysis of the elevation amplitudes of the Fourier modes shows the same importance of hurricane track. The amplitude spectra for the NW direction storms are clearly different than for the other storm scenarios These spectra show a peak at all locations for mode 7 and more noise at the higher frequencies.

All in all, the storm track influences all the indicators selected for the water level analysis and is therefore considered as an important parameter for the storm surge response. Not only the maximum surge is different, but also the whole process of the surge entering the basin happens shows a completely different pattern. This can also be found in the spectral response. Which reveals a different response to the Fourier modes per storm direction.

5.3.2 P_c & R_{max}

Comparing the results of two scenarios with same track (e.g. 1&2, 3&4, 5&6) shows that the surge response is almost insensitive to the different combinations of P_c and R_{max}.

Scenarios with the same storm direction show the same qualitative water level trend. The observed maximum surge level tend to be higher for scenarios with a lower central pressure. This can also be derived from the spectral response, where the spectral response per storm direction is comparable. The amplitudes for the scenarios with the lower pressure are slightly higher.

For scenarios with storm track NE and N the relative difference between water levels of the two storms is relative small, whereas for scenarios 5 and 6 this difference is bigger. Especially at locations A, I and K the water differences between the storms are around the 35 cm. For scenarios 1&2 and 3&4 this difference is in the order of a few cm (except for the maximum surge).

The results also demonstrate that timing of the maximum storm surge is scarcely influenced by different P_c and R_{max} combinations. The timing of the peaks deviates with a maximum 2 hours, which is the smallest time step for the calculations, meaning that the deviation could be even smaller.

In other words, hurricanes with a lower central pressure and smaller size tend to produce higher maximum water levels, whereas the course of the water levels is only slightly influenced. Scenario 5 and 6 on the other hand, show that the sensitivity to P_c and R_{max} depends on the track of the hurricane as well.

5.4 Physics behind the storm surge responses

The deviation in storm surge responses reveals that different physical processes take place for each landfall making hurricane. Depending on the scenario, some of these processes are more important than others. These processes can either be local factors or large scale factors as specified in Section 2.3. Since the storm scenarios do not cover change in forward speed and Holland-B parameter, processes related to these parameters are ruled out. The slope and the shape of the

coastal area are also kept the same for all scenarios, yet, these factors could still be of influence because of the different angles of approach.

Surge movement through basin

The difference in surge movement through the basin is shown in Figure 5.3. It can be seen that this is mainly dependent of the storm's direction and wind direction during its track over the basin. This can be deduced from the coastal basin's shape and the wind direction. It acts like a concave basin capturing the surge for the storms of direction NW, while for directions NE and N the Mississippi dikes form a solid barrier for the storm surge. Winds first blow towards the Mississippi river dikes and later blow away from the dikes onto the shore around location I.

Bouncing

As described in Section 1.2 hurricane Katrina seemed to be 'bouncing' from the Mississippi dikes to the northern coast of the basin. This bouncing can also be found in the surge response of storm directions N and NW when looking at the peak water levels (Figure 5.3). These tracks are both comparable to the track of hurricane Katrina in different stages of her approach to New Orleans. The NW track is applicable to the first part of hurricane Katrina's track entering the Gulf, while the N track is more comparable to Katrina's direction when making landfall.

   The results for water levels and amplitudes spectra indicate that this bouncing is a single event. The water levels at locations show no sign of a second peak between 5-6 hours, the spectra do not show a higher amplitude at modes with this period either. The surge only bounces from the Mississippi dikes to the northern shore where it is not reflected again. This bouncing is therefore not considered as a form of resonance within the coastal basin.

(Fore)runner

The storm surge responses of scenario 5 and 6 show influence of a large scale effect. An early rise of water level is simulated 20 hours before the storms makes landfall at the coasts of New Orleans. The early rise suggests a forerunner entering the basin. This forerunner is created at the coasts of Florida by the continued shore parallel winds. It propagates from east to west (to New Orleans). The forerunner reaches the basin one day ahead of the storm's surge.

   On the other hand, this forerunner can be seen as a runner creating a periodic signal as described in the following paragraph.

Geometry and bathymetry

Bathymetry and geometry of the Gulf have a large influence on the surge response. The shape of the Gulf and the continental shelf make it possible for a forerunner to develop if the storm direction is north west.

   Even so, the topographical step, near the coastal basin, increases the effect of the storm surge from all directions amplifying the surge compared to the deep water. The shallow part at the closed end however, indicates to decrease the surge or reflect the surge rather than to increase it. This can be caused by the higher friction in this shallow area.

The NW storm track shows also signs that can be related to shelf resonance. Looking at the amplitude spectra of scenario 5 and 6 (Figures 5.6 and G.3), these show higher amplitudes for modes 28-41 at locations I, K and L. The surface plots (Figures G.8 and G.9) show that these amplitudes follow the underling bathymetry lines. This increase in amplitude can be related to shelf resonance due to a reflecting wave at the topographical step. This is also observed during hurricane Ike (Hope et al. (2013)). According to Pugh (1987), the period of an open resonant basin is computed as:

$$T_{natural} = \frac{4L}{\sqrt{gh}} \tag{5.1}$$

where T is the resonant period (s), L the length of the open basin (m) and h the water depth (m). At locations I, K and L the water depth is 20 m. The distance to the topographical step is between 50 and 80 km (depending on the wind direction). The resonance period should than be between 4 and 6 hours. This is consistent with the period of modes 28-41.

5.5 Anomalies

Some of the results are remarkable compared with observed water levels of hurricanes and my expectations of the surge water levels. These exceptions are discussed here.

Spiky signal

The water level trends of scenarios 5 and 6 show a 'spiky' signal prior to the maximum surge. This behaviour was not expected beforehand and is also not observed in the other scenarios. An explanation could be the large grid size at the topographical step. The large change in water depth for different adjacent elements could lead to solutions which are less accurate. However, as discussed in Section 4.2.3, decreasing the element size resolves not all spiky signals.

A possible other explanation is given by Valle-Levinson (2015), who calls this signal 'wiggles' which arise from atmospheric forcing interacting with long ocean waves. These wiggles are observed to have periods in the order of 1 hour and are known as meteotsunamis.

Periodic signal

The periodic signal (observed in scenarios 5 and 6) cannot be explained by known physical processes from real hurricane surges. Nevertheless, it can be explained by a (fore)runner and the model boundary conditions.

This periodic signal suggest that the Dirichlet boundary conditions partially reflect the forerunner and keep the wave circulating inside the domain. Inside the basin it propagates like a Kelvin wave along the inverted barometer boundaries towards the coast of Florida again. The runner has a velocity of approximately 50 km/h along the coasts where the water depth is 20 m. This propagation speed is consistent with a Kelvin wave for this depth (50.4 km/h). In the deep part of the basin the amplitude of the circulating wave decreases while the propagation speed increases. This is also consistent with the wave speed in 1000 m deep water (as in the Gulf of Mexico). A wave with that depth should have a propagation speed of 100 km per hour.

The periodic signal has a period of 22-24 hours. This is consistent with the results in the Fourier spectra (Figure 5.6), that show a peak at mode 7 for all locations. This mode has a period of 24 hours. The surface plot of mode 7 also shows high amplitudes in the shallow parts and a lower amplitude in the deep part which is in accordance with a Kelvin wave in deep and shallow water.

If the runner was merely a forerunner consisting of one wave signal, this would have shown up in the amplitude of mode 1. Because this mode shows water elevations which happen only once every 7 days (T_{rec}), as would be expected from a forerunner.

No funnelling

Observed surge levels of hurricane Katrina and Isaac show that the maximum water level at locations D and E are among the highest. This can be explained by the funnelling effect of the basin and the shoaling effect of a decreasing water depth. In the simulations of the scenarios however this is not seen.

Compared to other locations the surges of storm directions N and NW (scenarios 3-6) show only a minor increase in water level at location D (closed end of the basin). This phenomenon is remarkable because both of these storm directions fill the basin and the surge moves to the closed end of the basin (Figure 5.3). The closed end of the basin is shallow (3 m), implying a higher friction which can reduce the surge levels. However, it seems as if the surge is possibly reflected at this shallow part and does not travel further into this shallow area.

5.6   Summary

To investigate the sensitivity to storm parameters, many scenarios can be created. For this study a synthetic set of 6 scenarios is composed. These scenarios represent storms that might occur in the New Orleans area.

Simulations of these scenarios show that surge response is more sensitive to storm direction than to the combination of P_c and R_{max}. All selected indicators (the water levels, peak levels, timing of the peaks and amplitude spectra) of different storm directions show a clear distinction. This difference is larger than for the different combination of P_c and R_{max}. A lower P_c and a smaller R_{max} only tend to produce a higher maximum surge in the order of centimetres. Not only the water levels are influenced by the storm direction, also the whole process of the surge entering the basin shows a completely different pattern.

This surge response can mainly be explained by a combination of local and large scale processes. The surge movement through the basin is mainly caused by the storm direction and local geometry of the basin. This results in the surge bouncing from one side to the other for NW and N storm directions, while for the NE direction the surge moves along the coasts.

Large scale processes on the other hand, are most important when the storm has a north western trajectory. The geometry and bathymetry of the Gulf combined with the continued shore parallel winds create a (fore)runner along the gulf of Florida which propagates with approximately the same speed as the hurricane towards New Orleans.

The spiky and periodic signal observed in the water level simulations. Both can be explained by made model choices. Nevertheless, the spiky signals could also be so-called meteotsunamies.

Chapter 6

Discussion

The previous chapters report the model set-up, model performance analysis and the conducted surge sensitivity study. This section discusses some important assumptions, model choices and the found results. Model input based on historical data is briefly discussed as well.

6.1 Storm surge model

In order to do a sensitivity study, model calculation time needs to be low. The storm surge model is therefore selected for this study due to its idealized character. The finite element method together with the Fourier transformation results in a relatively quick model. However, during the process of setting up the model multiple adaptations were made resulting in a calculation time of 3 hours. The linearised nature of the model affects the results, this effect is discussed in the following sections.

6.1.1 Linearised shallow water equations

Linearised shallow water equations are used for the model formulation. This means that the advection terms are absent and bottom friction is linearly implemented. Furthermore this implies that the model cannot deal with zero water levels at some locations. The domain is therefore formulated with a larger water depth than is comparable with reality. Compared with reality the bottom stress in shallow waters will be less resulting in an even higher surge than simulated in the model.

Excluding non-linear effects

The observed water levels at the coast are built up by several components (Section 2.3). The sum of these components results in the total water level used for coastal protection purposes. In this research, all components are excluded except the large scale processes. However by doing this, non-linear interactions between for example tide and storm surge are neglected.

The tides are not considered in the model. The used observed water levels however, did include tides before preparation. Tidal predictions are simply subtracted from the observed water levels. It is shown that non-linear effects are greatest when hurricanes make landfall during low tide (Rego and Li, 2010).

Non-linear effects could reach up top 80% of the tidal amplitude, which in this case is 0.4 m.

Tides could be included in the model by imposing a tidal signal on the open boundaries of the model. This would improve the computations of the surge levels but the inverted barometer cannot be applied at the same time. For this idealized study to storm parameters the tide is therefore neglected.

6.1.2 Grid size and bathymetry

The grid size should be smaller in areas with large variations in bathymetry (or geometry) to capture a smooth signal for all the changes. In this model set up the grid size is only reduced in areas along the coasts. The topographical step at the border of the continental shelf is covered with a bigger grid size. This could lead to large differences between elements and a solution which is not as accurate. This could be a possible explanation for the 'spiky' behaviour of the water level prior to landfall of the hurricane. Increasing the number of elements at the topographical step could diminish this effect. As seen in the model sensitivity, a finer grid reduces the amplitude of the 'spiky' signal but does not eliminate it completely. A drawback of this finer grid is the increasing computational time.

6.1.3 Boundary conditions and domain size

The boundary conditions in this study showed to be very important but at the same time very difficult to impose realistically. Especially the choice for the open boundary condition was a trade-off between calculation time, precision and link to reality. Simulations showed that domain size and the choice for an open boundary were coupled, therefore these are discussed together.

Closed boundaries

The choice for the closed reflecting boundaries representing the coastlines of the domain is quite straight forward. Water should be limited to flow only inside the basin. Still this choice for closed boundaries influences the results. In reality the coastline lies more inward during high water levels than during low water levels, and during a surge, water can flow land inward if water levels reach above the defence systems. The boundaries are modelled as a wall thus all waves are reflected. These aspects causes a higher simulated surge and less dissipation of energy. For this reason can simulated resonance or sloshing effects be larger than in reality.

Inverse barometric boundaries and domain size

The open boundary choice was more complex. Several model simulations were made to assess the effects of the different boundary conditions, either a non-reflecting boundary condition or an inverse barometric Dirichlet boundary condition. Furthermore different domain sizes were used for these considerations.

The Dirichlet boundary condition imposes a surface elevation and should therefore be located at locations where surface elevation due to wind is small compared to the inverse barometer effect of a hurricane. The boundaries should be far away from the dynamic area in the domain. This is not the case for the western boundary, from the Mississippi dikes to the most southern boundary. The boundary crosses the topographical step and is close to the New Orleans

coastal basin where many processes take place during a storm surge. At this boundary a discrepancy could arise between the imposed water levels and water levels inside the domain. Possibly creating an 'partially-reflecting' boundary condition. The simulations suggest that this is also happening. The periodic signal is simulated for the north west directed storms. These simulations show a wave travelling through the basin along both closed and open boundaries. The boundary should therefore be located further away.

The effect of this rotating wave is assumed to be small. The wave dissipates slowly and is in the order of a few cm at the end of the recurrence time.

The very first simulations started with merely the local domain (blue in Figure 3.4), but this showed to be inadequate to simulate large scale effect and not applicable with the open boundary condition. The larger domain used in this study showed to be able to include the large scale processes. Nevertheless as discussed, the open boundaries at some location are still too close to the dynamic area. Blain et al. (1994) emphasize that the domain should be even bigger; a domain capturing the whole west side of the Atlantic ocean, including Caribbean islands. For this study it was practically impossible to simulate with such a basin concerning the large increase in calculation time this would mean.

6.2   Historical data

Historical data were obtained from various sources. Uncertainty is already assessed in Section 4.1.3 and summarized in Table 4.3. Both sources for water level are considered as moderate to good. However the simulations can still deviate from these water levels since the domain does not includes Lake Pontchartrain. This lake is located north of New Orleans. A study on the closure of the lake during storm demonstrates that closing lake Pontchartrain results in water levels up to 4 ft (1.22 m) higher for a 100-year storm along the Biloxi marshes and the coasts of Lake Borgne surges (Southeast Louisiana Flood Protection Authority - East, 2012).

However, the simulated water levels at these locations (D to H) are lower than the observed water levels. These location are also situated at the coast of the shallowest part of the basin. At this closed end, the water depth is exaggerated resulting in a lower surge. It could be that the effect of closing the lake is reduced by the larger simulated water depth.

6.3   Model behaviour

The model behaviour is analysed in Chapter 4. This reveals that this idealized model is only capable reproducing a qualitative comparable surge response. This is an reasonable result, taking into account the idealized nature of the model. The model behaviour proves that the model does simulate the main processes of a storm surge and can be used to study surge response. However, it means that conclusions based on the simulated water levels and amplitudes spectra should be made with care.

The sensitivity to grid size implies that the simulated water levels are still dependent on numerical choices. This is undesirables because it means that found patterns in the water levels could be model induced instead of induced by the wind and pressure forcing. The size of the elements should be further refined

for following studies. Based on already made model improvements made by Chen (Appendix H) concerning grid size, it is shown that increasing the number of grid points improves the results.

6.4   Sensitivity study

The sensitivity study to storm parameters is the main objective of this study. The results of the storm scenarios are already shown in Chapter 5. Implications of these results are discussed here.

First, the number of storm scenarios is limited. At most two different values are used for a parameter which means that only limited conclusions can be based on these results. On the other hand, the simulations show enough deviation to conclude that the storm track is an important parameter. A step to increase the number of scenarios is already made and described in Appendix E.

Secondly, the simulations show a 'spiky' behaviour prior to landfall and in some cases a period signal after landfall of the hurricane. These phenomena cannot be explained entirely yet. Their impact on the storm surge cannot be predicted.

Finally, the sensitivity study reveals no big influence of the R_{max} or P_c whereas these are considered as important parameters for the surge levels in both the Saffir-Simpson scale and by Irish et al. (2008). This may be explained by the combined change of P_c and R_{max} in the scenarios. It could be that the higher central pressure decreases the effect of a larger R_{max}. Furthermore the effect of R_{max} or P_c is more apparent at one of the tracks. This suggests that parameters could be more or less important when a storm approaches New Orleans from another direction.

6.5   Summary

The storm surge model and the chosen model set-up result in several drawbacks. The grid size is too large at the topographical step and the open boundaries still partially reflect a wave. This affects the results by the seen 'spiky' signal and the period signal. However, the qualitative surge response is considered to be simulated fair despite of these phenomena. The model is therefore still considered appropriate for the sensitivity study to storm parameters.

Historical data is selected and prepared with care, nevertheless the locations of the simulated water levels are approximations. This way the simulated water levels could still deviate much from the observed ones.

The results of the sensitivity study are notable. The storm track is found to be the most important parameter for all factors concerning the surge. In literature however the focus is still on the storm intensity and storm size as main contributor for the maximum surge.

Chapter 7

Conclusions and Recommendations

This research is focussed on storm surges and the effects of storm parameter on the surge responses at the coasts of New Orleans, through idealized process-based modelling. This final chapter presents answers to the research questions posed in the first chapter. Recommendations will be made based on the answers to the research questions and the discussion in Chapter 6.

7.1 Conclusion

The research questions formulated in the first chapter will be answered here. Focus is on the last two questions because these are the main questions contributing to the objective of the study, whereas the first two questions address model properties and its performance.

1. How can the domain, parameters, forcing and boundary conditions of the idealized storm surge model be formulated to calculate the storm surges at the coasts of New Orleans?
This question has been answered in Chapter 3. Bathymetry and domain are chosen to schematically represent the New Orleans area. An inverse barometric Dirichlet boundary is used to represent the domain boundaries connected to the open water of the Gulf. The coastal boundaries are represented by reflecting boundaries where no normal flux is allowed.

Despite the relatively small area of interest the domain was chosen to simulate the whole north west part of the Gulf of Mexico. A small domain concerning only the local scale of the New Orleans area showed to be inadequate, large scale processes could not be simulated.

2. How does the idealized storm surge model behave and perform when applied to a realistic case study?
This question has been answered in Chapter 4, where model performance and sensitivity are investigated.

The model's performance is assessed by a hindcast of two historic storms. The reproduced water levels showed that the model is able to simulate qualitatively comparable surge levels. However, no quantitative comparison could be made because the simulated water level deviated too much. With a drag

coefficient of $2.54e^{-3}$ (-) the model reproduces comparable peak surges, while it underestimates the water level rise prior to landfall. The timing of the peak water levels is comparable, just as the overall simulated water level trends at the measurement locations.

The maximum surge levels are comparable but the water level trend is underestimated prior and after landfall. The timing of these peaks levels on the other hand, is comparable at all locations. The qualitative trend of observed water levels is reproduced by the model.

During the behaviour analysis it was pointed out that the simulated 'spiky' signal can be partially explained by the grid size. A new grid with smaller elements reduced the amplitude of the spikes, but those did not vanish completely and not at all locations. The behaviour study also revealed a high dependency to drag coefficient. The higher drag coefficient resulted in surge levels which were in better agreement with the observations. The default drag coefficient is therefore changed to this higher value for the sensitivity study.

The model demonstrates to be insensitive to friction parameters and the number of modes. The influence of changes in water depth was small as well, though changing the slope of the topographical step had a larger effect.

The model is judged to reproduces water levels which are in fair agreement with the observations. This is considered to be sufficient to study the sensitivity of surge response to storm parameters.

3. What is the sensitivity of the storm surge response to storm parameters?

This question has been answered in Chapter 5, where six different storm scenarios are presented.

The computed surge levels show that for this set of storm scenarios the track of the storm is the most important storm parameter. Water level trends for storms with different directions show a clear distinction. The storm direction affects all used indicators; maximum surge level, timing of the surge, the whole trend of the water level as the amplitude spectra. The deviation of surges caused by storm direction is in the order of tens of cm to several m, with a maximum of 2.36 m. The combinations of P_c and R_{max} on the other hand show only small differences in maximum surge, in the order of a few cm to 35 cm. The results also revealed that the sensitivity to P_c and R_{max} is depending on the storm track as well.

The simulated surges for the three different storm paths show a completely different pattern for the whole process of the surge entering the basin. Where the surge for the north east storm direction develops along the Mississippi dikes and goes to the east, the surges of the northern and north west track come from the east and are captured in the New Orleans coastal basin.

The direction of the storm has also affect water levels further away from the New Orleans coastal basin. The north western track is the only storm direction which generates a forerunner increasing also the water levels far away from the storm. This forerunner propagates from east to west along the coasts of Florida.

4. How can the (characteristic) storm surge response be explained?

This question has been answered in Chapter 5. The deviation in storm surge responses reveals that different physical processes are happening simultaneously.

Both local processes and large scale processes are affected. Depending on the storm the relative importance of these processes is different.

The sensitivity reveals that the storm direction mainly determines the important processes. The surge pattern moving through the basin is mainly caused by the local geometry of the basin and the wind direction. For the northern direction the surge moves out of the basin towards the east. While for the other directions the basin acts more like a funnel, capturing the surge at the closed end. This results in the observed surge to bounce once from one side to the other side of the basin.

large scale processes are more important for the storm with a north west direction. A forerunner is generated while this is not apparent for the other two storm directions. The geometry of the Gulf is a main contributor for this distinction. The north western path runs along the coasts of Florida inducing a set-up and the forerunner. The storms with other paths have no coastline and continental shelf at the east side of the hurricane where these processes can develop.

7.2 Recommendations

Based on this research multiple recommendations can be made. Both for further research as for improving the model. Furthermore recommendations can be formulated for policy makers. Most aspects have been discussed already in Chapter 6 and are only shortly touched upon.

7.2.1 Recommendations for further research

Further research should focus on extending the number of scenarios. A first start for this is already made. The focus should be on the sensitivity of different storm parameters as well as the sensitivity in combination with each other. Results of this study indicate that for instance the sensitivity for P_c and R_{max} is higher with a specific angle of landfall. With more scenarios the different surge responses between Isaac and Katrina (Chapter 1) could be explained in more detail.

Secondly, in my opinion more research is needed into storm surges on non-straight coastlines and the effect of large scale processes. Several storm surge studies are now focused on straight coastlines, only varying the storm parameters. The effect of large scale processes is then small or not considered. Yet this study shows that geometry of the coastline is important as well, for both the storm surge as well as the large scale processes contributing to storm induced water level changes.

7.2.2 Recommendations for improving the model

Further research using this model should start by improving the model. As discussed the results still show some unfathomed phenomena. Most important point of improvement is open boundary condition. The boundary conditions should be improved to allow a wave to travel out of the basin, without partially reflecting it. Even tides could be incorporated in the model by adding the periodic signal to the domain boundaries. Secondly, the element size of the grid should be decreased. The elements should be smaller especially at the topographical step

to ensure results are not affected by merely model induced signals. A start for this improvement is already made and shown in Appendix H Additionally, the domain of the study should be extended. Behaviour of large scale effects such as seiching of the entire Gulf is unknown at the boundaries of this domain. The accuracy of the forcing storms can be improved by using more modes representing the forcing.

Finally, the objective of this study is not to accurately predict extreme water levels. It cannot be recommended to use this model to predict extreme conditions during storm surges, since the model is used to determine the effects on only the most important processes of a storm surge. Other models should be used for that purpose. However, more information about storm surge response and characteristics obtained with this model can be used to improve the design of coastal defences.

7.2.3   Recommendations for policy makers

This study shows that the storms that approach the New Orleans coastal area with a NE direction are very important. Water levels are higher at most locations and a forerunner induces a higher set-up before landfall of the hurricane. Policy makers should focus on storms from this direction and steer more sensitivity studies to focus on this direction sensitivity and the specific geometry of the New Orleans coastal basin within the Gulf of Mexico.

Bibliography

Amorocho, J. and DeVries, J. J. (1981). A new evaluation of the wind stress coefficient over water surfaces. *Journal of Geophysical Research*, 86(C5):4308.

As-Salek, J. A. (1998). Coastal Trapping and Funneling Effects on Storm Surges in the Meghna Estuary in Relation to Cyclones Hitting Noakhali–Cox's Bazar Coast of Bangladesh. *Journal of Physical Oceanography*, 28(2):227–249.

Barras, J. (2005). Land Area Changes in Coastal Louisiana After Hurricanes Katrina and Rita. *Unites States Geological Survey*, pages 97–112.

Blain, C., Westerink, J. J., and Luettich, R. A. (1994). The influence of domain size on the response characterstics of a hurricane storm surge model. *Journal of Geophysical Research*, 99:467–479.

Bode, L. and Hardy, T. (1997). Progress and recent developmenst in storm surge modeling. *Journal of Hydraulic Engineering*, 123(4):315–331.

Brunt, D. (1934). *Physics and Dynamical Meteorology*. Cambridge University Press, Cambridge.

Chen, W. L. (2014). A 3D storm surge model using Finite Element Method.

Chen, W. L., Roos, P. C., and Schuttelaars, H. M. (2014). Storm surge response in large-scale basins: influence of topography. In *Physics of Estuaries and Coastal Seas*, number October, pages 17–20.

Chen, W. L., Roos, P. C., Schuttelaars, H. M., and Hulscher, S. J. M. H. (2015). Resonance properties of a closed rotating rectangular basin subject to space- and time-dependent wind forcing. *Ocean Dynamics*, 65:325–339.

Cobell, Z., Zhao, H., Roberts, H. J., Clark, F., and Zou, S. (2013). Surge and Wave Modeling for Louisiana 2012 Coastal Master Plan. *Journal of Coastal Research*, pages 88–108.

Dietrich, J. C., Tanaka, S., Westerink, J. J., Dawson, C. N., Luettich, R. a., Zijlema, M., Holthuijsen, L. H., Smith, J. M., Westerink, L. G., and Westerink, H. J. (2012). Performance of the unstructured-mesh, SWAN+ ADCIRC model in computing hurricane waves and surge. *Journal of Scientific Computing*, 52(2):468–497.

Dijkman, J. (2007). A Dutch perspective on coastal Louisiana flood risk reduction and landscape stabilization. Technical Report October, Netherlands Water Partnership, London.

Fitzpatrick, P. J. (1999). *Natural disasters: hurricanes: a reference handbook.* Abc-Clio Incorporated.

Harris, D. L. (1959). An interim hurricane storm surge forecasting guide. *U.S. Weather Bureau Tech*, 32:24.

Holland, G. J. (1980). An Analytic Model of the Wind and Pressure Profiles in Hurricanes. *Monthly Weather Review*, 108(8):1212–1218.

Homeland security Council (2006). The federal response to hurricane Katrina. Technical Report February, Homeland security Council.

Hope, M. E., Westerink, J. J., Kennedy, a. B., Kerr, P. C., Dietrich, J. C., Dawson, C., Bender, C. J., Smith, J. M., Jensen, R. E., Zijlema, M., Holthuijsen, L. H., Luettich, R. a., Powell, M. D., Cardone, V. J., Cox, a. T., Pourtaheri, H., Roberts, H. J., Atkinson, J. H., Tanaka, S., Westerink, H. J., and Westerink, L. G. (2013). Hindcast and validation of Hurricane Ike (2008) waves, forerunner, and storm surge. *Journal of Geophysical Research: Oceans*, 118(9):4424–4460.

Irish, J. L., Resio, D. T., and Ratcliff, J. J. (2008). The Influence of Storm Size on Hurricane Surge. *Journal of Physical Oceanography*, 38(9):2003–2013.

Jong, de, M. S. (2012). Developing a parametric model for storms to determine the extreme surge level at the Dutch coast. Technical report, Delft University of Technology.

Kennedy, A. B., Gravois, U., Zachry, B. C., Westerink, J. J., Hope, M. E., Dietrich, J. C., Powell, M. D., Cox, A. T., Luettich, R. a., and Dean, R. G. (2011). Origin of the Hurricane Ike forerunner surge. *Geophysical Research Letters*, 38(8):1–5.

Kumar, M., Schuttelaars, H. M., and Roos, P. C. (2015). Three-Dimensional Semi-Idealized Model for Tidal Motion in Tidal Estuaries An application to the Ems estuary. *Ocean Dynamics*, submitted.

National Climatic Data Center (2014). Historical Hurricane Tracks [Database record HURDAT2]. Technical report, NOAA.

National Oceanic and Atmospheric Administration (NOAA) (2015). Tides and Currents [Database record Water levels]. Technical report, Center for Operational Oceanographic Products and Services (CO-OPS).

National Weather Service (2014). National Hurricane Centre. URL: http://www.nhc.noaa.gov/. Date accessed: 20-12-2014.

Orders, T. (2006). Final Coastal and Riverine High Water Mark Collection for Hurricane Katrina in Mississippi.

Peng, M. L., Xie, L., and Pietrafesa, L. (2006). A numerical study on hurricane-induced strom surge and inundation in Charleston Harbor, South Carolina. *Journal of Geophysical Research*, 111(C8).

Population Division (2012). Population estimates. Technical report, U.S. Consensus Bureau.

Proudman, J. (1953). *Dynamic Oceanography*. Methuen and Co, London.

Pugh, D. (1987). *Tides, Surges and Mean Sea-Level*. John Wiley & Sons, New York, Swindon, UK.

Rego, J. L. and Li, C. (2010). Nonlinear terms in storm surge predictions: Effect of tide and shelf geometry with case study from Hurricane Rita. *Journal of Geophysical Research: Oceans*, 115(6):1–19.

Resio, D. T. and Westerink, J. J. (2008). Modeling the physics of storm surges. *Physics Today*, 61(9):33–38.

Roth, D. (2010). Louisiana Hurricane History. Technical report, National Weather Service, Camp Springs, MD.

Simpson, R. (1974). The hurricane disaster-potential scale. *Weatherwise*, 27:169.

Southeast Louisiana Flood Protection Authority - East (2012). New Orleans East Land Bridge Study. Technical Report December.

Straatsma, L. (2015). On the influence of storm characteristics on surge response in the New Orleans coastal basin: Literature study. Technical Report University of Twente, University of Twente, Enschede.

The Times-Picayune (2014). The Times-Picayune. URL: http://media.nola.com/news_impact/photo/map-stjohn-090112jpg. Date accessed: 19-12-2014.

U.S. Army Corps of Engineers (2006). Appendix B: History of hurricane occurences. Louisiana coatal protection and restoration (LACPR) Preliminary Tech. Rep. Technical report, New Orleans District Rep.

U.S. Army Corps of Engineers (2008a). Flood Insurance Study : Southeastern Parishes , Louisiana Intermediate Submission 2 : Offshore Water Levels and Waves.

U.S. Army Corps of Engineers (2008b). Flood Insurance Study: Southeastern Parishes, Louisiana. Technical report, New Orleans district.

Valle-Levinson, A. (2015). IMAU-colloquium: What are those 'wiggles' in storm surges? Utrecht.

Vickery, P. J. and Wadhera, D. (2008). Statistical models of Holland pressure profile parameter and radius to maximum winds of hurricanes from flight-level pressure and H* wind data. *Journal of Applied Meteorology and Climatology*, 47(10):2497–2517.

Weather Underground (2014). Subtropical storms. URL: http://www.wunderground.com/hurricane/subtropical.asp?. Date accessed: 18-11-2014.

Weenink, M. (1956). The 'twin' storm surge during 21st-24th December 1954. A case of resonance. *Deutsche Hydrograpische Zeitschrift*.

Weisberg, R. and Zheng, L. (2006). Hurricane strom surge simulations for Tampa Bay. *Estuaries Coasts*, pages 899–913.

Westerink, J. J., Feyen, J. C., Atkinson, J. H., Luettich, R. a., Dawson, C. N., Powell, M. D., Dunion, J. P., Roberts, H. J., and Ethan, J. (2005). A New Generation Hurricane Storm Surge Model for Southern Louisiana. Technical report, University of Notre Dame, Notre Dame.

Williams, L. (2007). Higher Ground - A study finds that New Orleans has plenty of real estate above sea level that is being underutilized.

Appendix A

Model set-up

This appendix presents extra figures illustrating the model set-up. This model set-up is described in Chapter 3.

Figure A.1 shows all observation and measure locations which are mentioned throughout the report. Figure A.2 shows the nodes for the unstructured mesh used for this study.
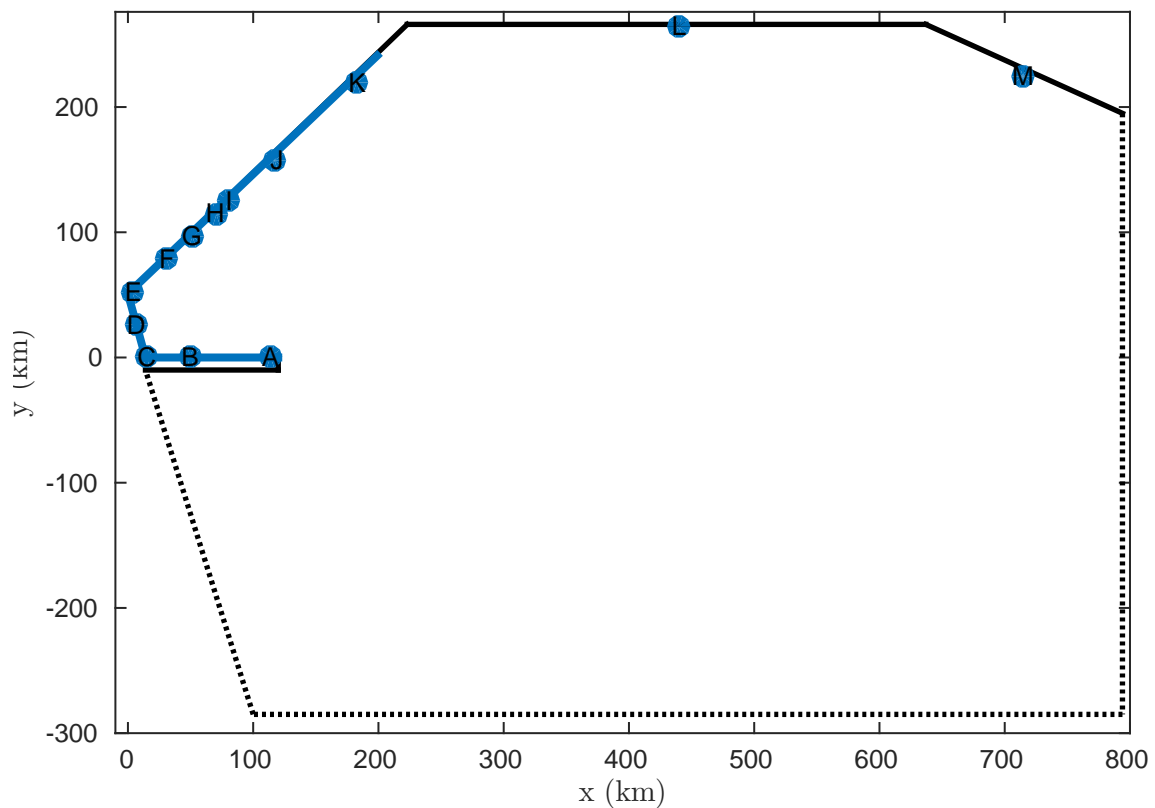
Figure A.1: Schematic representation of observation and measuring locations in the New Orleans area used for calibration and validation. All stations are listed in Section 4.1.1
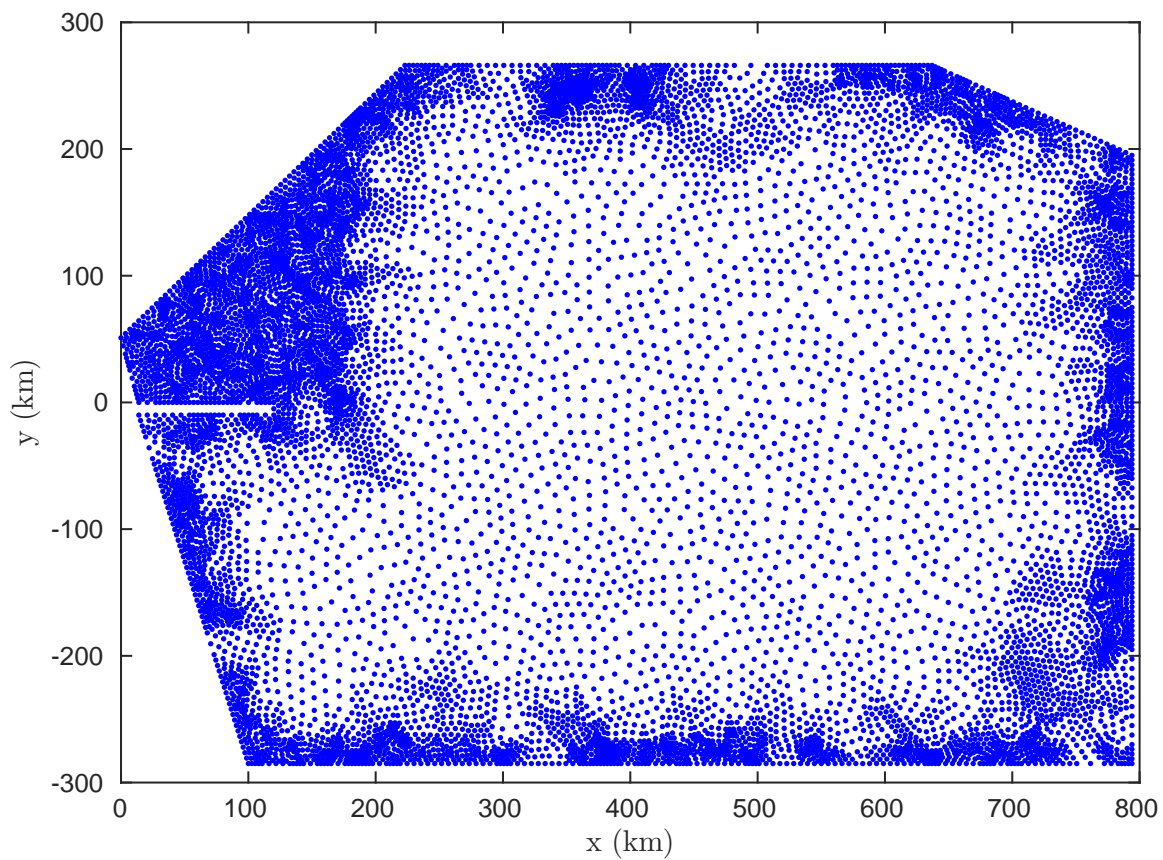
Figure A.2: Grid nodes (total of 10130 nodes) of the unstructured triangular mesh used for the simulations. Along coasts and in New Orleans coastal zone grid size is 6 km and 20 km in the middle of the domain.

Appendix B

Storm parameters

This appendix presents the storm parameters for hurricanes Katrina, Ivan and Rita. These are referred to in Section 4.1.2. First a table is presented with the used direction of each storm, then the other parameters are presented in Figures B.1 and B.2. Parameter of hurricane Katrina are shown in Figure 4.2.

B.1 Use of parameters

The values of 5 out of six storm parameters are given in the table and figures in this appendix. The sixth parameter, the location of the storm's centre at each time step, is derived from the forward speed C_f and the storm direction $/phi$.

All parameters are only specified for the first 67 (Katrina) or 73 (Ivan and Rita) hours. After these time steps the calculation continues with fixed parameter values to the last time step, $t = T_{rec} * 24 = 168$. The last prescribed value of all parameter are used for this remaining period. Meaning that the storm's wind- and pressure-field do not change over time and that the storm direction is one straight line.

Table B.1: *Parameter values of storm direction (ϕ) for hurricanes Katrina, Ivan and Rita.*

Time (h)	Katrina (°)	Ivan (°)	Rita (°)
1	255.96	295.64	233.23
2	255.96	295.64	233.23
3	255.96	295.64	233.23
4	255.96	295.64	233.23
5	255.96	295.64	233.23
6	255.96	295.64	233.23
7	256.23	294.57	228.41
8	256.23	294.57	228.41
9	256.23	294.57	228.41
10	256.23	294.57	228.41
11	256.23	294.57	228.41
12	256.23	294.57	228.41
13	264.17	295.77	233.49
14	264.17	295.77	233.49

Continued on next page

Table B.1 – continued from previous page

Time	Katrina	Ivan	Rita
(h)	(°)	(°)	(°)
15	264.17	295.77	233.49
16	264.17	295.77	233.49
17	264.17	295.77	233.49
18	264.17	295.77	233.49
19	286.70	311.00	250.00
20	286.70	311.00	250.00
21	286.70	311.00	250.00
22	286.70	311.00	250.00
23	286.70	311.00	250.00
24	286.70	311.00	250.00
25	297.03	322.00	252.00
26	297.03	322.00	252.00
27	297.03	322.00	252.00
28	297.03	322.00	252.00
29	297.03	322.00	252.00
30	297.03	322.00	252.00
31	317.39	330.32	259.56
32	317.39	330.32	259.56
33	317.39	330.32	259.56
34	317.39	330.32	259.56
35	317.39	330.32	259.56
36	317.39	330.32	259.56
37	317.82	324.61	258.00
38	317.82	324.61	258.00
39	317.82	324.61	258.00
40	317.82	324.61	258.00
41	317.82	324.61	258.00
42	317.82	324.61	258.00
43	317.82	324.61	258.00
44	317.82	324.61	258.00
45	317.82	324.61	258.00
46	317.82	324.61	258.00
47	317.82	324.61	258.00
48	317.82	324.61	258.00
49	317.82	324.61	263.37
50	317.82	324.61	263.37
51	317.82	324.61	270.00
52	317.82	324.61	270.00
53	317.82	324.61	270.00
54	317.82	324.61	270.00
55	317.82	324.61	270.00
56	317.82	324.61	270.00
57	317.82	324.61	270.00
58	317.82	324.61	270.00
59	317.82	324.61	270.00
60	317.82	324.61	272.00

Continued on next page

Table B.1 – continued from previous page

Time (h)	Katrina (°)	Ivan (°)	Rita (°)
61	317.82	324.61	271.03
62	317.82	324.61	280.00
63	317.82	324.61	280.00
64	317.82	324.61	280.00
65	317.82	324.61	280.00
66	317.82	324.61	281.00
67	317.82	324.61	281.89
68		324.61	281.89
69		324.61	281.89
70		324.61	281.89
71		324.61	281.89
72		324.61	281.89
73		324.61	281.92
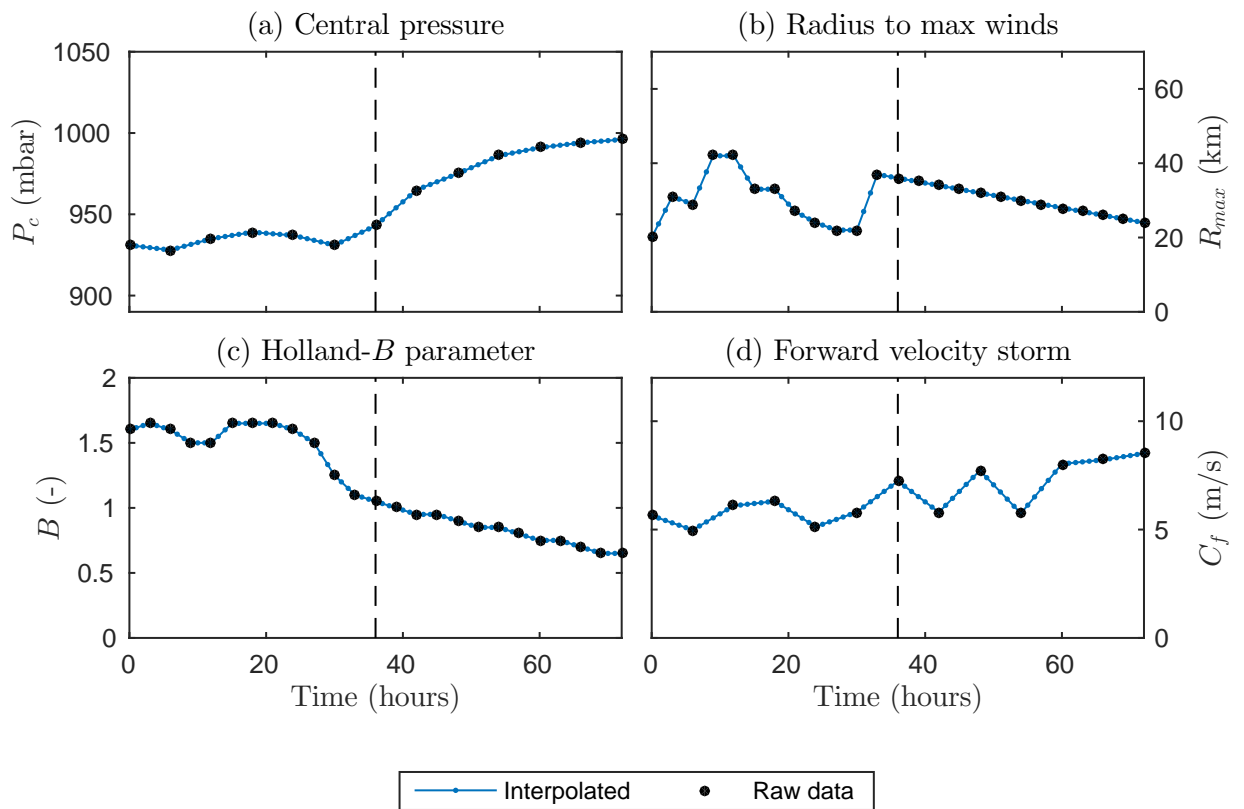
Figure B.1: Hourly storm parameters P_c, B, R_{max} and C_f of hurricane Ivan from 14-9-2004 0.00h till 18-9-2004 0.00h.
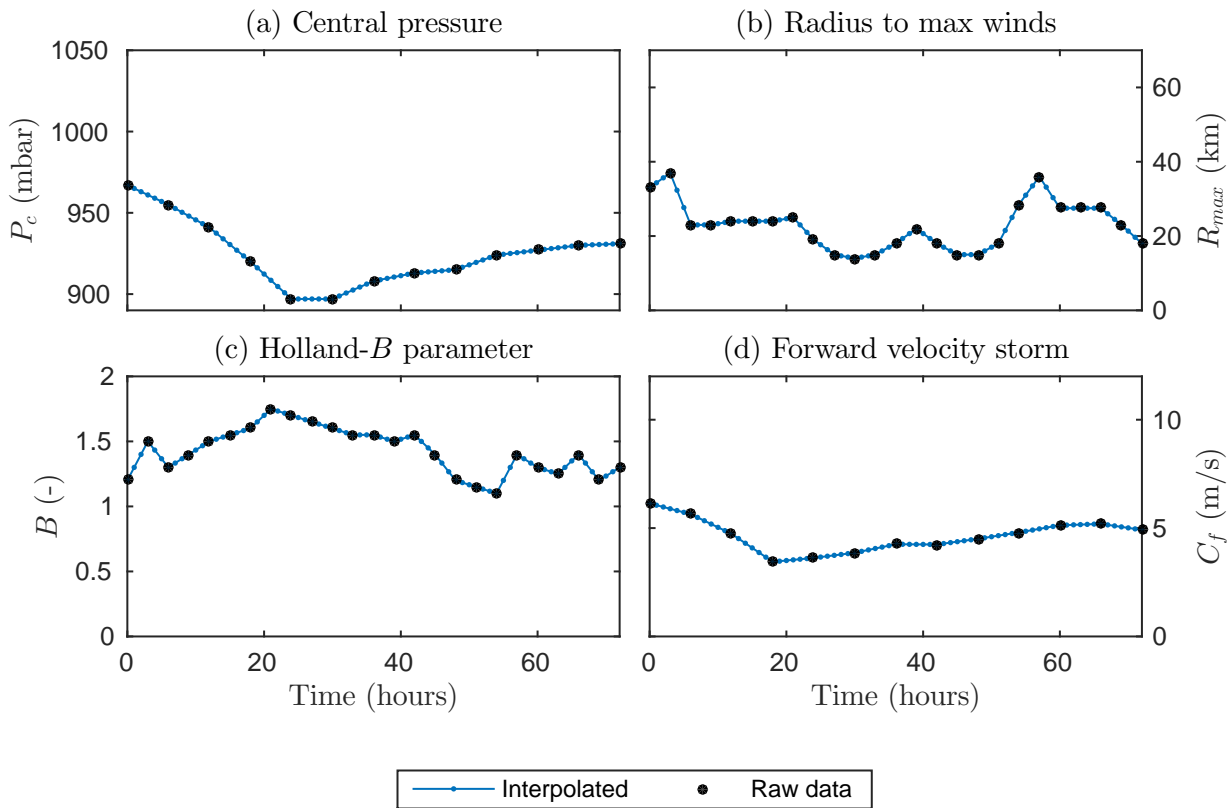
Figure B.2: Hourly storm parameters P_c, B , R_{max} and C_f of hurricane Rita from 21-9-2005 0.00h till 24-9-2005 0.00h.

Appendix C

Base case simulations

This appendix shows results of the base case simulations which are referred to in Chapter 4 . Base case simulations use the default model set-up as described in Chapter 3 and the storm parameters as specified in Appendix B.

Results of the water levels of hurricane Katrina are already presented (Figure 4.3). Water levels of hurricane Ivan and Fourier spectra of Katrina and Ivan are shown in this appendix.
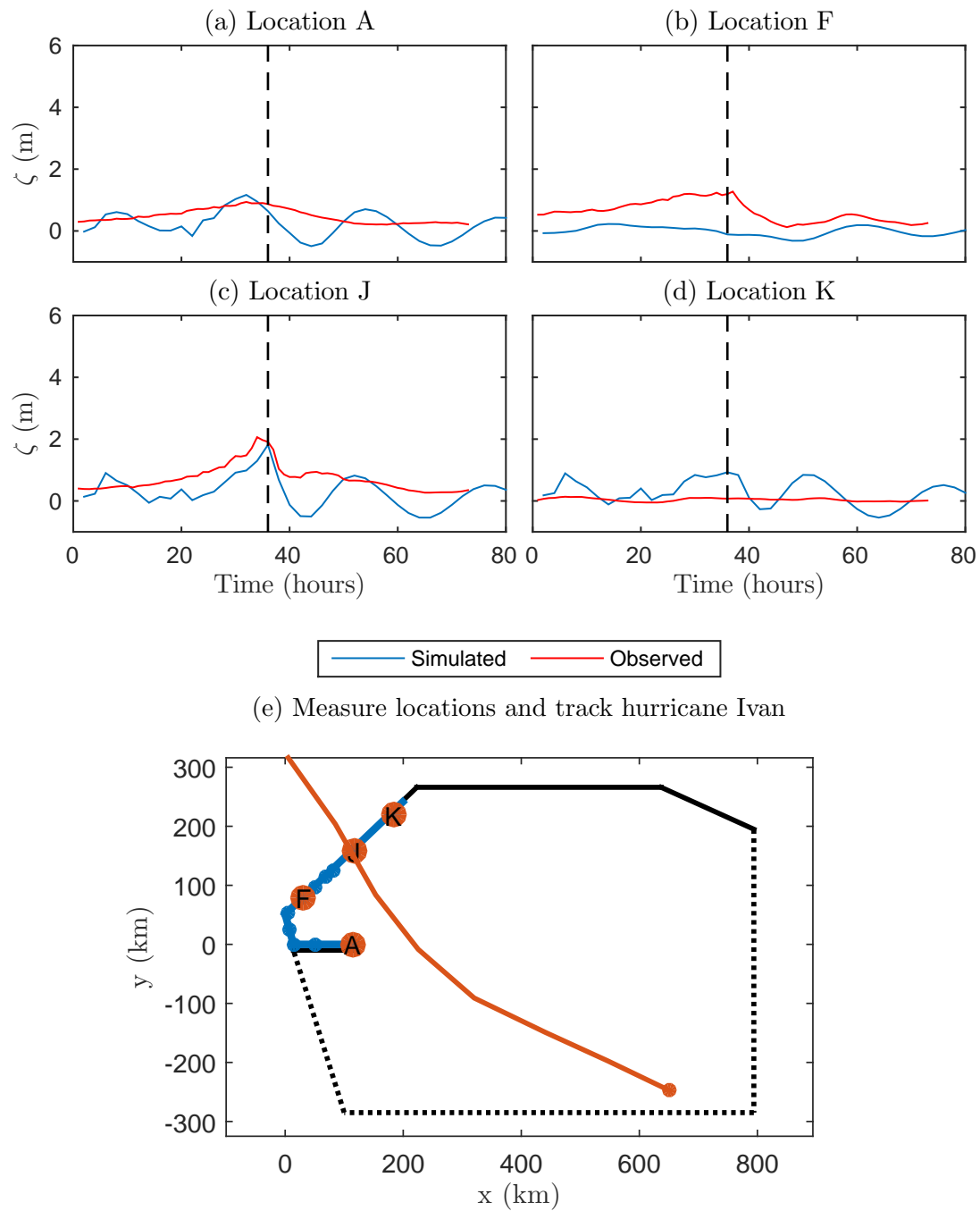
Figure C.1: Simulated water levels for hurricane Ivan (a-d). Vertical dashed line represents the time of landfall (t=36). (e) shows measuring locations and the track of hurricane Ivan.
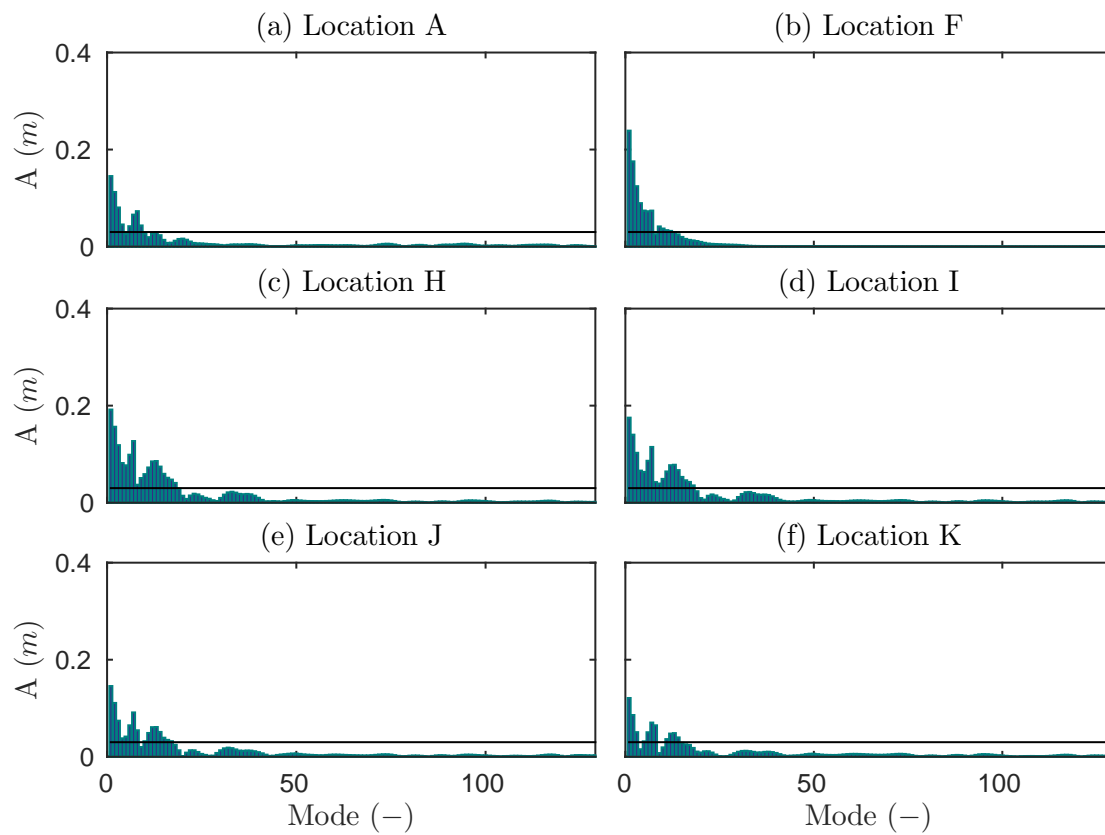
Figure C.2: Fourier spectra of elevation amplitude (m) for base case of hurricane Katrina.
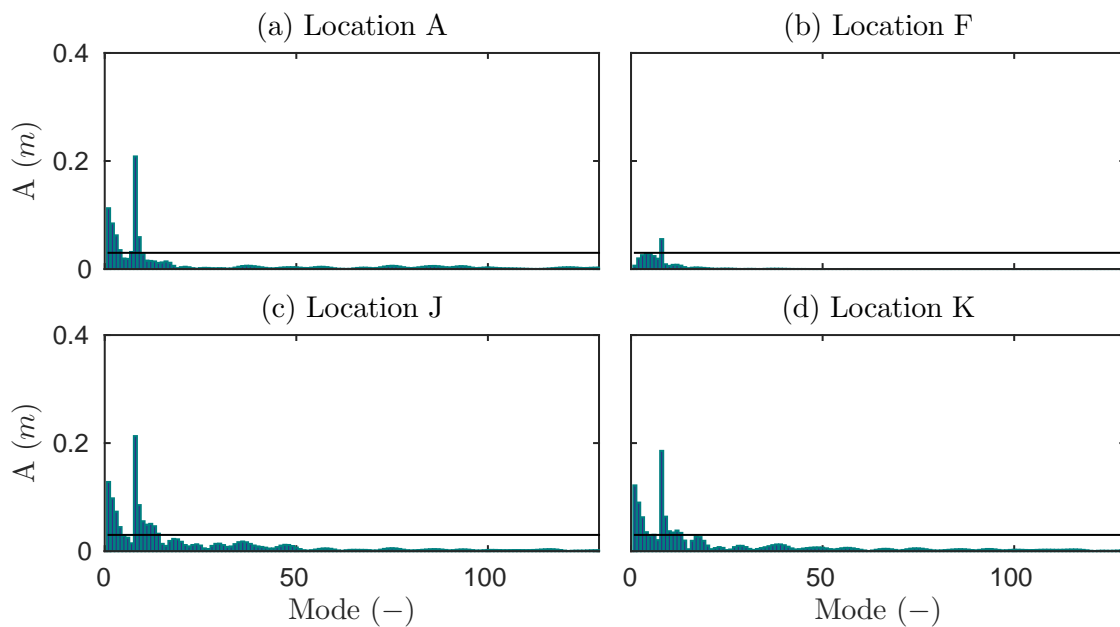
Figure C.3: Fourier spectra of elevation amplitude (m) for base case of hurricane Ivan.

Appendix D

Model performance

This appendix presents input and results of different simulations made to assess the model performance and behaviour. First the used input values and varied values are shown in Table D.1, followed by two extra figures visualizing the changes in input for bathymetry and grid size.

Second, the results of the different simulations are shown in Figures D.3 to D.9. These results are referred to in Section 4.2.3.

Table D.1: Default and varied physical parameters used to assess model behaviour.

Physical parameter	Default value	Changed values
Friction	A_v (m/s^2) and s (m/s)	A_v (m/s^2) and s (m/s)
	0.025, 0.01	0.035, 0.01
		0.015, 0.01
		0.025, 0.001
		0.025, 0.1
Bathymetry	Water depth (h)	Water depth (h)
	Figure 3.5	-20%
		+20%
		Smooth (Figure D.1)
Drag coefficient	C_f (-)	C_f (-)
	1.4e^{-3}	2.54e^{-3}
Number of modes	k (-)	k (-)
	128	256
Grid size	Element size (km)	Element size (km)
	6, 20 (Figure A.2)	3, 10 (Figure D.2)

(a) Countours of bathymetry

(b) Depth profile
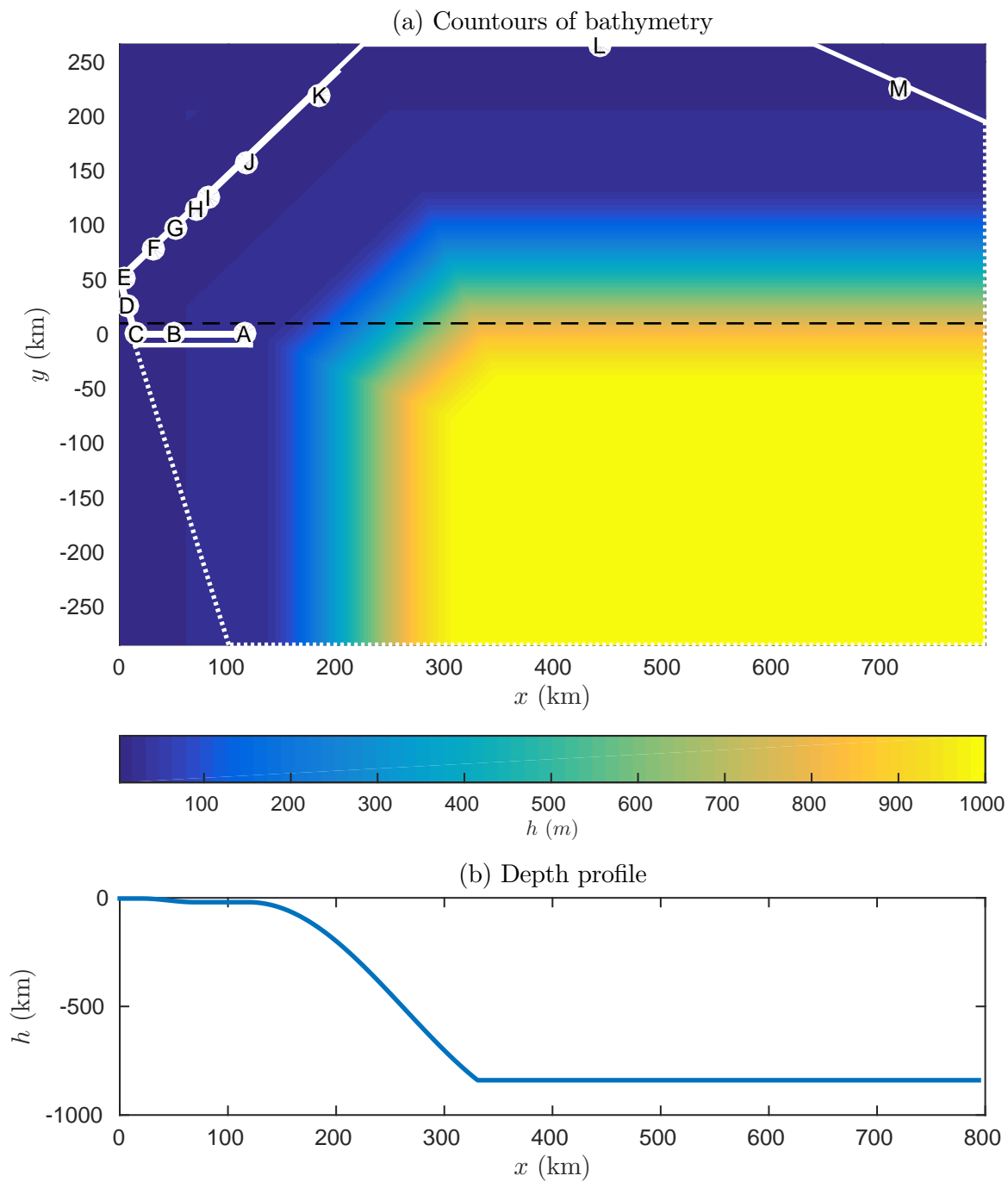
Figure D.1: Smooth bathymetry used for model behaviour assessment including domain boundaries and locations.
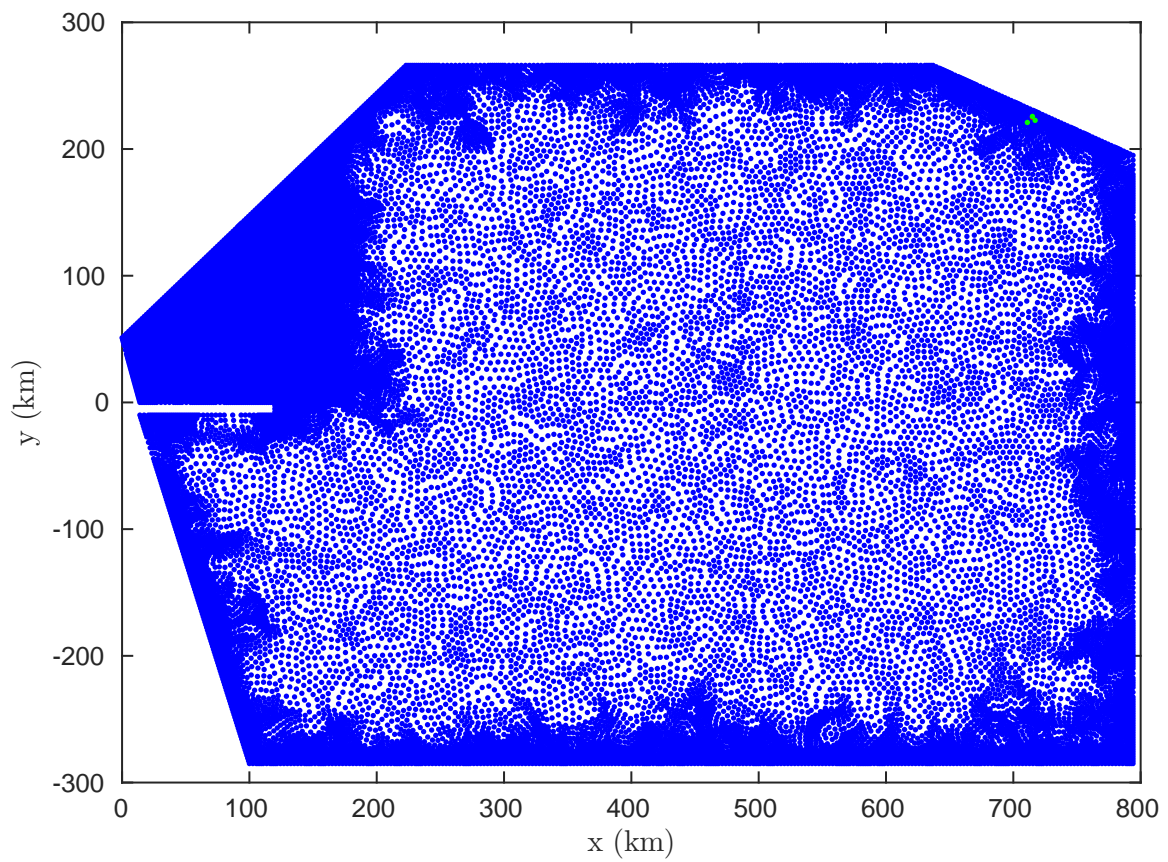
Figure D.2: Fine grid (total of 31673 nodes) of the unstructured triangular mesh used for model behaviour assessment. Along coasts and in New Orleans coastal zone grid size is 3 km and 10 km in the middle of the domain.
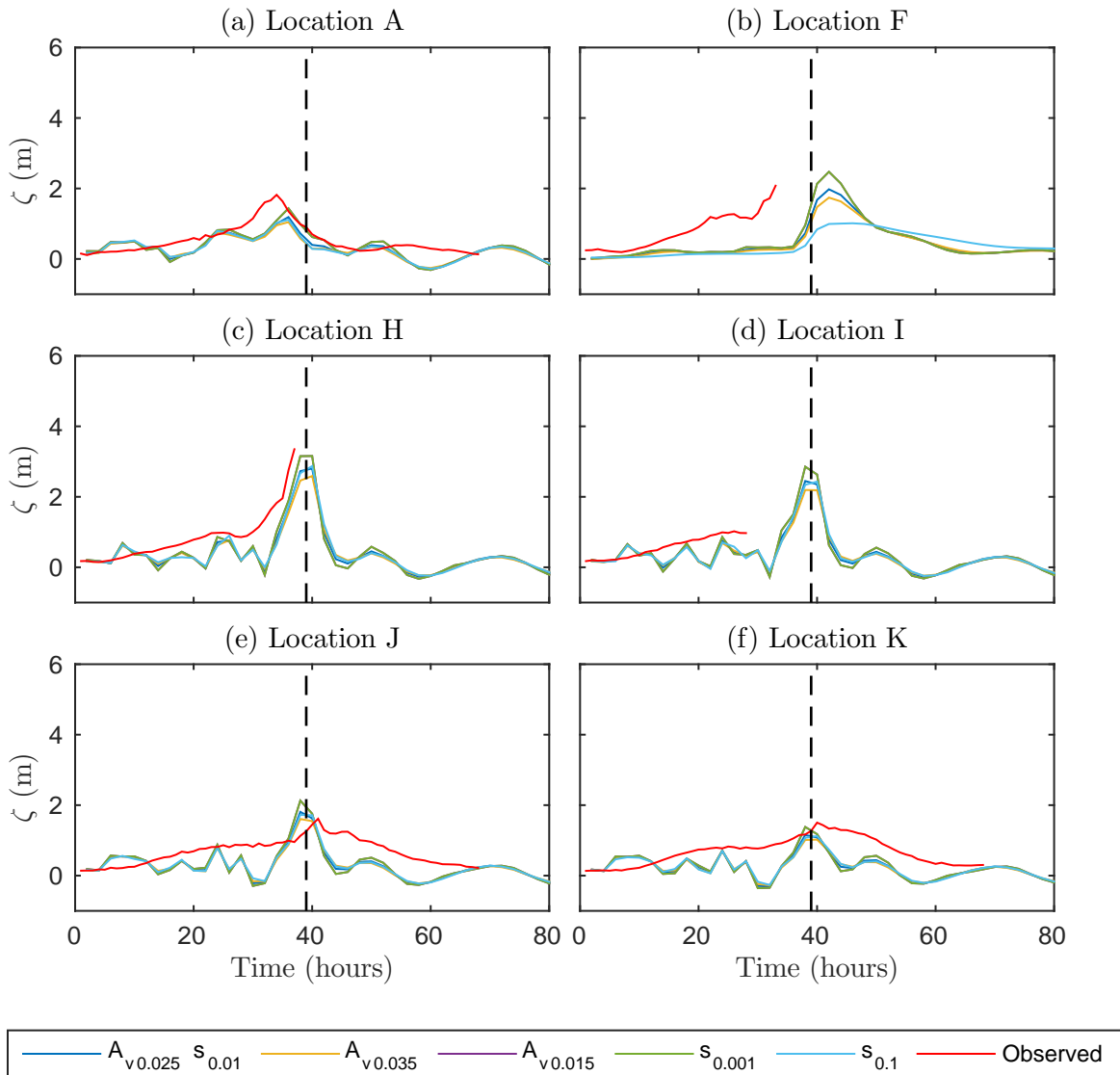
Figure D.3: Simulated water levels for hurricane Katrina with different combinations of A_v and s. Vertical dashed line represents the time of landfall (t=39). $A_v = 0.025$ (m^2/s) and $s = 0.01$ (m/s) are the base case values, other numbers in legend show deviations from this combination.
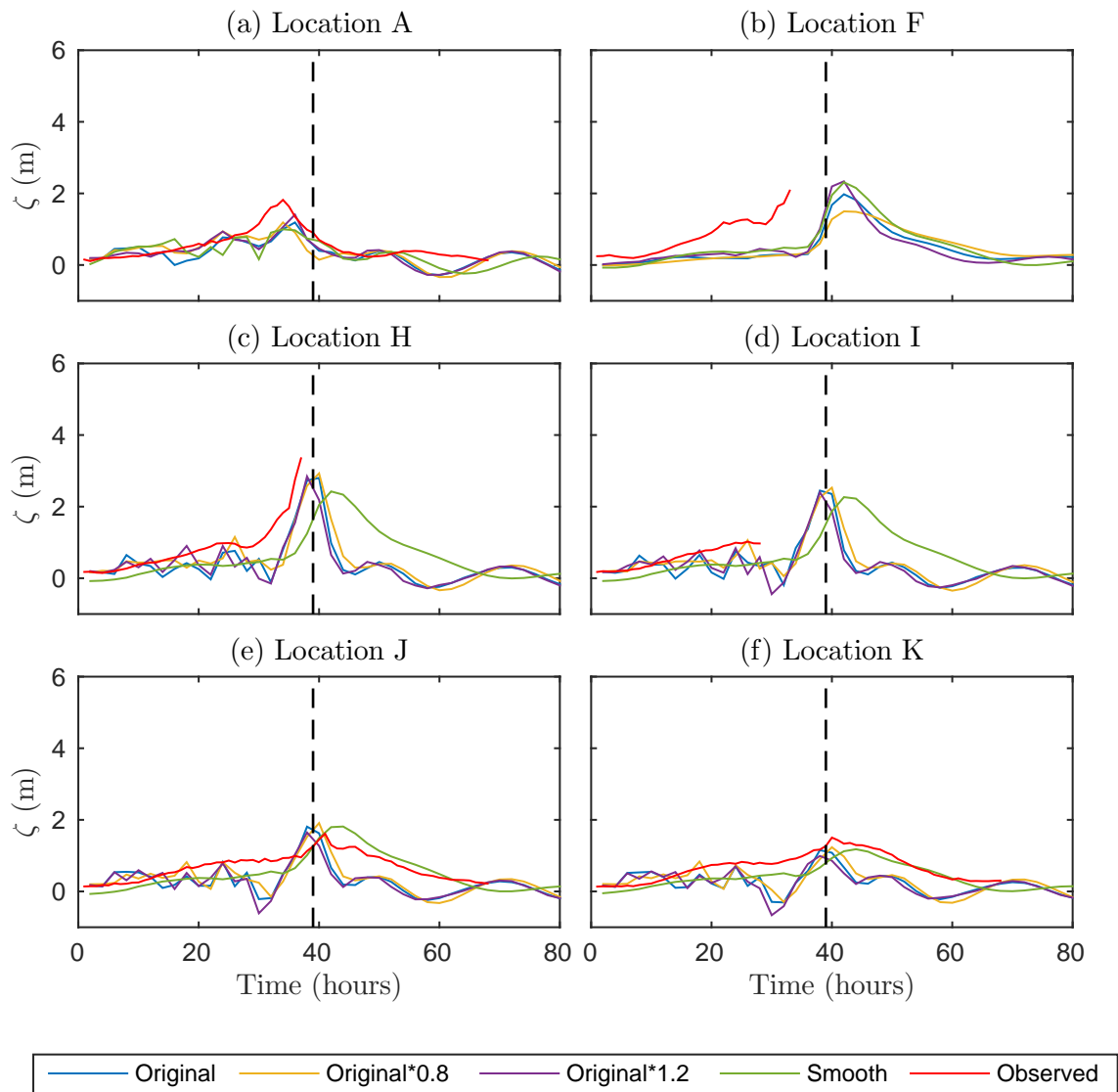
Figure D.4: Simulated water levels for hurricane Katrina with different depths and shapes of the bathymetry. Original bathymetry is shown in Figure 3.5, smooth bathymetry is shown in Figure D.1. Vertical dashed line represents the time of landfall (t=39). $A_v = 0.025$ (m²/s) and s (m/s) are the base case values.
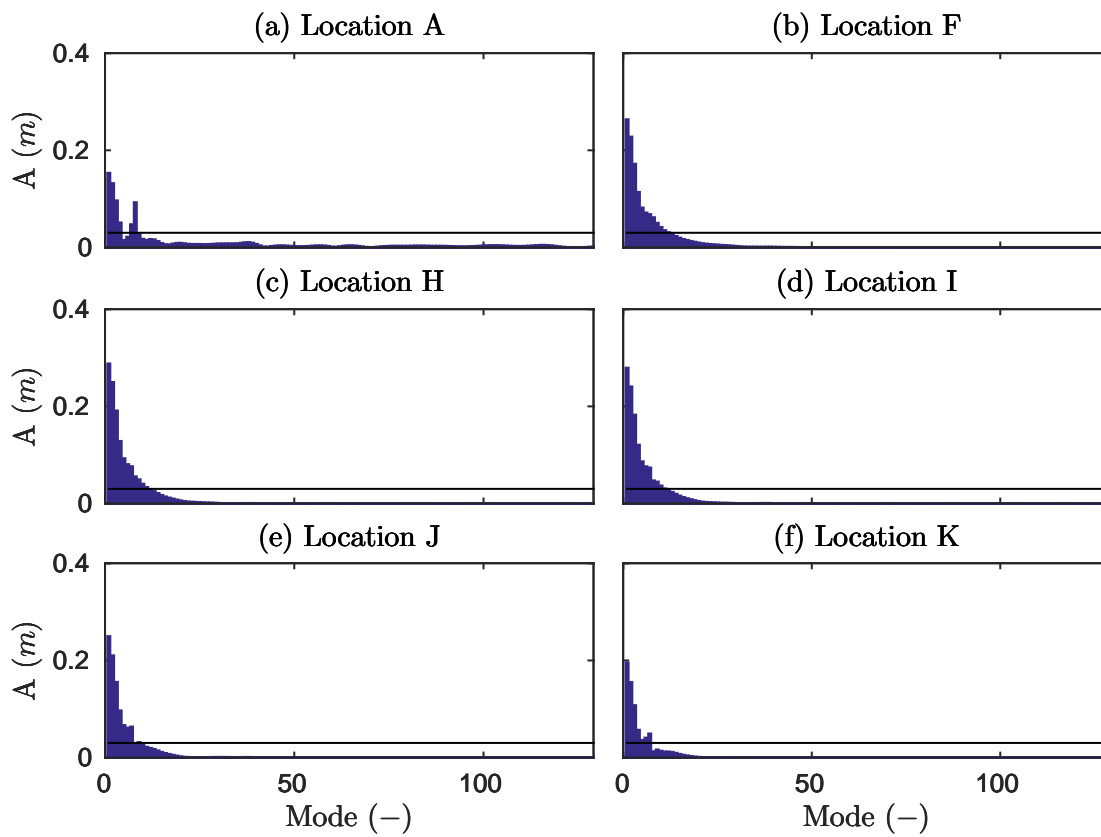
Figure D.5: Fourier spectra of elevation amplitude (m) for hurricane Katrina and a smooth bathymetry (Figure D.1).
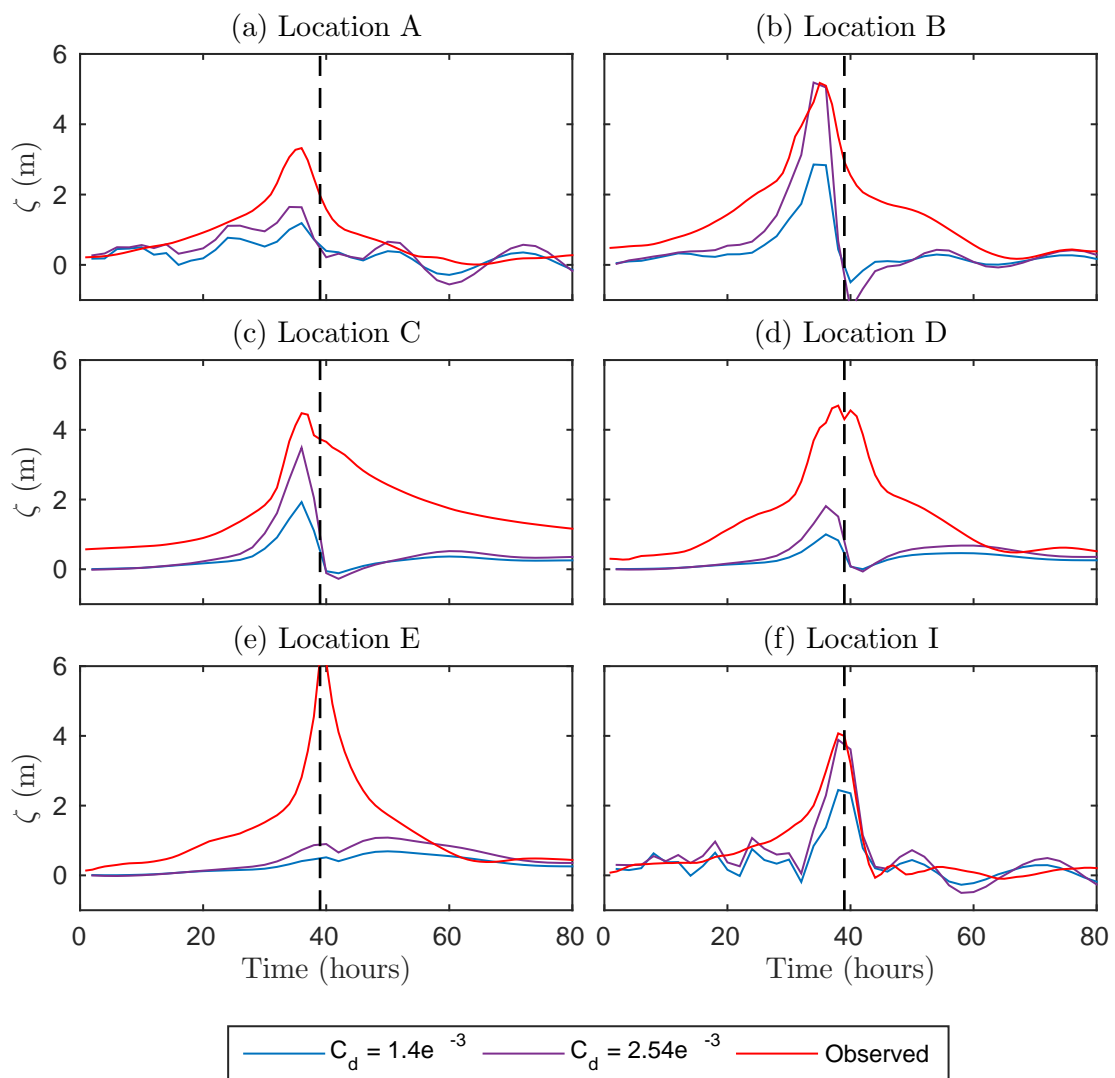
Figure D.6: Simulated water levels for hurricane Katrina with different C_d-values compared to ADCIRC simulations. Vertical dashed line represents the time of landfall (t=39).
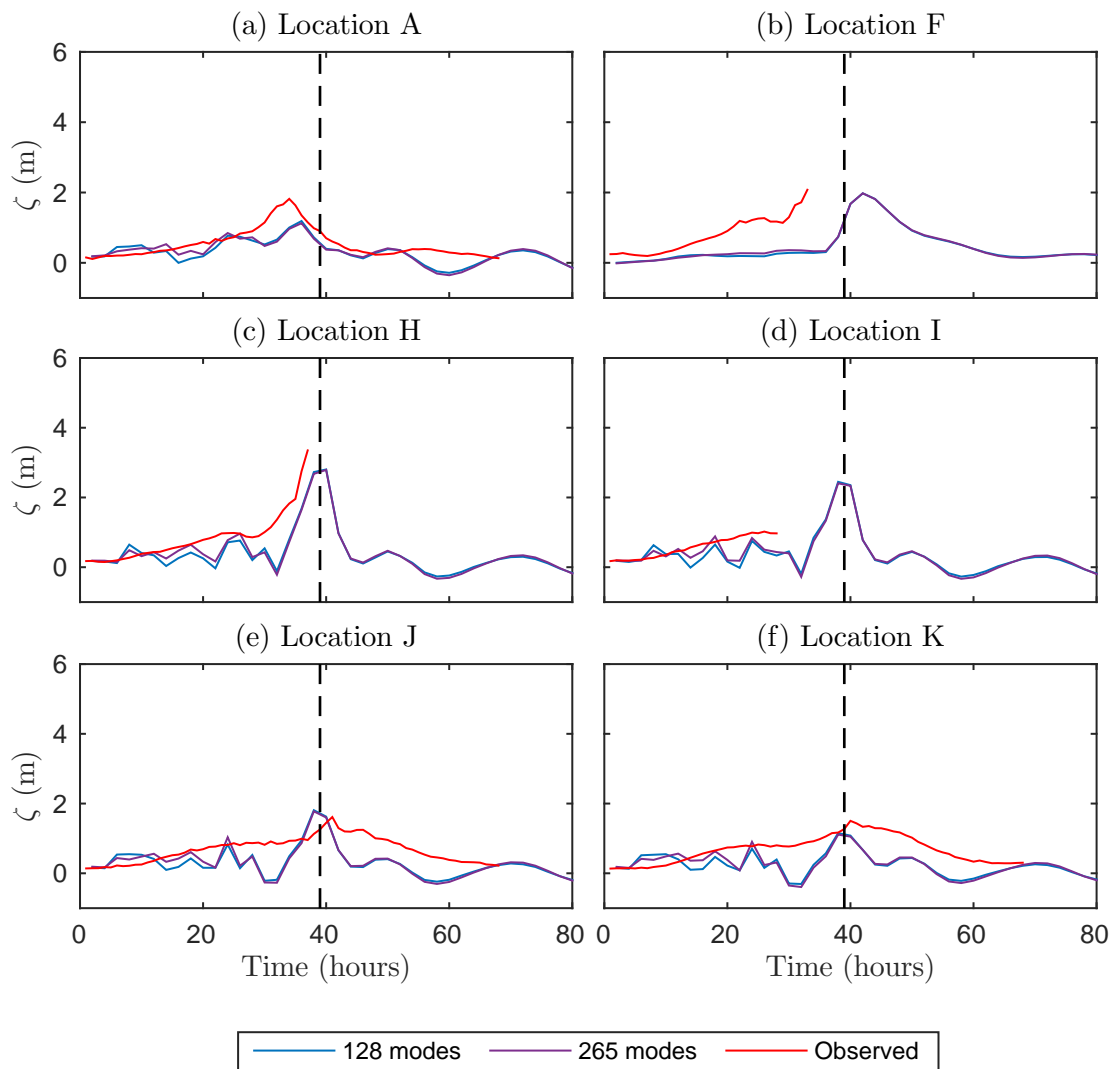
Figure D.7: Simulated water levels for hurricane Katrina with a different number of modes (T_{rec} is kept the same). Vertical dashed line represents the time of landfall (t=39).
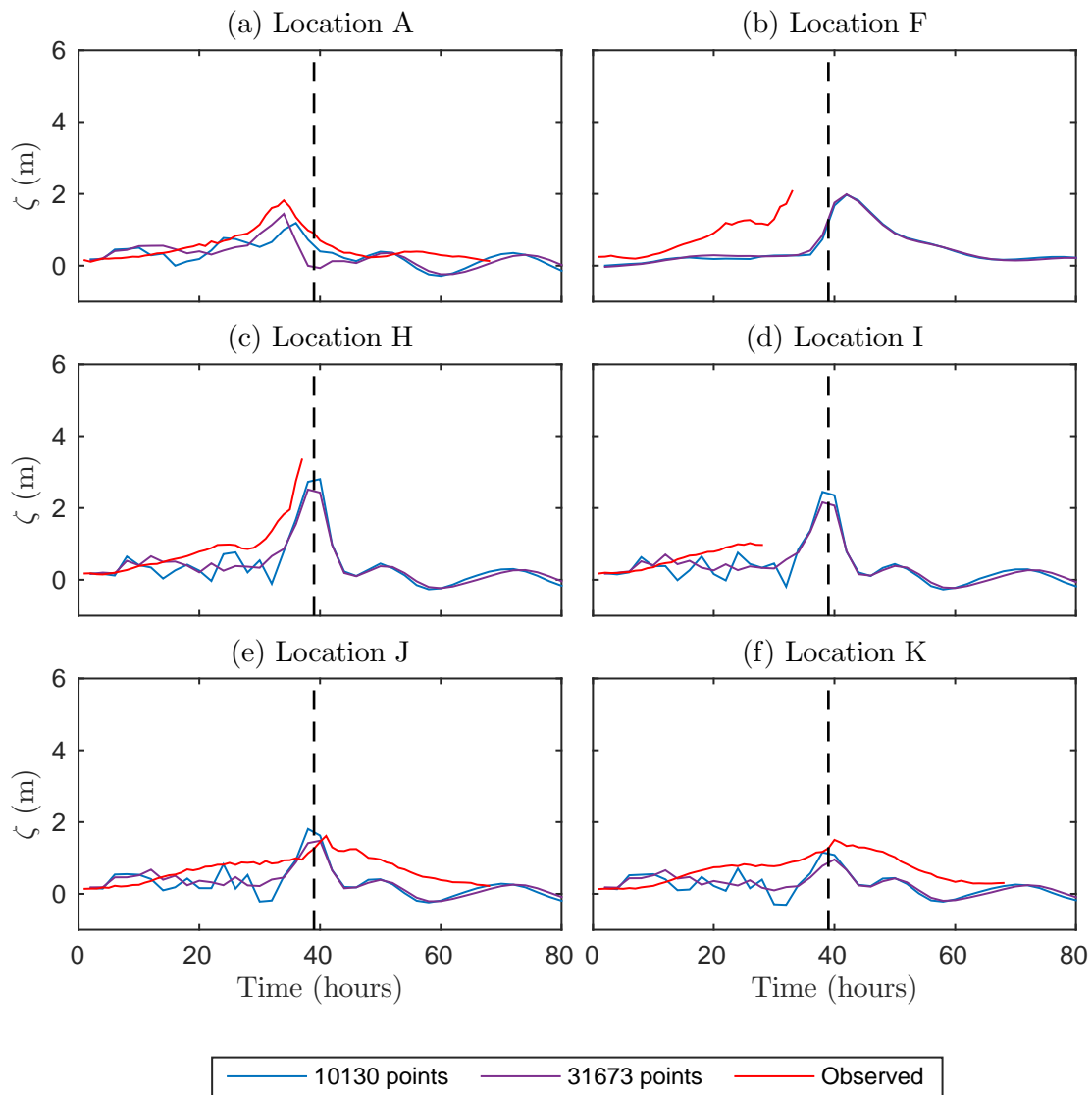
Figure D.8: Simulated water levels for hurricane Katrina with different grid sizes. Original grid is shown in Figure A.2, fine grid is shown in Figure D.2. Vertical dashed line represents the time of landfall (t=39).
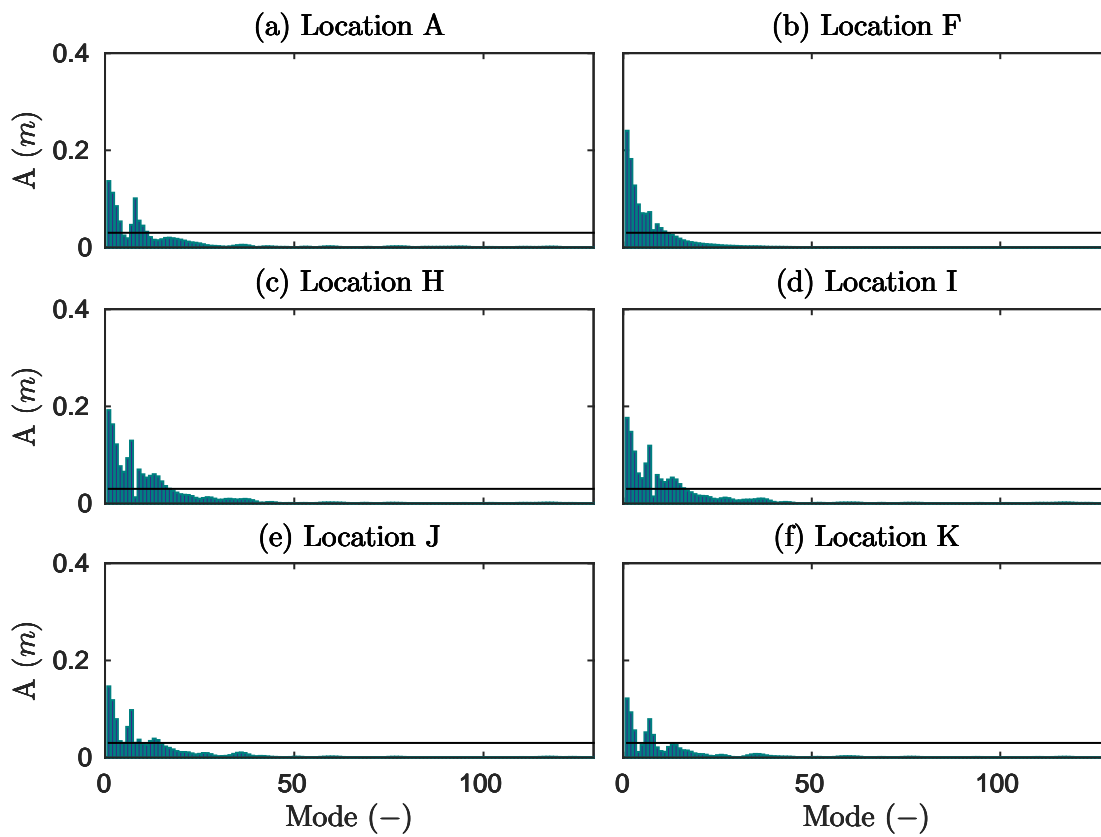
Figure D.9: Fourier spectra of elevation amplitude (m) for hurricane Katrina and a fine grid (Figure D.2).

Appendix E

Storm scenario selection

This appendix presents the selection of storm parameter and scenarios. These scenarios referred to in Section 5.1.

For this study a set of 6 scenarios is simulated and 9 other scenarios are proposed. Based on historical and probable combinations many more scenarios can be composed. In an ideal situation a plan is made for 108 storm scenarios. Based on the storm parameters 18 different storms are composed which can approach the coast over the 6 different paths.

E.1   Parameter constraints

Selection of parameters and combinations of parameters for a scenario is based on three different things; (i) Realistic ranges for storm parameters in the New Orleans area. (ii) Interrelations between storm parameters. (iii) Assumptions and constraints for parameters in combination with the FEM-model. Each of these three is covered below. A synthetic set of probable hurricanes is chosen. An advantage of this over methods that depend heavily on historical storms is that this also considers storms that might happen, whereas one otherwise only considers storms that did happen.

E.1.1   Realistic ranges

Straatsma (2015) summarized in the literature study the historical ranges for these parameters in the New Orleans area:

- P_c: 910 to over 970 mbar.

- R_{max}: 11 to 74 km.

- B: theoretically from 1 to 2.5, however values used in studies about hurricanes around New Orleans range from $0.9 - 1.9$.

- C_f: around 5.6 m/s.

- Paths (ϕ and $(x, y)_{origin}$) between 110 and 230 degrees with respect to the north.
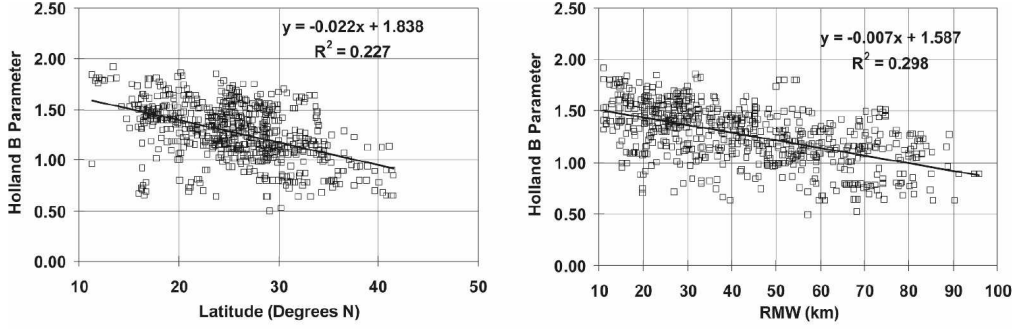
Figure E.1: Relationships between B (left) and R_{max} (right) *Vickery and Wadhera (2008)*.

E.1.2   Parameter interrelations

Relations between storm parameters imply that the parameters cannot be selected without caution. Parameters, P_c, R_{max} and C_{fw} are most important storm parameters (Resio and Westerink, 2008) describing the wind and pressure fields. However, as found by Vickery and Wadhera (2008) these parameters are not completely independent of each other. They found statistical proof for a relation between R_{max} and B and B and latitude (Figure E.1).

This research is focused on a fixed location of 29 (°) latitude which means that B parameter can still vary between 0.9 and 1.6. The interrelation of B with R_{max} shows that B decreases when R_{max} increases, the range of B is still very large so not more restricted than the already mentioned one.

Furthermore, Vickery and Wadhera (2008) found a relation between R_{max} and (ΔP_c). Even though this relation is not statistically proven for hurricanes at the Gulf of Mexico, it is 94% statistical proven for all hurricanes of the Atlantic Ocean. Therefore it is recommended to use the following relation between P_c and R_{max}:

$$\ln(R_{max}) = 3.858 - 7.7 \times 10^{-5} \Delta P_c^2;$$
$$r^2 = 0.290, \quad \sigma_{lnR_{max}} = 0.390 \tag{E.1}$$

U.S. Army Corps of Engineers (2008b) stresses this apparent differences between hurricanes at the Gulf of Mexico compared with hurricanes along the whole coast of the Atlantic. Therefore the relationship E.1 is used as guidance and not as strict constrain for the storm scenarios.

Together, these relations indicate that for instance the likelihood of a storm with a P_c less than 930 mbar and a R_{max} greater than 40 km , combined with a B value of greater than 1.1, is remote.

E.1.3   Parameters and the storm surge model

The storm scenarios are used to generate probable hurricanes to simulate with the idealized storm surge model. Because of this, some simplifications are made for the parameter and scenario selection:

- In contradiction to reality storm parameters are kept constant during the hurricanes approach to the coast to estimate the surge. However, it is
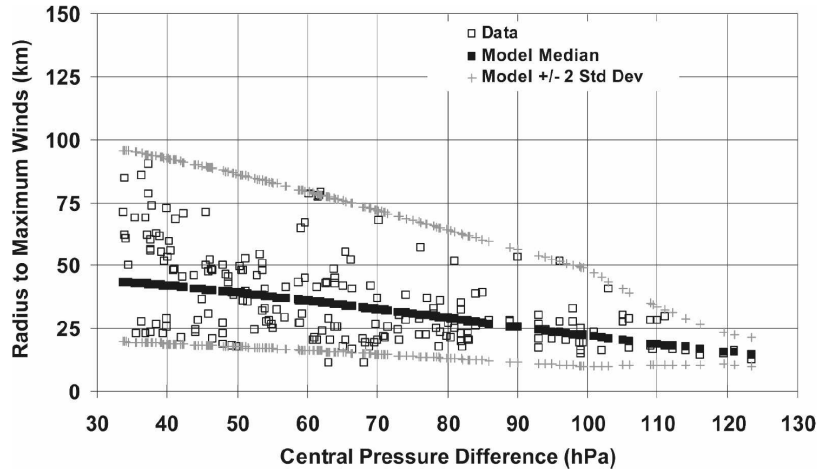
Figure E.2: Modelled and observed P_c and R_{max} for Gulf of Mexico hurricanes Vickery and Wadhera (2008).

shown this idealized approaches is not a good assumption for predicting the real surge at the coast, this is neglected because the objective is not about predicting water levels but about the general mechanism of the storm surge.

- The paths of hurricanes are simulated as a straight line.

- The calculation time of the model is about 200 minutes. It is impossible to simulate many storm scenarios within this study.

E.2   Parameter choice

The storm scenarios were chosen based on the previous considerations. For each of the parameters is described why these values are chosen. In general the scenarios are aimed to represent relative severe storms (category 3 and higher).

P_c is based on intense hurricanes which have a normally a central pressure lower than 960 mbar. Because central pressure is a very important factor determining the wind and pressure fields three values are chosen: 900, 930 and 960. These values are in accordance with both historical data and scenarios used by FIS and Irish.

R_{max} could be based on relation found by Vickery. For the pressures 900, 930 and 960 this gives the following radii: 13, 21 and 32 km. However, these radii are small and much bigger radii fall within the range of 2 times the standard deviation of this relationship (Figure E.2). Furthermore, the radius of 13 km is quite exceptional, while radii bigger than 32 km have happened more often in historic storms with a pressure of 930 or 960 mbar. Therefore, the radius of 13 km is exchanged for a large radius of 47 km. And nonetheless this large radius is remote for a storms with a central pressure of 900 mbar, hurricane Katrina fitted in this category on its biggest moment.

B is on average 1.21 according to Vickery and Wadhera (2008). In the last few hours before landfall the B parameter tends to decrease 0.21. Both of

these values (1 and 1.21) are close to the values used in U.S. Army Corps of Engineers (2008a). This study however uses a fixed B for the whole storm track, thus it is chosen to select a value of 1.1.

C_f has a large range of values in several model studies. Based on historic storms the value will be around 5.6 m/s, but (Peng et al., 2006) also used a value of 10 m/s. Which is high but not unrealistic. Therefore two selected values for forward speed are 6 and 10 m/s.

ϕ is derived of the possible storm tracks in New Orleans. Historic storms show that tracks with a angel of lower than $110°$ and higher than $240°$ are highly unlikely. This is because of the shape of the Gulf of Mexico and Florida lying to the east of New Orleans. Hurricanes with a track lower than $110°$ first make landfall in Florida, this will diminish the strength of the hurricane considerable and change the track. Three different angles are selected; one angle due north (N) and two inclined track, respectively $+45°$ (NE) and $-45°$ (NW) due north. For the coordinate system of the model the angles will be respectively $7.5°$, $322.5°$ and $277.5°$.

$(x, y)_{origin}$ pairs are specified for each angle of approach. These tracks (A and A') have the same angle of approach but are 30 nmi (55.5 km) apart from each other. The surge elevations along the coast scale with this parameter for a wide range of storm sizes on a straight coastline. Even though New Orleans is not a straight coastline, U.S. Army Corps of Engineers (2008a) roughly examined this impact and found a 30 nmi difference still acceptable to reasonably estimate the storm surge. Choosing for the 30 nmi interval between the two tracks gives a bias of 20% in the most extreme case (when a hurricane with small R_{max}, makes landfall precisely in between two tracks).

E.3   Scenarios

The chosen parameter variations are shown in Table E.1, systematically varying the parameters results in the list of scenarios shown in Table E.2. However for this study a selection must be made which is shown in Table 5.1. Therefore, the number of scenarios and different parameter values are limited. It is chosen to select a maximum of six scenarios. The selection is mainly based on the path and intensity & size of the storm (orange scenarios). Nine extra scenarios (blue scenarios) are proposed as a good extension for the study if more time is available.

Table E.1: Selected storm parameters

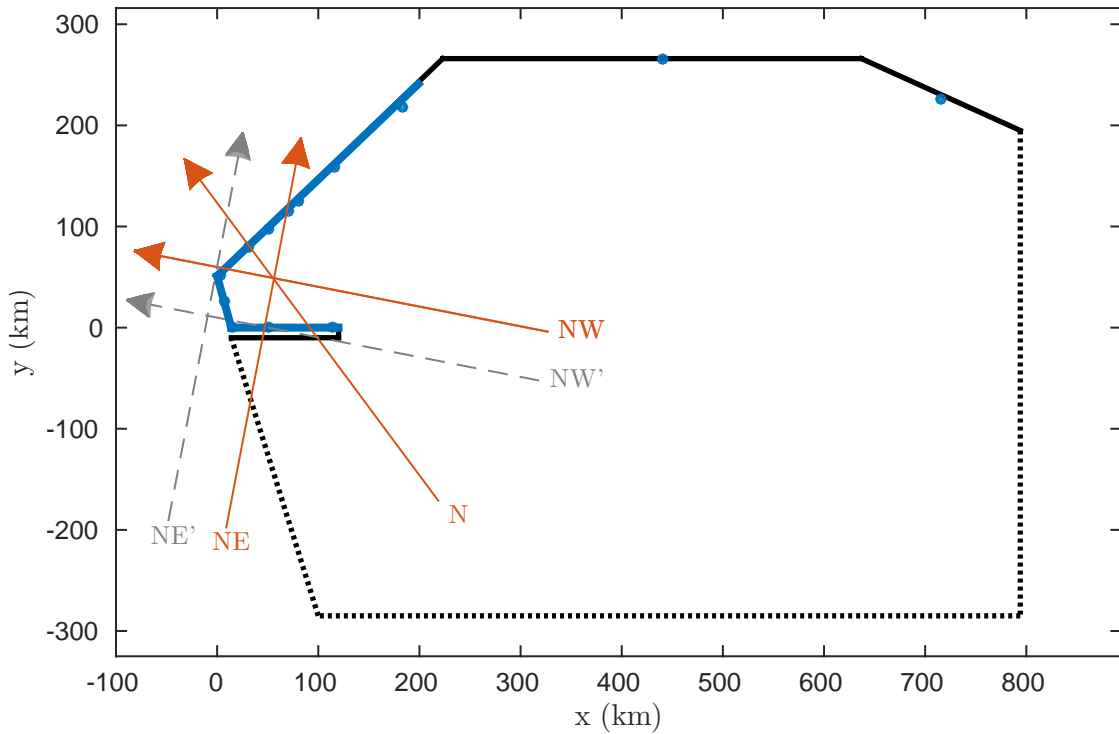| P_c (mbar)	R_{max} (km)	B (-)	C_f (m/s)	ϕ (°)	$(x, y)_{origin}$ (-)
900, 930, 960	21 32 47	$\sim$1.1	6 10	7.5 322.5 277.5	A A'

*relative to the North.

Figure E.3: **Orange:** *The three main storm directions as specified in Table E.1. Where NE, N and NW represent 7.5°, 322.5° and 277.5° respectively.* **Grey:** *Also the three secondary tracks based on the original paths are shown. These are parallel to the orange tracks only 55.5 km apart.*

Table E.2: *Storm scenarios.* **Orange:** *run scenarios in this study.* **Blue:** *first scenarios to run in a follow up of this study.*

Scenario	P_c (mbar)	R_{max} (km)	C_f (m/s)	ϕ (°)	$(x, y)_{origin}$ (-)
-	900	21	6	7.5	A
1	900	32	6	7.5	A
-	900	47	6	7.5	A
-	900	21	10	7.5	A
-	900	32	10	7.5	A
-	900	47	10	7.5	A
-	900	21	6	322.5	B
3	900	32	6	322.5	B
-	900	47	6	322.5	B
-	900	21	10	322.5	B
-	900	32	10	322.5	B
-	900	47	10	322.5	B
10	900	21	6	277.5	C
5	900	32	6	277.5	C
11	900	47	6	277.5	C
-	900	21	10	277.5	C
-	900	32	10	277.5	C

Continued on next page

Table E.2 – continued from previous page

Scenario	P_c (mbar)	R_{max} (km)	C_f (m/s)	ϕ (°)	$(x,y)_{origin}$ (-)
-	900	47	10	277.5	C
-	900	21	6	7.5	A'
-	900	32	6	7.5	A'
-	900	47	6	7.5	A'
-	900	21	10	7.5	A'
-	900	32	10	7.5	A'
-	900	47	10	7.5	A'
-	900	21	6	322.5	B'
-	900	32	6	322.5	B'
-	900	47	6	322.5	B'
-	900	21	10	322.5	B'
-	900	32	10	322.5	B'
-	900	47	10	322.5	B'
-	900	21	6	277.5	C'
-	900	32	6	277.5	C'
-	900	47	6	277.5	C'
-	900	21	10	277.5	C'
-	900	32	10	277.5	C'
-	900	47	10	277.5	C'
-	930	21	6	7.5	A
-	930	32	6	7.5	A
2	930	47	6	7.5	A
-	930	21	10	7.5	A
-	930	32	10	7.5	A
-	930	47	10	7.5	A
-	930	21	6	322.5	B
-	930	32	6	322.5	B
4	930	47	6	322.5	B
-	930	21	10	322.5	B
-	930	32	10	322.5	B
-	930	47	10	322.5	B
12	930	21	6	277.5	C
13	930	32	6	277.5	C
6	930	47	6	277.5	C
-	930	21	10	277.5	C
-	930	32	10	277.5	C
-	930	47	10	277.5	C
-	930	21	6	7.5	A'
-	930	32	6	7.5	A'
7	930	47	6	7.5	A'
-	930	21	10	7.5	A'
-	930	32	10	7.5	A'
-	930	47	10	7.5	A'
-	930	21	6	322.5	B'
-	930	32	6	322.5	B'
8	930	47	6	322.5	B'

Continued on next page

Table E.2 – continued from previous page

Scenario	P_c (mbar)	R_{max} (km)	C_f (m/s)	ϕ (°)	$(x,y)_{origin}$ (-)
-	930	21	10	322.5	B'
-	930	32	10	322.5	B'
-	930	47	10	322.5	B'
-	930	21	6	277.5	C'
-	930	32	6	277.5	C'
9	930	47	6	277.5	C'
-	930	21	10	277.5	C'
-	930	32	10	277.5	C'
15	930	47	10	277.5	C'
-	960	21	6	7.5	A
-	960	32	6	7.5	A
-	960	47	6	7.5	A
-	960	21	10	7.5	A
-	960	32	10	7.5	A
-	960	47	10	7.5	A
-	960	21	6	322.5	B
-	960	32	6	322.5	B
-	960	47	6	322.5	B
-	960	21	10	322.5	B
-	960	32	10	322.5	B
-	960	47	10	322.5	B
-	960	21	6	277.5	C
-	960	32	6	277.5	C
14	960	47	6	277.5	C
-	960	21	10	277.5	C
-	960	32	10	277.5	C
-	960	47	10	277.5	C
-	960	21	6	7.5	A'
-	960	32	10	7.5	A'
-	960	47	10	7.5	A'
-	960	21	6	322.5	B'
-	960	32	6	322.5	B'
-	960	47	6	322.5	B'
-	960	21	10	322.5	B'
-	960	32	10	322.5	B'
-	960	47	10	322.5	B'
-	960	21	6	277.5	C'
-	960	32	6	277.5	C'
-	960	47	6	277.5	C'
-	960	21	10	277.5	C'
-	960	32	10	277.5	C'
-	960	47	10	277.5	C'

Appendix F

Sensitivity analysis: Water level results

This appendix presents 3 separate figures of the simulated storm scenarios, one for each storm direction. The figures are referred to in Section 5.2.1.
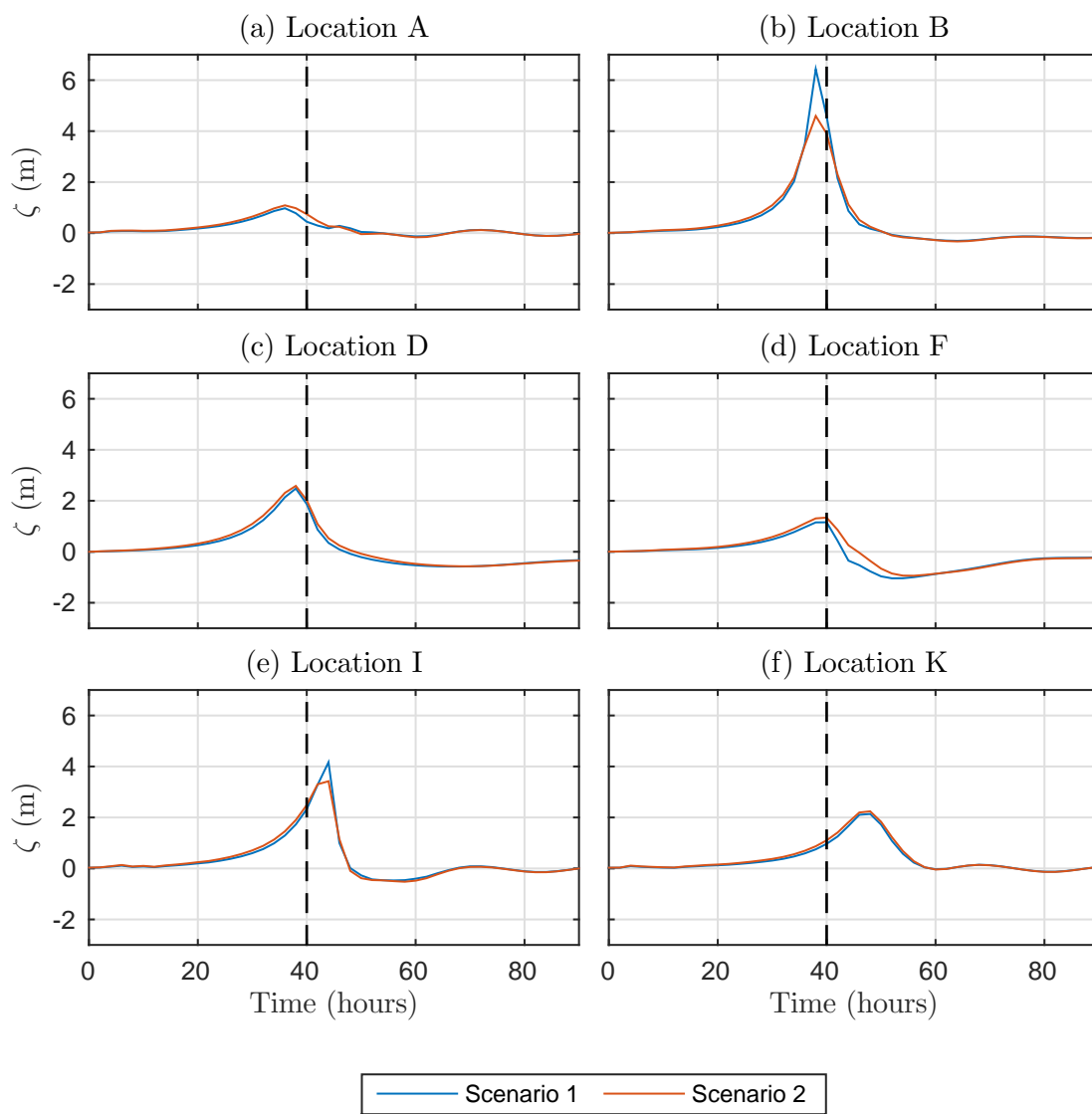
Figure F.1: Simulated water levels for scenarios 1 and 2 at 6 locations. Locations are shown in Figure 5.1.
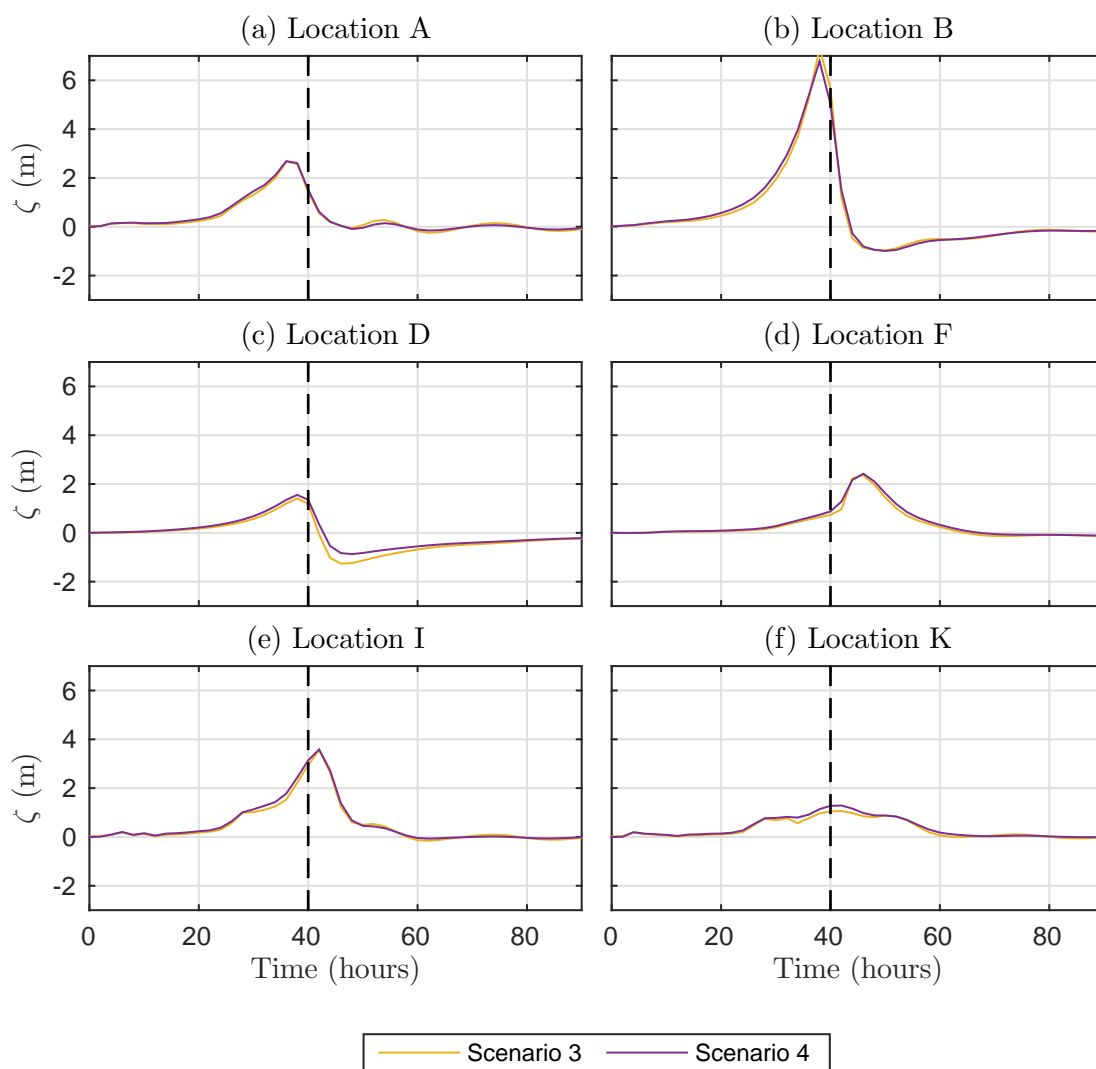
Figure F.2: Simulated water levels for scenarios 3 and 4 at 6 locations. Locations are shown in Figure 5.1.
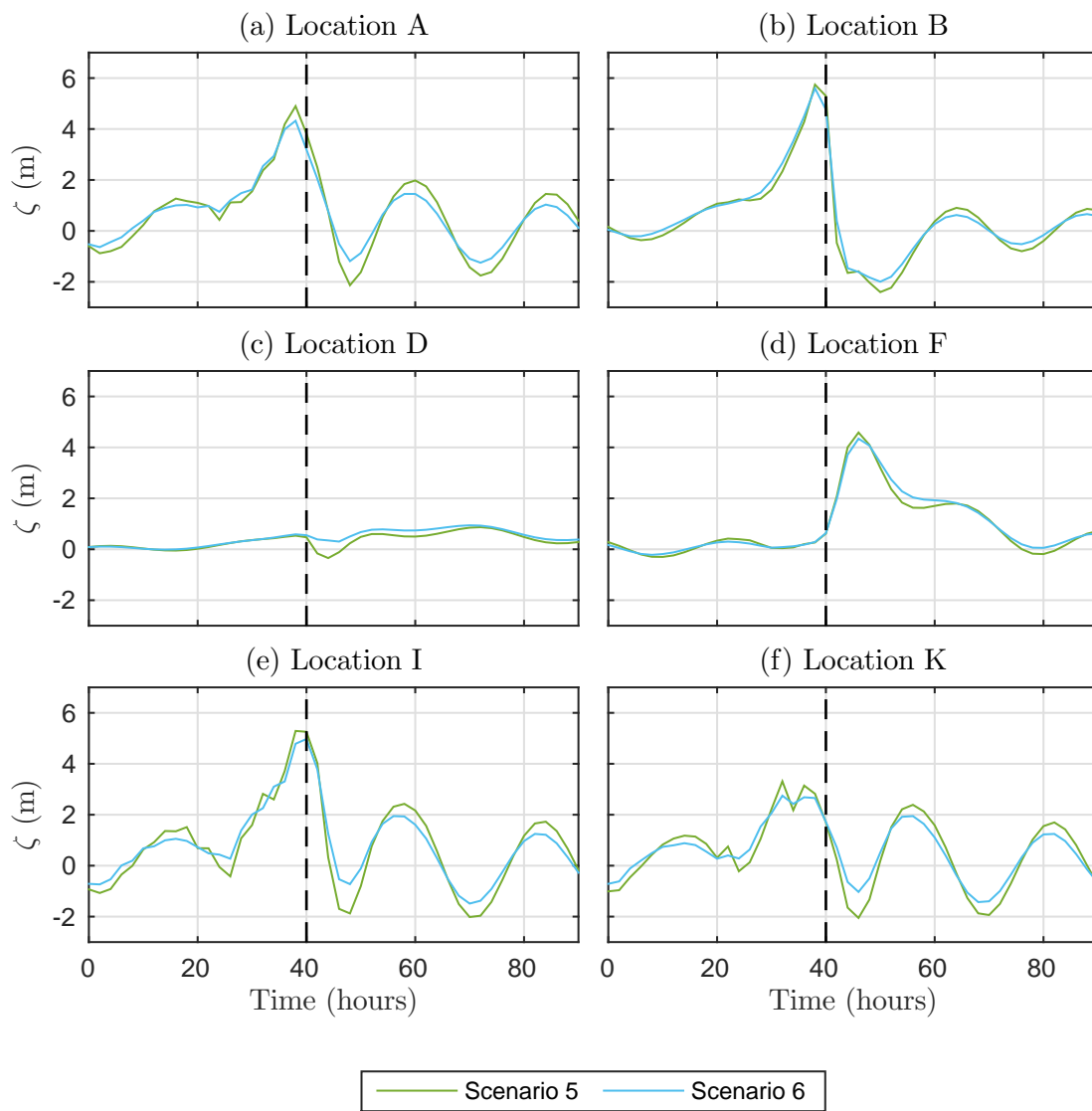
Figure F.3: Simulated water levels for scenarios 5 and 6 at 6 locations. Locations are shown in Figure 5.1.

Appendix G

Sensitivity analysis: Fourier results

This appendix presents the amplitude spectra for scenarios 2, 4 and 6 (Figures 5.4 to 5.6) (scenarios 1, 3 and 5 are presented in Section 5.2.2). Furthermore, amplitude surface plots of the six simulated storm scenarios are shown. The figures are referred to in Section 5.2.
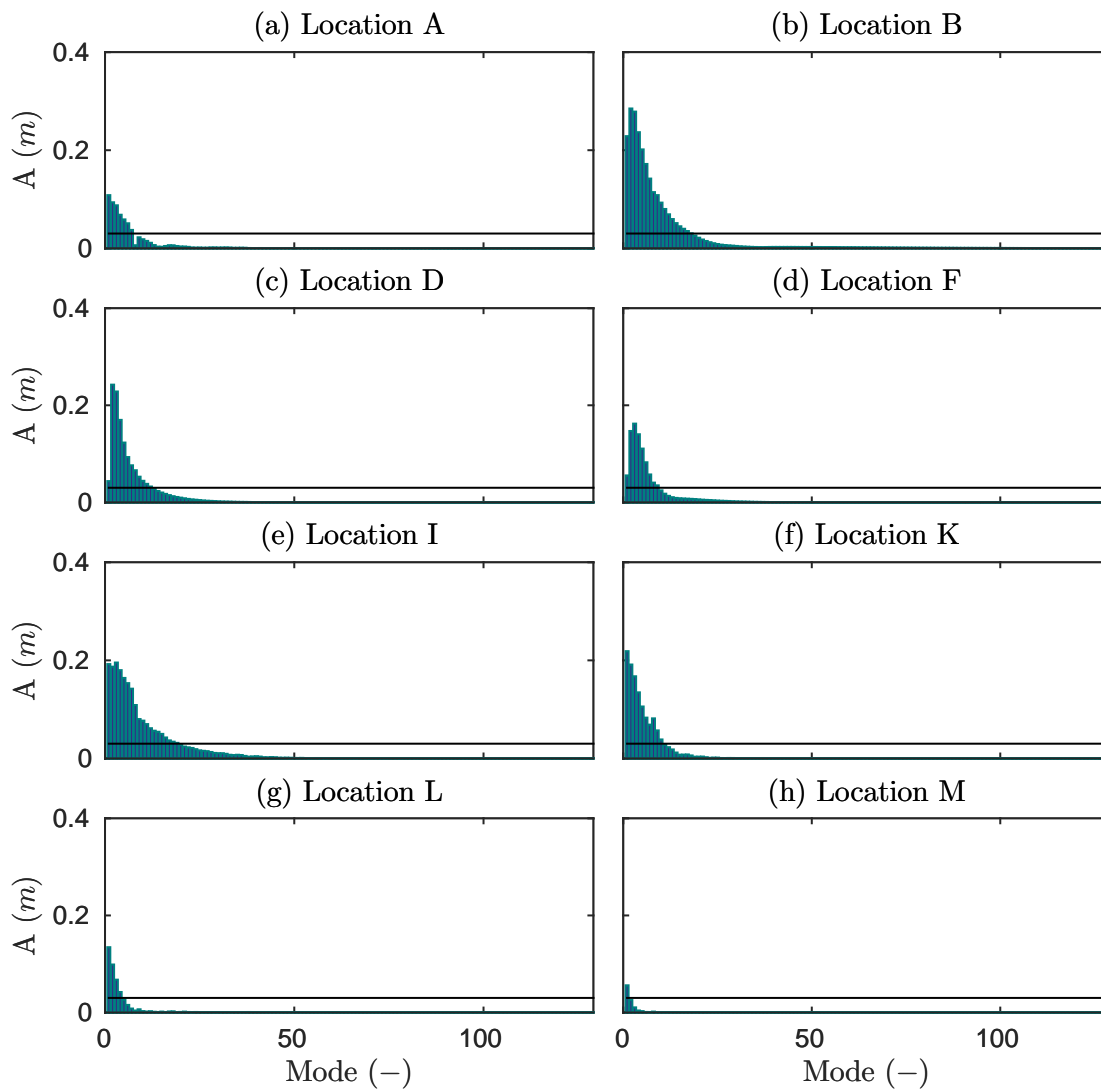
Figure G.1: Fourier spectrum of elevation amplitude (m) for scenario 2.
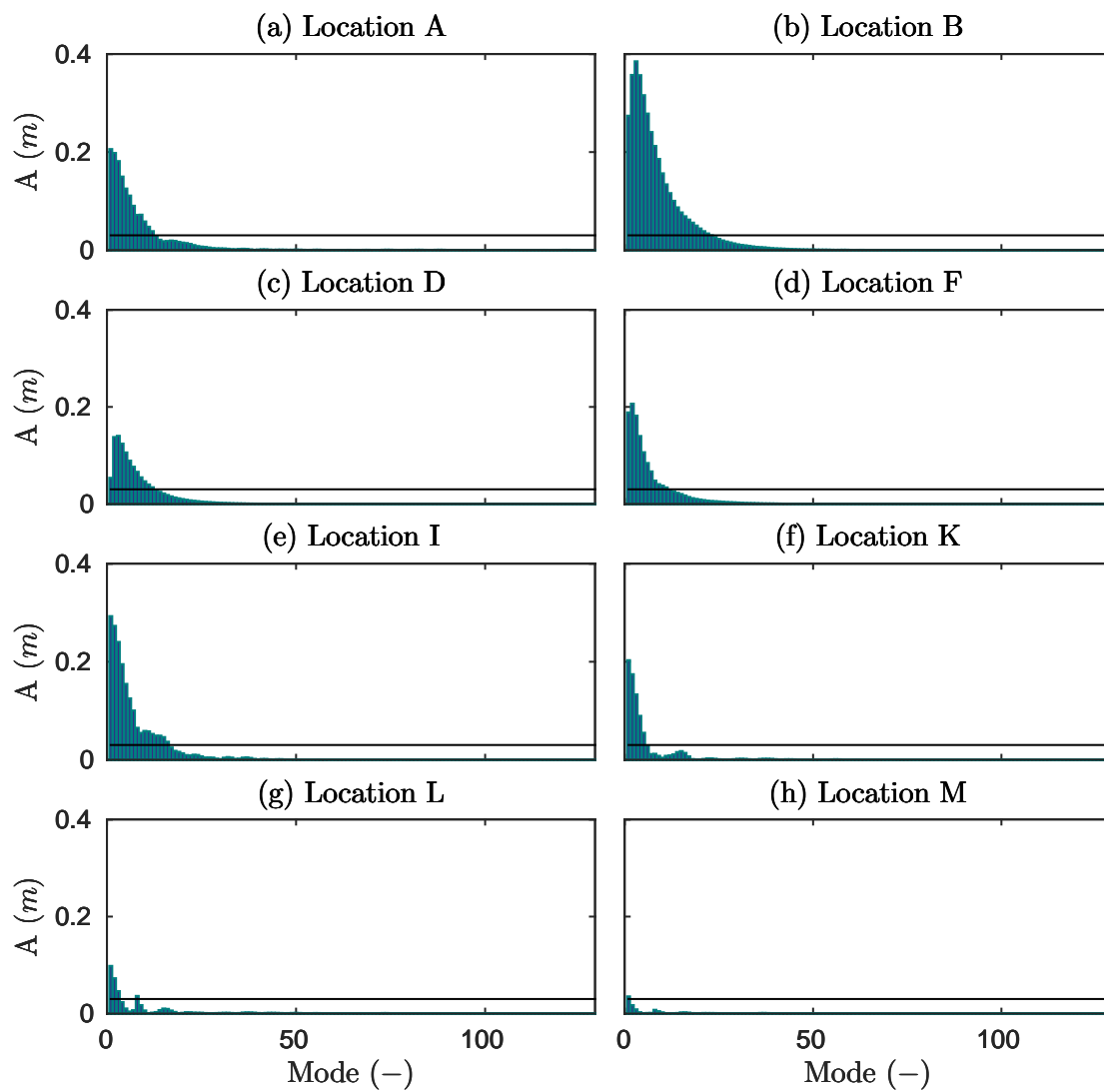
Figure G.2: Fourier spectrum of elevation amplitude (m) for scenario 4.
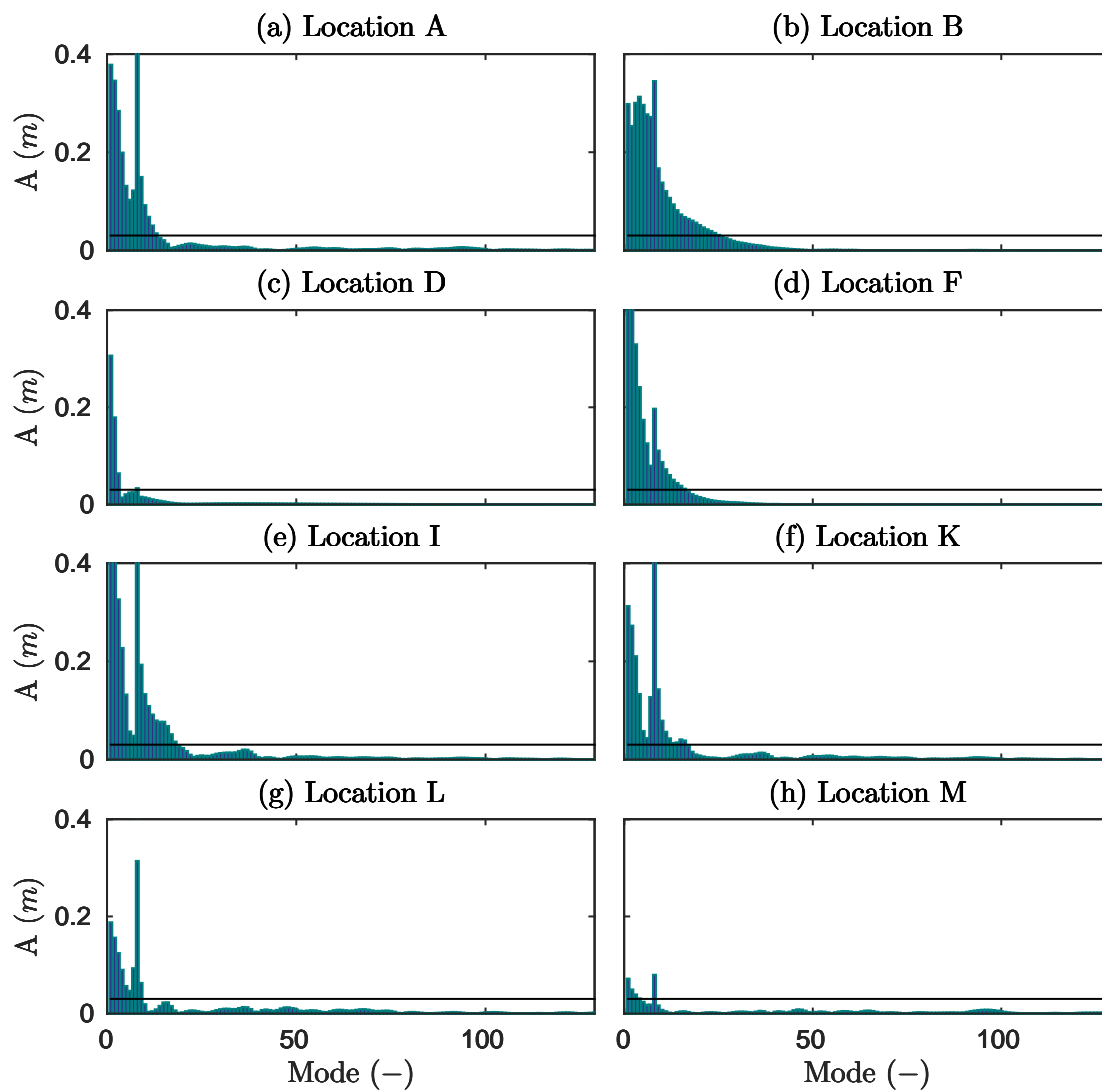
Figure G.3: Fourier spectrum of elevation amplitude (m) for scenario 6.
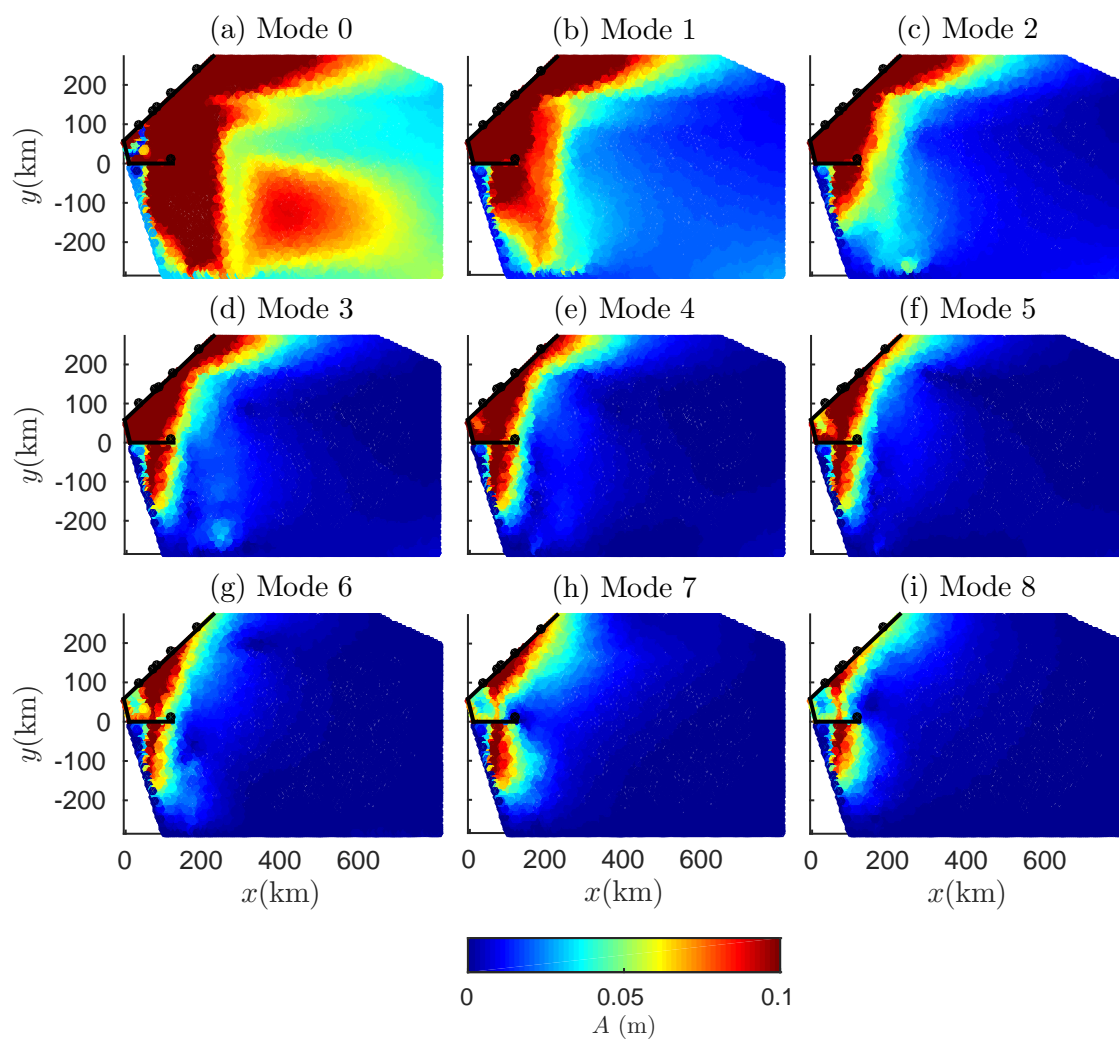
Figure G.4: Elevation amplitude of Fourier modes 0-8 of scenario 1.
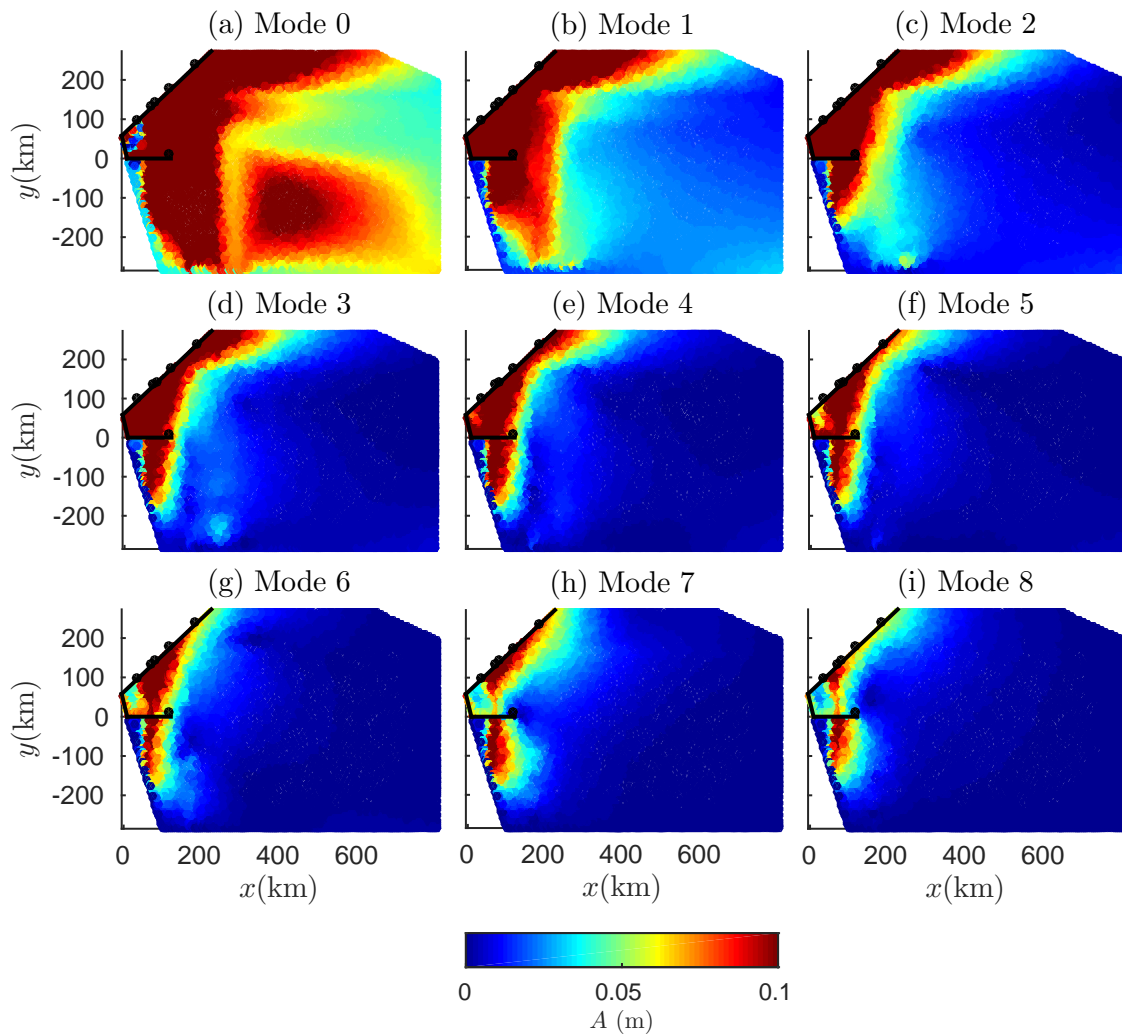
Figure G.5: Elevation amplitude of Fourier modes 0-8 of scenario 2.
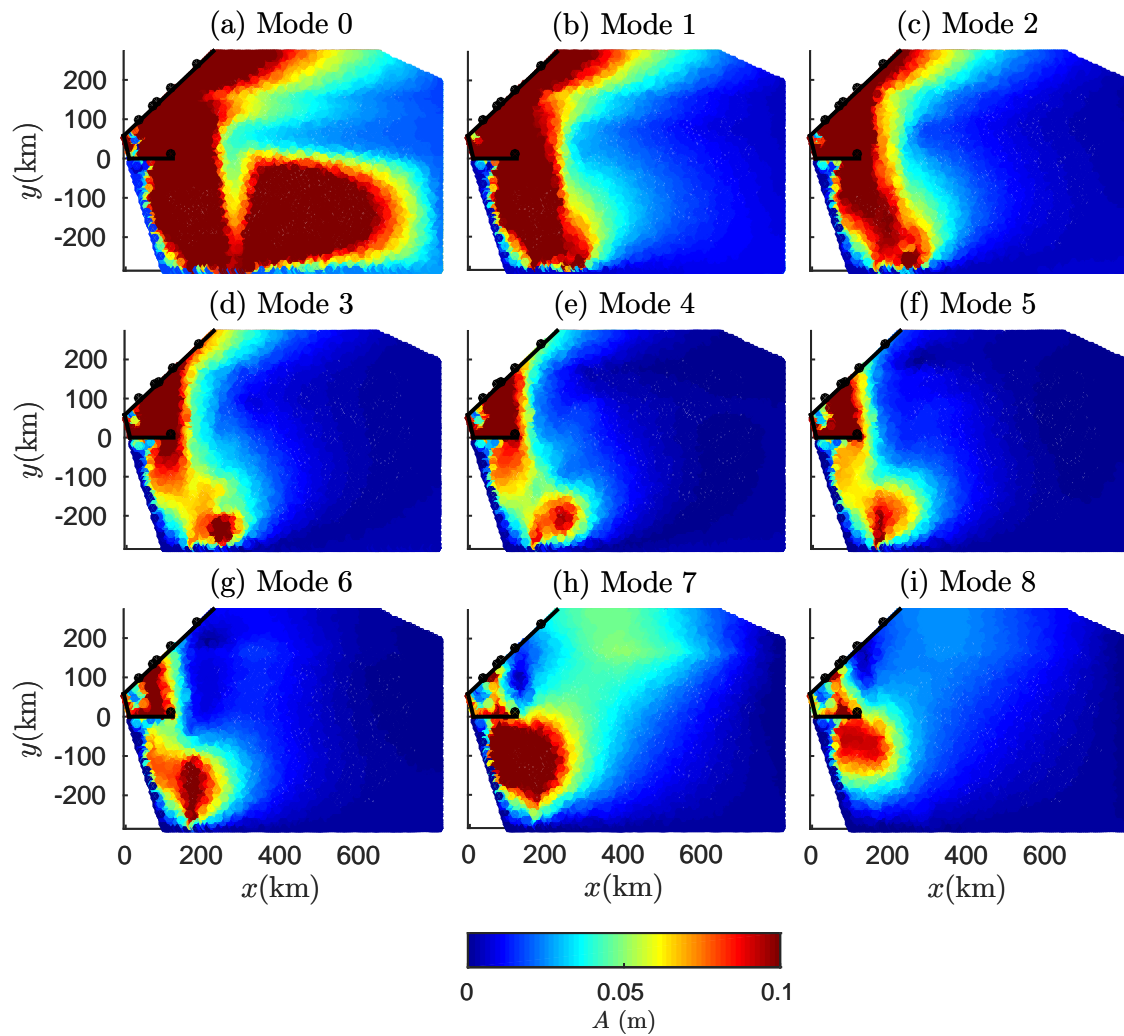
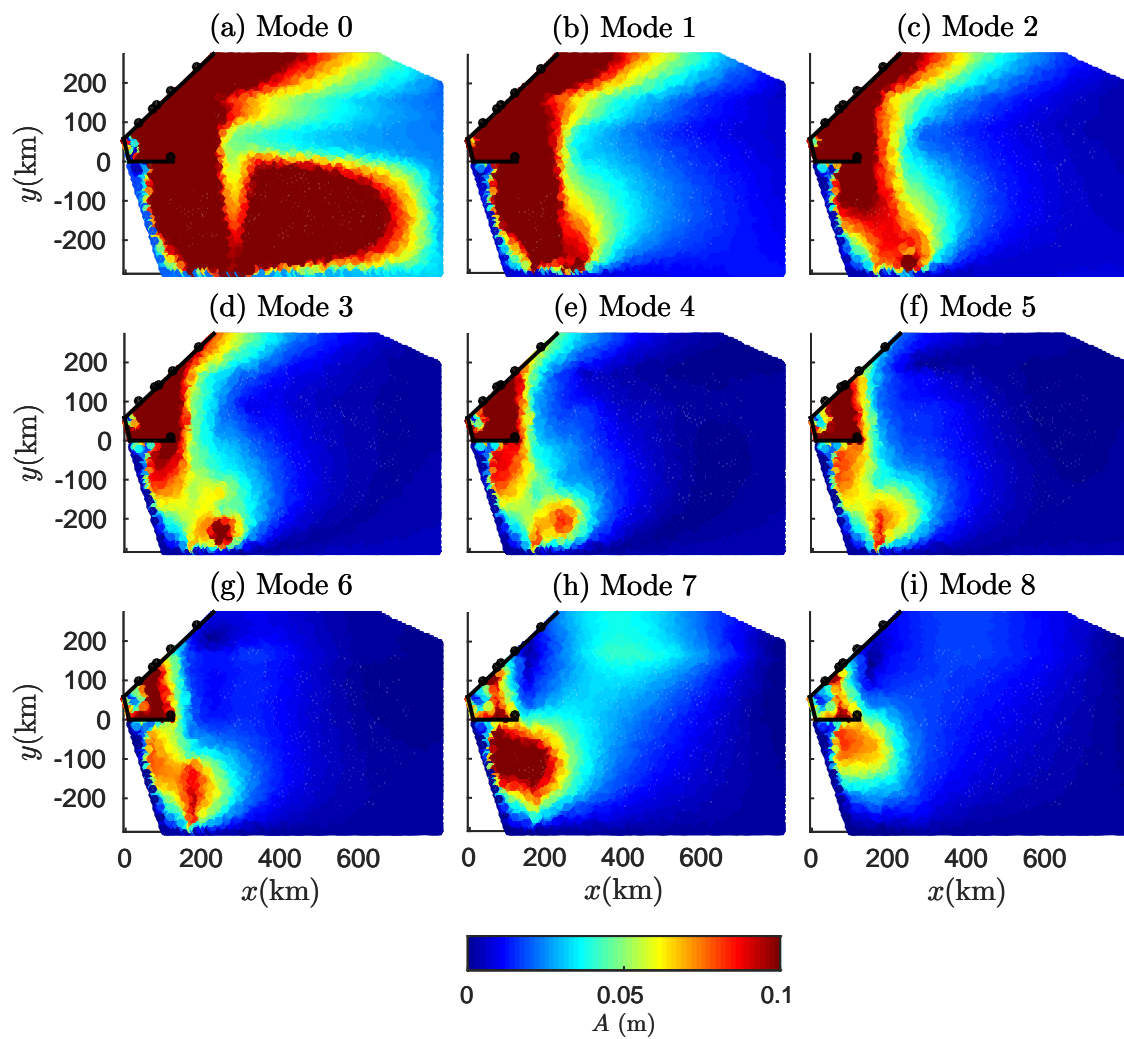Figure G.6: Elevation amplitude of Fourier modes 0-8 of scenario 3.

Figure G.7: Elevation amplitude of Fourier modes 0-8 of scenario 4.
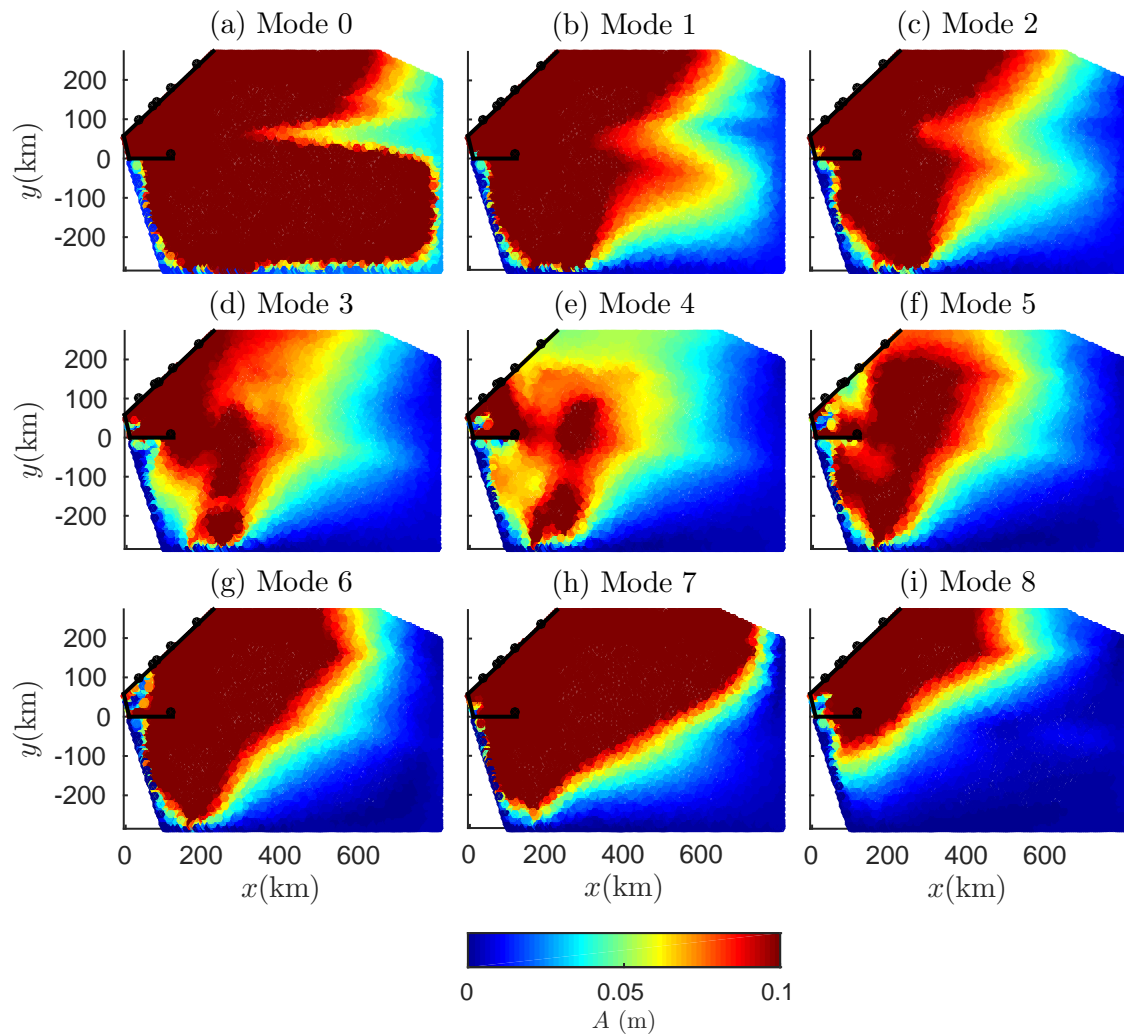
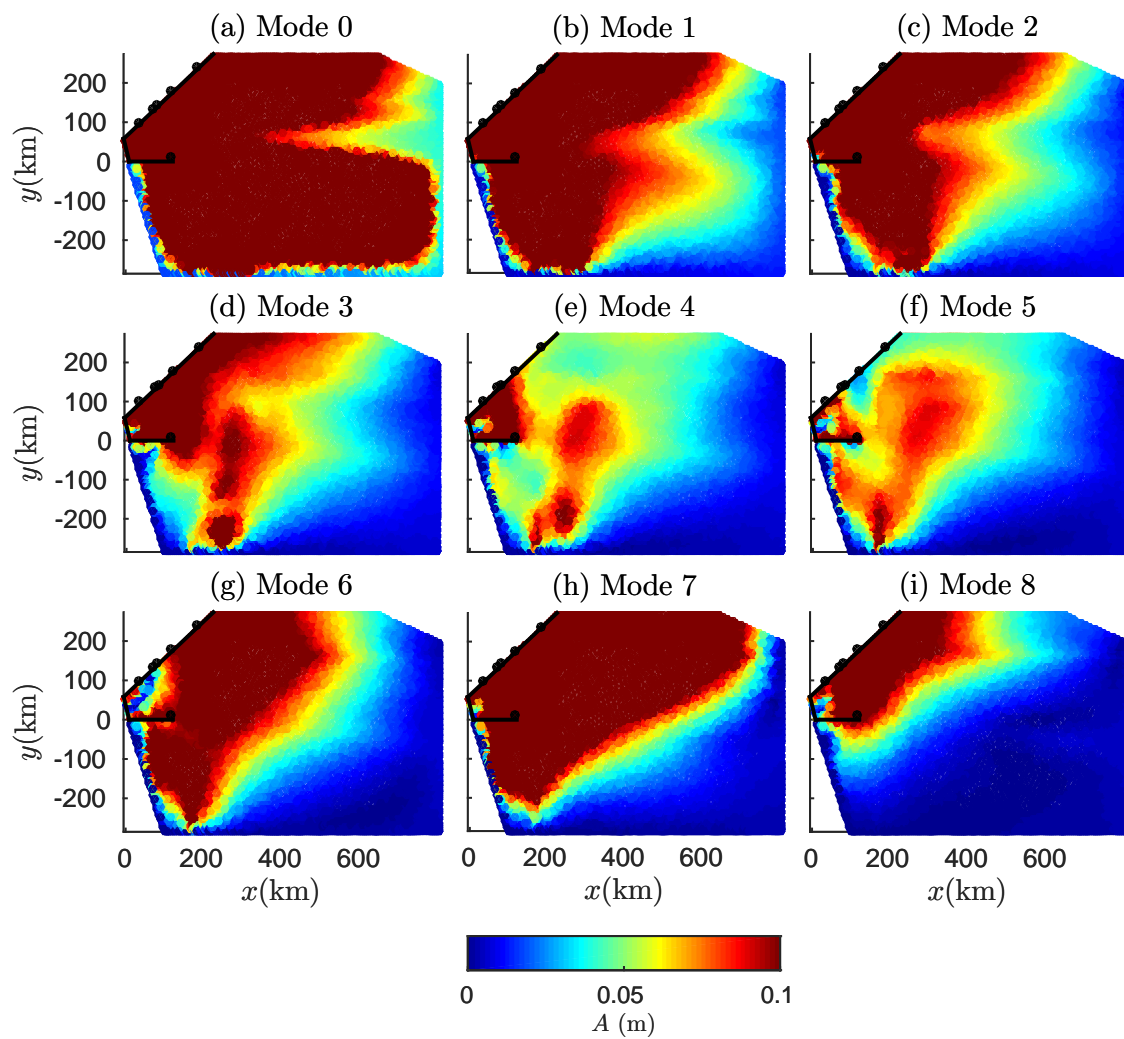Figure G.8: Elevation amplitude of Fourier modes 0-8 of scenario 5.

Figure G.9: Elevation amplitude of Fourier modes 0-8 of scenario 6.

Appendix H

Model development

While writing this thesis model development did not stop. Chen kept busy improving the model and its applicability to a case study. The following figures (Figures H.1 and H.2) show the results of the made improvements made. The table (Table H.1) presents the parameters and model changes used to acquire these results. These results are referred to in Chapter 6 and section 7.2

Table H.1: New values of physical parameters used during the model development.

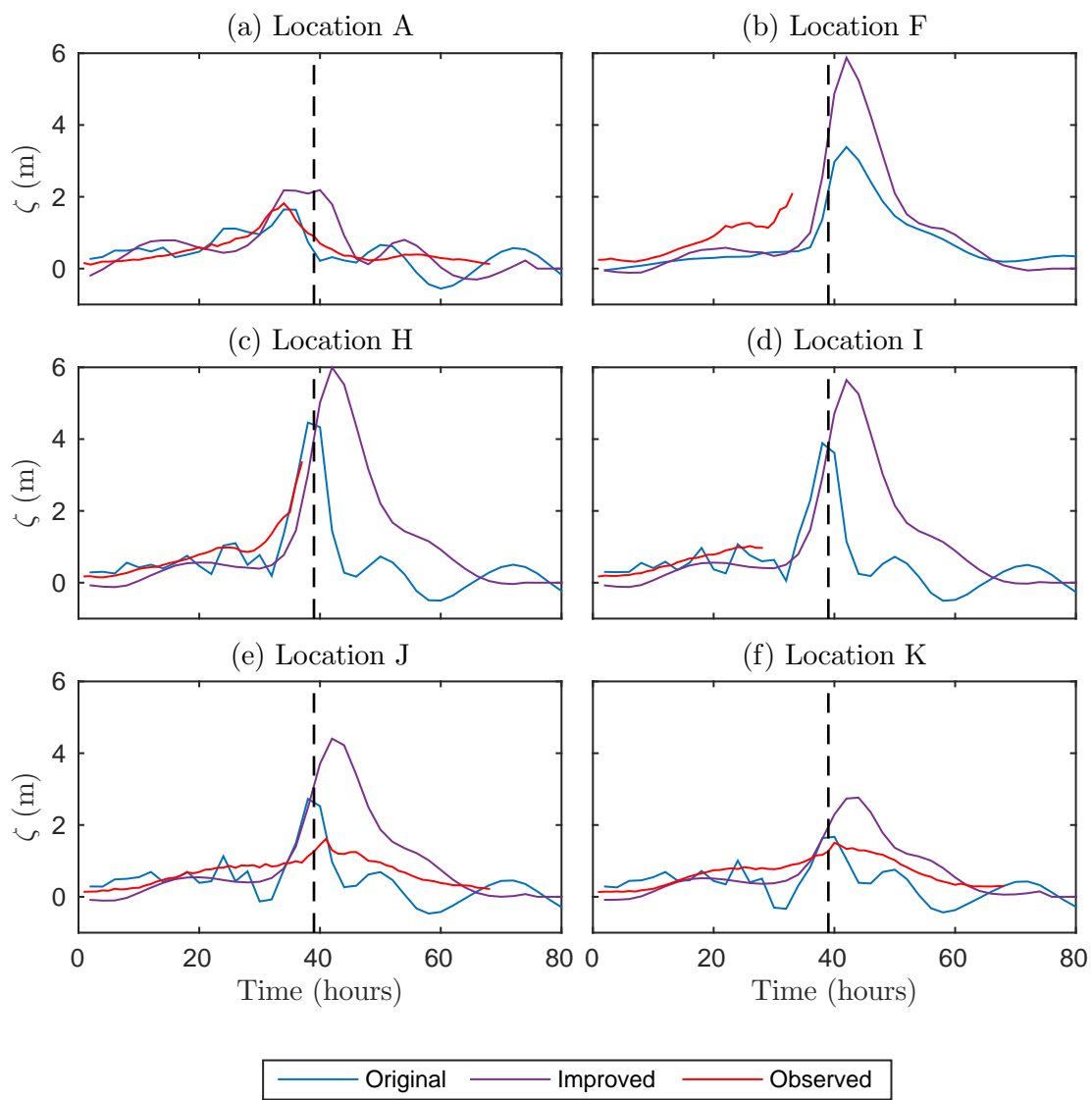| Physical parameter	Original value	New value
Friction	A_v (m/s^2) and s (m/s)	A_v (m/s^2) and s (m/s)
	0.025, 0.01	0.01, 0.015
Bathymetry	Water depth (h)	Water depth (h)
	Figure 3.5	Smooth (Figure D.1)
Drag coefficient	C_f (-)	C_f (-)
	2.54e^{-3}	2.54e^{-3}
Number of modes	k (-)	k (-)
	128	128
Grid size	Element size (km)	Element size (km)
	6, 20 (Figure A.2)	2, 3

Figure H.1: Simulated water levels for hurricane Katrina with the improved parameters as described in Table H.1. Vertical dashed line represents the time of landfall (t=39).
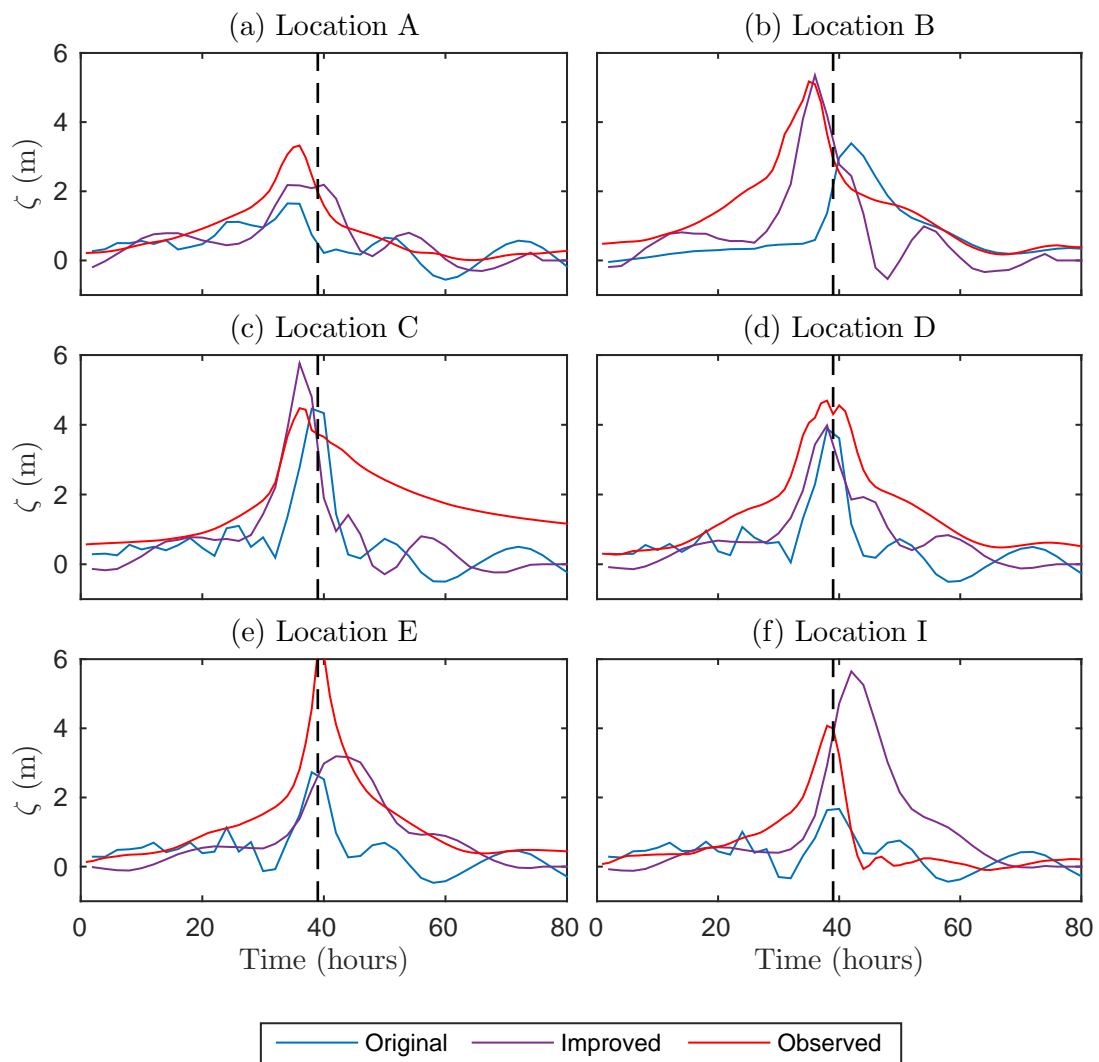
Figure H.2: Simulated water levels for hurricane Katrina compared to ADCIRC simulations The improved parameters as described in Table H.1. Vertical dashed line represents the time of landfall (t=39).